TECHNISCHE UNIVERSITÄT WIEN

Diploma Thesis

Electroporation of human tumor cells on a micro structured chip

Under supervision of

Ao. Univ. Prof. Dipl.-Ing. Dr. techn. Heinz Wanzenböck

Univ. Ass. in Neda Karami

by

Antun Štetić

18833157

…….. ……...……

Wanzenböck Heinz Karami Neda

TECHNISCHE UNIVERSITÄT WIEN

Affidavit

I have taken note that I am only authorized to publish my work under the designation:

Diploma-Thesis (Diplomarbeit)

With the approval of the examination committee. I solemnly declare that the presented work was created by myself independently. This work was created in accordance with the recognized principles for academic papers. All used resources, especially the underlying literature, are mentioned and listed in this work. The passages taken verbatim from the source are clearly identified as such.

The topic of this work has not been submitted for evaluation in any for as an examination paper, neither domestically nor internationally, by any examiner. This work corresponds to the work evaluated by the examiners.

I acknowledge that the submitted work will be electronically and technically reviewed using appropriate tools, including plagiarism detection software within the framework of the applicable rules or safeguarding good scientific practice, “Code of Conduct” at TU Wien, have been adhered to in creating the submitted work. On the other hand, by comparing with other students theses, violations of my personal copyright are avoided.

29.5.2024 Antun Štetić

Abbreviations

ATP	Adenosine triphosphate
C	Capacitor
CTMP	Critical transmembrane potential
DAPI	4′,6-diamidino-2-phenylindole
DEP	Dielectrophoresis
E	Electrical field
ECF	Extracellular fluid
FBS	Fetal bovine serum
ICF	Intercellular fluid
IDE	Interdigitate electrodes
IRE	Ireversable electroporation
MLA	Maskless aligner
PBS	Phosphate buffered saline
PECVD	Plasma enhanced chemical vapor deposition
PI	Propidium Iodide
PVD	Physical vapor deposition
R	Resistor
RE	Reversable electroporation
RIE	Reactive ion etching
RF	Radiofrequency
SiN	Silicon nitride
TMP	Transmembrane potential
X	Reactance
Z	Impedance
5R0ELA	Name of self-made electroporation device used throughout the thesis

Content

Abstract 3
Abstrakt 4
1.Introduction 5
1.1 Cell 7
1.1.1 Cell cycle 7
1.2 Tumor 9
1.2.1 Development of tumor 10
1.2.2 Carcinogens 11
1.3 Electroporation 13
1.3.1 Electrical Engineering 101 14
1.3.2 Electrical model of the cell 15
1.3.3 Mechanics of electroporation 16
2. Microelectrodes 20
2.1 Chip design 21
2.2 Chip fabrication 28
2.2.1 Spin coating 28
2.2.2 Maskless aligner 30
2.2.3 Sputter deposition 35
2.2.4 Plasma-enhanced chemical vapor deposition 40
2.2.5 Etching 41
2.2.6 Microwell 49
2.3 Chip holder 51
3. Electroporation device 53
3.1 Device design and function 55
4. Experiment 65
4.1 Experiment Setup 65
4.2 CASY 66
4.3 Cell staining 70
Conclusion 82
Appendix- Schematic 84
Appendix-Code 85
Appendix-Cell staining 87

Appendix- Cell count 97
Literature 98
Supplemental literature 101
Biography 103
Appreciation 104

Abstract

Cancer today is the second leading cause of death in the modern world. While often treatable, it is very expensive and for patients exhausting process, involving a lot of drug and radiation uptake. To avoid this new treatment methods are being investigated, most of them involving electroporation. Electroporation is a process where specific signals are stimulated, inducing an electrical field, which in turn causes the cell membrane to become more porous. Depending on the strength of said electrical field, those pores in cell membranes could reseal. In case the pores are not able to reseal, irreversible electroporation occurs, and the cell will die eventually. If the cell membrane can reseal, reversible electroporation occurs, allowing higher cellular drug uptake. Since the threshold of electroporation changes from cell type to cell type, a lot of research and optimization still needs to be done. For that sake, a custom electroporation device named 5R0ELA was designed and constructed during this thesis. Along the electroporation device, two types of microelectrode chips were designed and constructed, which would allow quick and easy experimentation on the cells. Finally, both the electroporation device and chips were tested, using two different methods (bioimpedance and cell staining), to conclude whether this simple and cost-efficient setup could cause electroporation.

Keywords: Electroporation, electrical field, tumor, membrane microelectrodes, chip, device, cell staining, HT-29

Abstrakt

Krebs ist heute die zweithäufigste Todesursache in der modernen Welt. Er ist zwar oft behandelbar, aber ein sehr teurer und für die Patienten anstrengender Prozess, der mit einer hohen Medikamenten- und Strahlenaufnahme verbunden ist. Um dies zu vermeiden, werden neue Behandlungsmethoden erforscht, von denen die meisten die Elektroporation beinhalten. Die Elektroporation ist ein Verfahren, bei dem bestimmte Signale stimuliert werden, die ein elektrisches Feld erzeugen, das wiederum die Zellmembran poröser werden lässt. Je nach Stärke des elektrischen Feldes können sich diese Poren in der Zellmembran wieder verschließen. Sind die Poren nicht in der Lage, sich wieder zu schließen, kommt es zu einer irreversiblen Elektroporation, und die Zelle stirbt schließlich ab. Wenn sich die Zellmembran wieder verschließen kann, kommt es zu einer reversiblen Elektroporation, die eine höhere zelluläre Arzneimittelaufnahme ermöglicht. Da sich der Schwellenwert für die Elektroporation von Zelltyp zu Zelltyp ändert, ist noch viel Forschungs- und Optimierungsarbeit zu leisten. Aus diesem Grund wurde im Rahmen dieser Arbeit ein maßgeschneidertes Elektroporationsgerät mit der Bezeichnung 5R0ELA entwickelt und gebaut. Zusammen mit dem Elektroporationsgerät wurden zwei Arten von Mikroelektrodenchips entworfen und gebaut, die ein schnelles und einfaches Experimentieren mit den Zellen ermöglichen sollen. Schließlich wurden sowohl das Elektroporationsgerät als auch die Chips mit zwei verschiedenen Methoden (Bioimpedanz und Zellfärbung) getestet, um festzustellen, ob dieser einfache und kostengünstige Aufbau Elektroporation bewirken kann

Schlüsselwörter: Elektroporation, elektrisches Feld, Tumor, Membran-Mikroelektroden, Chip, Gerät, Zellfärbung, HT-29

1.Introduction

Cancer is a group of diseases involving abnormal cell growth, with the potential to spread to other parts of the body. After heart disease, it is the second leading cause of death worldwide, estimated to be nearly 10 million in 2020 [s1]. Besides that, it is estimated that in 2020 there were 18.1 million new cancer cases, with 9.3 million in men and 8.8 in women. Many factors contribute to cancer formation, like age, alcohol and tobacco consumption, diet, genes, and gender. Overall, the most common cancer is breast cancer, with 2.26 million new cases in 2020 alone, followed by lung (2,2 million), colorectal (1.9 million), prostate (1.4 million), and stomach cancer (1.1 million) [s2].

If cancer is detected early in its onset, it can be somewhat easily treated, be it with chemotherapy, radiation therapy, stem cell transplantation, hormone therapy, or simply surgery [1,2]. Both chemotherapy and radiation therapy are widely used nowadays, and they work on somewhat similar principles. Chemotherapy is a drug treatment that uses powerful chemicals that circulate in a person's bloodstream in the hope that it will kill or shrink cancer cells. Radiation therapy uses invisible bursts of energy in localized areas in the hope of killing cancers. Both of them have unfortunate side effects that, besides damaging cancer cells, they damage healthy cells as well. This leads to tiredness, hair loss, nausea, vomiting, skin irritation, anemia, and a lowering of overall life quality.

Besides these two methods, surgery is also well very common method for treating cancer. Cancer surgery is an operation or procedure to remove a tumor from the body. This is the oldest kind of cancer treatment. While this method does not have previously mentioned side effects, it lowers life quality as well, as sometimes, surrounding healthy tissue is also removed [3]. As breast cancer is the most common cancer type, (but for different body parts as well, like testicles), due to aesthetic reasons patients will often refuse surgery or act too late, at which point the cancer will metastasize. Cancer metastasis is a state when cancer spreads to other parts of the body, besides the origin point. This complicates cancer treatment and lowers the survival rate drastically.

To circumvent this in late 1990, the thermal ablation technique was developed. During tumor ablation, thermal energy is used to heat or cool the tumor in the hope of killing it [4]. While this method is minimally invasive (unlike surgery), there is a risk of damaging surrounding tissue. As well it has also been observed that cancer tends to reoccur using this method. In response to this, in 2005 a new method, called electroporation was performed for the first time to destroy cancer cells. During electroporation, high-energy electrical fields are used to create pores in cancer cell membranes, which in turn should increase the uptake of anti-cancer drugs [5,6].

Electroporation as a cancer treatment method is still in an experimental phase, where a lot of optimizations still need to be done. As such, this thesis proposes and fabricates a unique, effective, and at the same time cost-optimized electroporation device named "5R0ELA" (covered in *3. Electroporation device*). Due to morality reasons, as well as for time efficiency, the experimental phase was not performed on a conscious being (be it human or animal), but rather on HT-29 tumor cells (*4.1 Experiment Setup*). Considering the cell's relatively small size (on µm scale) and to lower amplitudes of a generated electrical field, two types of microelectrode chips were fabricated (2. Microelectrodes). With said two types of microelectrodes, it is possible to observe how different electrical field amplitudes in combination with different isolation types of electrodes affect electroporation efficiency. Interfacing between the 5R0ELA electroporation device and microelectrode chips is done via a simple and elegant solution of a custom-built chip holder (2.3 Chip holder). Finally, electroporation efficiency was checked with two methods, which were impedance counting (*4.2 CASY*) and cell staining (*4.3 Cell staining*). Since electroporation causes the membrane to become more porous, cell impedance is changed, which can be observed with impedance counting method. Likewise, due to membranes increased porosity, as theory suggests, the cell drug uptake rate should be increased. This is exploited with the cell staining method, where cells should, instead of drugs, uptake certain color staining's, which is then observed via microscope.

The background needed for a complete understanding of electroporation is covered in the upcoming sub-chapters of the introduction. Be it biology of the cell (*1.1 Cell*), a theory of tumors (*1.2 Tumor*), or mechanic of electroporation with a corresponding electrical engineering background (*1.3 Electroporation*).

1.1 Cell

Cells are considered the basic unit of life, and all living this are made up of them. Some organisms consist of only a single cell and they are called unicellular organisms, while humans, animals, and plants are considered multicellular organisms. The basic rules of cells to be considered alive are: uptake and processing of nutrients, excretion of waste, response to environmental stimuli, and reproduction. Collections of similar cells (e.g. muscle cells) with specific tasks are called tissue (e.g. muscle tissue). Organs (e.g. Bladder, kidney) are structures made up of two or more tissues organized to carry out a particular function. A group of organs with related functions make up organ systems (e.g. urinary system). The human body consists of over 30 trillion cells [7].

In general, cell structure can be divided into extracellular (ECF) and intracellular (ICF) fluids. ECF is not a part of the cell but it is cells surrounding, literally fluid outside the cells. Cells nutrients and oxygen needed for cell survival are found here. ICF makes approximately 40% of the whole-body weight and includes everything that is enclosed in cells by their membrane. The membrane consists of a phospholipid bilayer that has hydrophilic heads and hydrophobic tails, and its function is to protect the organelles (mitochondrion, chloroplast, or nucleus) of the cell and to separate ECF and ICF.

1.1.1 Cell cycle

The cell cycle refers to a series of highly regulated events that include cell growth, development, and division into daughter cells. As visible in *Figure 1* it has two main phases, interphase and mitotic (M) phase. Interphase consists of several steps, that is G_1, S, and G_2 and it is mostly associated with cell growth and development. G_1 or the first gap, is a step during which there is little to no visible change in the cell. However, during G_1, the cell is quite active at the biochemical level. The cell is accumulating the building blocks of chromosomal DNA and the associated proteins, as well as accumulating enough energy reserves to complete the task of replicating each chromosome in the nucleus [8]. S or synthesis is the phase during which DNA replication (two identical copies) occurs. This stage is the most error-prone since DNA errors will be carried over and degenerated cells will emerge. During G_2, a cell continues to grow, proteins

are made and the content of a cell is reorganized in final preparations for the mitotic phase.

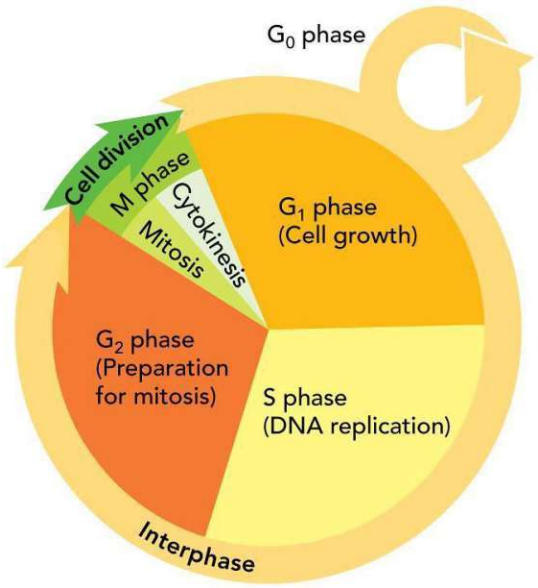

Figure 1 Cell cycle [8]

Figure 1 presents cell cycle, with the M phase including Mitosis and Cytokinesis. Mitosis is divided into a series of phases (prophase, prometaphase, metaphase, anaphase, and telophase) that result in the division of the cell nucleus [7]. Cytokinesis is responsible for the complete physical separation of the cytoplasmic components into two daughter cells (genetically identical cells). After that cell has several options. Depending on the tissue type that cell is part of it can rapidly go back to G_1, and be divided again (like blood cells) or it can go to the G_0 (resting phase). In this phase cell fulfills its function and it is capable of division. It remains in this phase until it receives a special signal (growth factor) at which point goes back to the G_1. Finally, cells can experience apoptosis, which is programmed "natural" cell death.

During the cell cycle, so-called checkpoints can be found at the "entrance" of the S and M phases and at the exit of the M phase. The purpose of these checkpoints is to inhibit cell growth if previous events (S/M) were not completed fully or if an error was detected. This way, the replication of "faulty" cells is stopped. If those errors go under the radar and if the cell instead of going to apoptosis, uncontrollably divides (with mutated DNA), it becomes a tumor cell. That is why, tumor occurrence increases with age, as more times (higher probability) have passed for such an event to occur, as well as accumulated DNA damage. The theory behind tumors, the way they spread through the body, and their promoters is covered in the following chapter *1.2 Tumor*.

1.2 Tumor

A tumor is any abnormal proliferation of cells, that results in abnormal growth of tissue, generally without inflammation. One of the fundamental features of tumor cells is clonality, that is, tumors can develop from a single cell (copies) that begins to proliferate abnormally. Changes in cell properties towards uncontrolled growth is called dysplasia.

While there are hundreds of different distinct types of tumors, in general, they can be separated into two distinct groups, that being benign and malignant tumors. Benign tumors have slower growth and they increase their size by expansion and displacement of other tissue. An example of a benign tumor is a wart. A distinct difference is that benign tumors don't invade/spread to other organs/body parts, unlike malignant ones. Malignant tumors are capable of both invading surrounding tissue and spreading throughout the body via circulatory or lymphatic systems. This process is called metastasis (*1.2.1 Development of tumor*). While benign tumors can be somewhat easily surgically removed, malignant tumors' ability to spread to different parts of the body complicates that. Malignant tumors, besides surgery, are treated with previously mentioned chemo and radiation therapies.

The goal of this thesis is to develop an effective electroporation setup, by interfacing a self-made electroporation device named "5R0ELA" (*3. Electroporation device*), and two types of microelectrode chips (*2.* Microelectrodes*)* by increasing tumor cell (drug) uptake. Together with tumor's ability to metastasize, they increase their size by invasion and destruction of other tissues, and that is what makes them so dangerous. Malignant tumor is better known by its other name, cancer.

Most cancers can be further separated into four categories, according to the tissue from which they have originated. Those four categories are carcinomas, sarcomas, leukemias, and lymphomas. Carcinomas make up approximately 90% of all human cancers and are malignancies of epithelial cells. Epithelial cells (tissue) are cells that cover bodies (skin) and line internal organs. Sarcomas are rare type and they are cancer of connective tissues, such as bones, muscle, fibrous tissue, and cartilage. Leukemias and lymphomas make up 8% of all cancers and they arise from the blood-forming cells and immune system cells respectively [7].

1.2.1 Development of tumor

As previously mentioned, cancer develops as a "faulty" cell as part of a tissue. These cells multiply much faster than surrounding tissue, and as such tumors grow much faster than the rest of the tissue. All body tissues are covered with a membrane that keeps cells of that tissue inside. As cancer cells grow much faster than regular tissue, this membrane will be broken by cancer cells and they will "spill" to other tissues. Likewise, cancer, due to its size, will exert pressure on the surrounding tissue including surrounding blood vessels as well. This leads to lower/omission of blood flow to the normal tissues and in such cases, some of the tissue will die off. Tumor cells, like normal ones, require a supply of blood, nutrients, and oxygen to survive. This way cancer is "stealing" a higher percentage of the total blood supply. As cancer gets bigger, it gets further and further away from the blood vessels, and that way center of the tumor gets less and less oxygen and nutrients [s3]. To avoid this tumor cells, send out signals called angiogenic factors. This encourages new blood vessels to be formed into a tumor. This process is called angiogenesis.

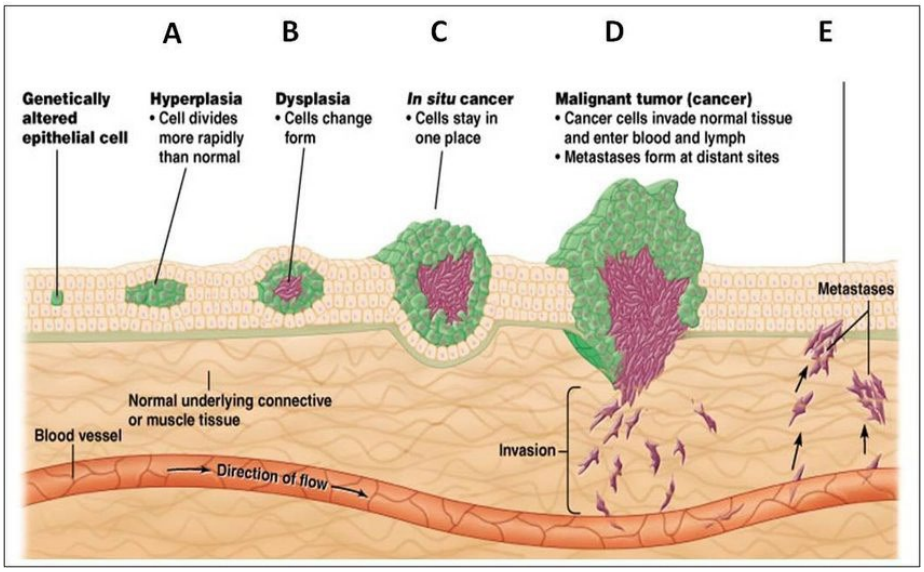

Figure 2 Development of the cancer cells [9]

Figure 2 describes the development of the cancer, with all corresponding stages, and beforehand mentioned angiogenesis (new blood vessel formation). Via new blood supply, tumors can grow even further. Since the tumor has its "own" blood supply now, it receives all the nutrients it requires, but it can also spread its cells through said blood supply, and thus, travel throughout the

rest of the body. This is the second way cancer can metastasize.

To influence/suppress metastasis, the uptake of anti-cancer drugs by cells is an important part of cancer therapy. To increase drug uptake, the use of electroporation (*1.3 Electroporation*) has been recognized as highly beneficial which is caused by a device (*3. Electroporation device*) that introduces an intensive electrical field onto the tumor cells. While anti-cancer drugs suppress cancer development, carcinogens (*1.2.2 Carcinogens)* promote it.

1.2.2 Carcinogens

While the reasons for tumor cancer formation are still not fully understood, substances that cause cancers are called carcinogens. As previously mentioned, cancers start as normal cells but during normal their life cycle, errors in cells are introduced. If those errors are not recognized by the checkpoint systems (and faulty cell is eliminated), cancer or tumors will be formed.

Malignancy of tumors is a complex and additive process, where many factors influence the likelihood of cancer formation. Agents like radiation, chemicals, viruses, and genetics are the main perpetrators. Radiation and many chemical carcinogens act by damaging DNA and inducing mutations. These carcinogens are generally referred to as initiating agents since the induction of mutations in key target genes is thought to be the initial event that leads to cancer development [5]. These “errors” are then carried out during the cell cycle. For example, solar ultraviolet radiation (skin cancer) and chemicals in tobacco smoke are one of the most common causes of DNA damage that leads to cancer.

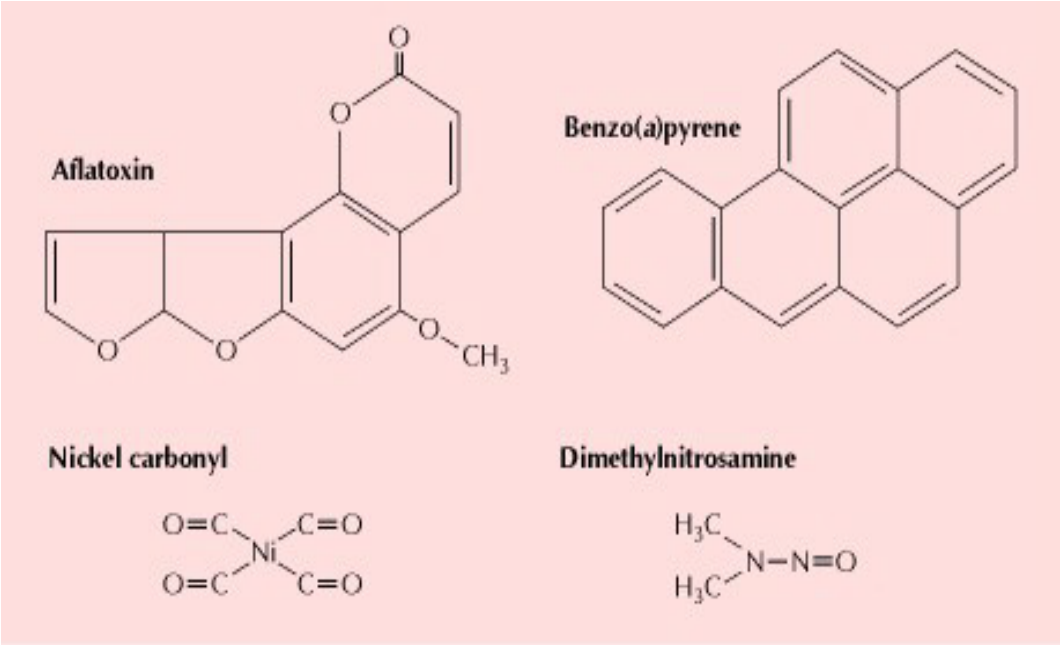

Figure 3 Structure of tobacco carcinogens [9]

Figure 3 represents the structure of the carcinogens in tobacco smoke. Benzo(α)pyrene, dimethyl nitrosamine, and nickel compounds are the major identified causes of cancer in humans and make up to 90% of the total causes of cancer in the lungs. This is important, since as mentioned in *1.Introduction*, lung cancer is the deadliest one, and thus tobacco is particularly problematic.

For a virus to survive it must enter a living cell and take over the cell's reproduction mechanism so that the virus can reproduce itself. Some viruses do that by inserting their DNA into the host's cell and that can affect the host's DNA which in turn can lead to cancer. The most common are Human papillomaviruses (HPVs), Epstein-Barr virus (EBV-herpes virus), Human immunodeficiency virus (HIV), and Hepatitis B/C viruses.

Besides initiating cancers, some carcinogens do not induce cancers, but rather they contribute to cancer development, by stimulating/increasing the speed of cell proliferation, without causing mutations. They are called tumor promoters and are most importantly made up of hormones (particularly estrogens).

1.3 Electroporation

Electroporation is a method in which a large external electrical field is used to create pores in the membrane of the cell thus increasing its permeability. This increase in permeability can be, depending on the strength of the used electrical field, temporary (RE) or permanent (IRE) which causes eventual cell death.

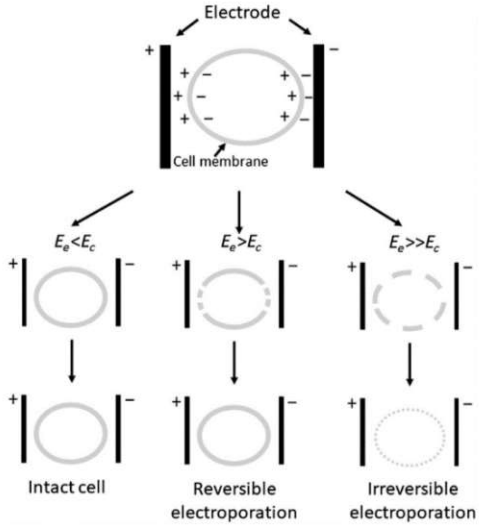

Figure 4 Possible outcomes of electroporation in relation to electrical field (E_e) strength and cells critical value (E_c) [10]

Figure 4 shows a schematic of the possible outcome of electroporation (RE, IRE, or non-affected) depending on the strength of the applied electrical field (E) and cell-specific critical value (E_C).

With increased permeability, there is a wide range of applications, like gene transfection, bacteria deactivation, tissue ablation, or most importantly for this thesis, increased drug uptake. Increased drug uptake improves suppression of the further metastasis of tumors (*1.2.1 Development of tumor*) and its viability which is a vital part of cancer treatment therapy.

To fully understand the mechanics of electroporation (*1.3.3 Mechanics of electroporation*), a short introduction to the field of electrical engineering is needed (*1.3.1 Electrical Engineering* 101) alongside understanding how a can cell be represented with electrical components (*1.3.2 Electrical model of the cell*).

1.3.1 Electrical Engineering 101

First, there exists an electrical potential. The potential is the presence (or lack of it) of electrons at a point in space, and a single electron has a charge of $1.6 * 10{-}10$ Columbus. The more electrons that are present, the higher the potential. The difference in potential (concentration) in two different, spatially separated points is called voltage (U), and its unit is expressed in Volts (V). Since the basic law of nature dictates that everything wants to be in some sort of balance, electrons from the point of higher potential want to migrate to the point of lower potential. This will continue to happen until equilibrium between two points is achieved. The flow of these electrons from higher to lower potential is called electrical current (I), and its magnitude is expressed in Amperes (A). During the flow, electrons will "interact" with other atoms/electrons on the path which usually lowers this flow, and this effect is called resistance (R) and is expressed in Ohms (Ω). This leads to Ohm law which is expressed as:

$$I = \frac{U}{R} \tag{1}$$

From formula 1 it is visible that current is proportional to voltage and reversible proportional to resistance. If resistance is too high, an isolator is present in tween two potential points and there is no current flow. But, due to still present potential imbalance, electrical force is created between them, and thus the electrical field is created (E). The electrical field generated between two points is expressed as a voltage per unit of distance between them.

Field can be detected by putting "experimental" electrons in it (or any other charged particle). On the said electrons, the force will be exerted (field), and the electrons will move to the corresponding gradient (from higher to lower concentration). In case cells are found in this field, ions (atoms or molecules that have gained or lost one or more electrons, resulting in a net electrical charge) will move toward the corresponding point of the electrical field. Positive ions will move toward the point of higher potential, while negative ones will move toward lower potential, to satisfy the previously mentioned equilibrium.

While the electrical field will be used mainly for electroporation during this thesis, it is also a very important part of the microelectrode chip fabrication process, as discussed in *2.2.3 Sputter deposition* or *2.2.5 Etching.*

1.3.2 Electrical model of the cell

The effects of electroporation on a cell can be understood by observing the electrical model of the cell. Both ICF and ECF are considered to be conductors and as such are represented as resistors. As mentioned, the barrier between ICF and ECF is a cell membrane, which is an isolator. Two conductors separated between an isolating layer are a building block for a capacitor (C) which represents the cell membrane. A capacitor is a device for storing electrical energy.

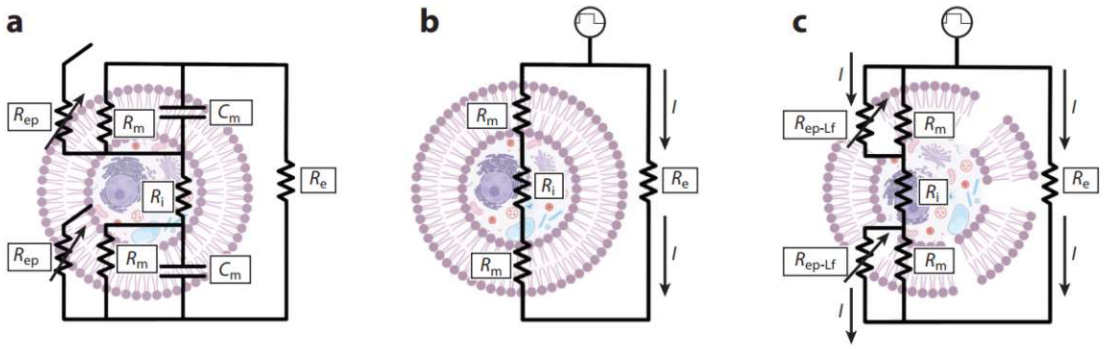

Figure 5 Cell as an electrical model, in different states: intact, low frequency stimulated, and successfully electroporated cell [11]

Figure 5 represents a cell in three different states (a, b, and c). R_e and R_i are ECF and ICF resistances, while R_{ep} (in electroporated state) and R_m are membrane resistances. The most left case (a) of the cell represents a "normal", functional cell, which is under no influence. In case a low-frequency current is applied (b) to the cell, it will go around the cell, using ECF as the only conductive path. This can be explained with the following formula:

$$Xc = \frac{1}{2*\pi*f*C} \qquad (2)$$

X_c is the reactance of the capacitor, and it can be interpreted as the "resistance" of the capacitor to current flow. C is capacitance, in this case, it differs from cell-to-cell type (or from the same cell types, as it is used to determine cell membrane integrity). The combination of "real" R resistance and reactance X is called impedance (Z) and it is only present in an alternating current circuit.

As visible from formula 2, reactance is inversely dependent on the frequency (f), and because of

that cell will be "ignored" at low frequencies as its reactance will be too big. At high frequencies, reactance will be low, and this phenomenon is important for bioimpedance measurements since the resistance of ICF is now measurable. While not related to electroporation, bioimpedance is important, for electroporation detection, via CASY device. This method is more explored in chapter *4.2* CASY. When electroporation occurs, pores are formed on the cell membrane which allows even low-frequency current to flow through the cell, and this case is explored in c state in *Figure 5,* where $R_{ep\text{-}Lf}$ represents the resistance of electroporated cell membrane, which is now low, which in turn allows current to flow through the cell, as membrane became porous.

1.3.3 Mechanics of electroporation

While today, there is still no agreed-upon explanation for electroporation mechanics, two theories are prevalent. One theory suggests that, since the membrane separates the ICF of the cell from the rest of the environment, it will "block" previously mentioned ions (*1.3.1 Electrical Engineering* 101) from movement. As an electrical field will exert force on ions, and if that field is sufficiently strong, ions will be pulled out, creating nanopores in a membrane, and increasing its permeability. Another theory suggests that the cell membrane phospholipid bilayer is differently charged. Specifically, hydrophilic heads are negatively charged. Whit that, heads will orient according to the field, which will cause cell shape deformation and eventual pore formation [12]. In both theories, the size of these nanopores depends on the strength of the field.

In a healthy cell, there is always so-called cellular transmembrane potential (TMP), and it is usually -0.07 V. It is caused by the difference in ion concentration of the ICF and ECF. TMP can be manipulated by applying an external electrical field, which in turn causes pores in the membrane. If pores are sufficiently small, they will, after a few seconds to a minute, seal again preserving the integrity of the membrane and with it the cell. This is called reversible electroporation. In case the field is stronger, higher TMP will be caused and thus bigger pores will be formed. Once TMP surpasses so-called critical transmembrane potential (CTMP) the created pores will be too big, and the membrane will not be able to reseal itself again. This will lead to leakage of ICF out of the cell and eventual cell death. This is called irreversible electroporation [11].

Thus, the main factor for successful electroporation is the electrical field and its components. An external electrical field is generated using electrical signals. In most cases for electroporation, a square signal is used, due to its simple generation nature and effectiveness [11]. The most obvious factor of the signal is its amplitude and it represents the maximal value (voltage) of the signal. In electroporation, a continuous signal is never used, thus pulse width is present. Pulse width represents the duration of the signal when it is at a certain (non-zero) voltage value (time duration of the positive half). The duration of the signal while, it is at a zero value, is called the negative half. The combined duration of the positive and negative half is called the signal period (T-cycle), and it is the time duration before the signal repeats itself. The percentage of the time of the positive half compared to the signal period is called the duty cycle. Finally, frequency (f) is the number of signal repetitions in one second and it is the inverse of the period ($f = \frac{1}{T}$). All signal components are visible in the picture below.

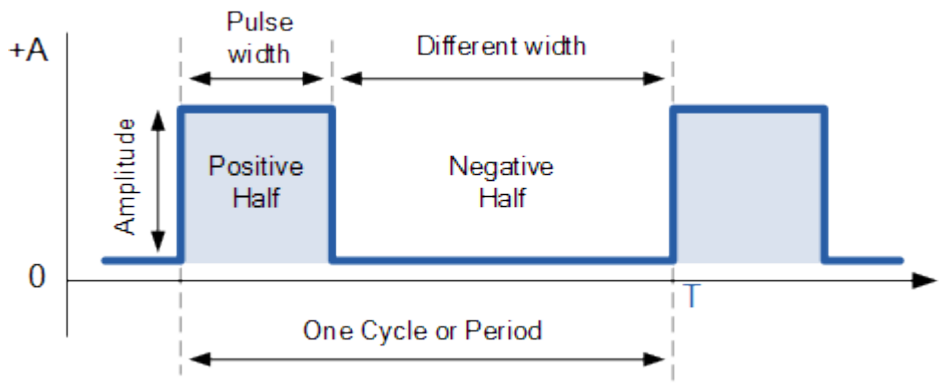

Figure 6 Signal components of DC pulsed signal, often used in electroporation [12]

Figure 6 demonstrates the example of possible pulsed signals that are prevalent in electroporation. When deciding which signal will be used for electroporation, it has to be considered the amplitude, pulse width, frequency, and signal repetition number, all increase the likelihood of electroporation proportionally. Likewise, negative half and period, proportionally decrease the likelihood of electroporation. The bottom line is, that it all comes down to the total energy the cell is subjected to. The area of the positive half (multiplication of amplitude and pulse with) is energy and increases electroporation, while the rest phase (negative half) decreases electroporation likelihood.

While the excitation signal is the main component that determines whether the electroporation of the cell happened, it is not the only one. Each cell type responds differently to electroporation in relation to its dimension, shape, and orientation. This is described using the Schwan equations [13] as follows:

$$TMP = F * E * r * \cos(\varphi) * (1 - e_{\tau}^{t}) \tag{3}$$

Where *TMP* is current transmembrane potential, the membrane is subjected to, *F* is a form factor that describes the impact of the cell shape on the distribution of the electrical field on the cell (for example, 1.5 for a perfectly spherical cell), *r* is a radius of the cell, φ is a polar angle measured from the center of the assumed spherical cell to the direction of the electrical field and *t* is elapsed time since electroporation started.

Factor F is determined using the following relation:

$$F = \frac{3\sigma_e[3d_m r^2\sigma_i + (3d_m^2 r - d_m^3)(\sigma_m - \sigma_i)]}{2r^3(\sigma_m + 2\sigma_e)\left(\sigma_m + \frac{1}{2}\sigma_i\right) - 2(r - d_m)^3(\sigma_e - \sigma_m)(\sigma_i - \sigma_m)} \tag{4}$$

Where: σ_e - extracellular conductivity

σ_m - membrane conductivity

σ_i -intercellular conductivity

d_m – membrane thickness

Finally, τ charging time of the membrane (as it is represented as a capacitor) and it is given with the following formula:

$$\tau = r * C_m * \left(\rho_i + \frac{\rho_e}{2}\right) \tag{5}$$

Where: C_m-cell capacitance per unit area

ρ_i- resistivity of the intercellular domain

ρ_e- resistivity of the extracellular domain

Due to these many factors, electroporation (especially reversible) is still a method that is being researched as optimal stimulating signal changes from cell type to cell type.

These forlmulas (3, 4, 5) are used to optimize the stimulating signal, for each type of (tumor) cell, but some general, broad guidelines exist, where 8 pulsed signals are used, with 1 Hz, duration of 100 µs and generating electrical field out of several kV/cm [11,14].

Optimization is important since irreversible electroporation or damage to the cells wants to be avoided. However, for medical tumor treatment, irreversible electroporation is the oldest method but it has been falling out of favor in recent times. The point of it was to electroporate tumor cells permanently, so that intercellular content is let loose, causing cell death. Some newer research finds that patients treated with this method are susceptible to cancer reappearance. [15]

Newer methods, where optimization is really important, induce reversible electroporation which in turn increases cellular medication uptake preventing/or suppressing metastasis, as discussed in *1.2.1 Development of tumor*. Using electroporation, targeted membranes of tumor cells will open, which in turn, allows higher uptake of medication, compared to normal healthy cells (whose membrane opens up at different stimulating values). Since it is still a novel method a lot of optimization research has to be done. This method minimizes damage to the patient's healthy cells and thus the rest of the body.

The newest method, which has just recently entered clinical trials uses reversible electroporation as well. This method involves injecting a patient with Ca in the area of the tumor. Tumor cells, for now, unknown reasons, have a high uptake of Ca molecules that are needed for ATP (Adenosine triphosphate) [16]. ATP is a nucleotide that provides energy to drive and support many processes in living cells. While Ca is not poisonous to the cells/body by itself, by electroporating tumor cells, their uptake goes into “overdrive”, so much so that they cause their own demise.

Due to both methods utilizing reversible electroporation, the purpose of this thesis is only to prove that electroporation is possible with “5R0ELA” (*3. Electroporation device*) in combination with fabricated microelectrodes (*2. Microelectrodes*). As such, this cost-effective setup can be used for future research in the area of electroporation signal optimization.

2. Microelectrodes

As mentioned in *1.3 Electroporation*, for electroporation to take place, huge electrical fields are needed (in the range of kV/cm). This complicates things as high voltages can be dangerous for health (subject and operator), leading to stricter safety regulations. Additionally, this complicates the electroporation device from an electrical standpoint and its size, further increasing its price. Electroporation being a novel method, a lot of experiments still need to be done, to optimize signals used in electroporation. This can be done by testing on real patients or animals, both of these options raise morality concerns. To avoid that, tumor cells can be used, electroporating them, thus leading to the optimization of simulating signals and testing of new drugs. Since cells are relatively small, the distance between negative and positive electrodes can be small as well to successfully electroporate them. Since the electrical field is dependent on the distance, this leads to using smaller stimulating signals. Thus comb-shaped interdigitated microelectrodes (IDE), with a spacing of 100µm were constructed, bringing down stimulating signal from the kV range to two-digit values.

For the material of the electrodes, gold was chosen due to its excellent properties, which were fabricated on a 49 by 49 mm glass substrate. Gold has moderately good conductivity ($4.11*10^7$ S/m) [s5], and is resistant to oxidation and corrosion. An isolating layer out of SiN was used, to prevent short-circuiting between electrodes, and so that an electrical field could be formed. Most of the modern literature [17] uses this isolating layer only in between electrodes, thus forcing current to take a non-optimal path, and avoiding short-circuiting. The second design was built as well, where the electrodes are completely covered with an isolating layer [18,19].

The following subchapters will cover the ideas behind the design of custom microelectrodes (*2.1 Design*), their fabrication process alongside all necessary testing (*2.2 Chip* fabrication) and finally wrapping it up with a custom-made chip holder (*2.3 Chip holder*) that allows interfacing between the chip and electroporation device.

2.1 Chip design

Before the chip fabrication process can be initiated, the design for the first layer of the electrodes needs to be created. It was done using the program KLayout. KLayout is computer-aided design software that is used to layout patterns for lithography [s6]. All the sizes and scales during chip design were done in µm.

The design was made in such a way that it can fit onto a 49 by 49 mm glass substrate. Glass was chosen due to its cost-effectiveness alongside its properties, like transparency (for microscope usage), high heat resistance, and chemical and biological inertness. 49 by 49 mm size of the glass substrate was chosen due to its availability and preexistence of chip holders with said size. Those chip holders would be used if the fabrication of a custom chip holder had failed.

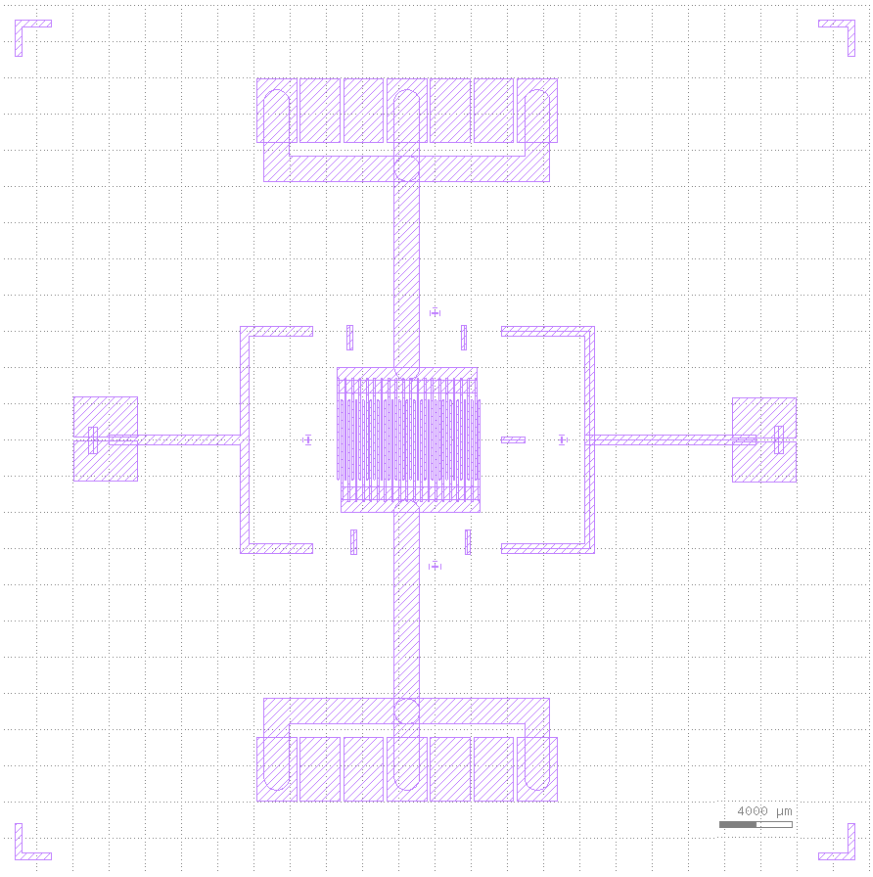

Figure 7 Design of the first layer design of the chip

Figure 7 represents the final design for the first layer of the chip. A critical part of the work of electroporation are electrodes themself. They are located in the central part of the chip and there

are 40 of them (20 positive and 20 negative). As stated in *1.3 Electroporation*, electroporation requires high electrical fields, and thus electrodes need to be relatively close, so that high voltages (fields) can be avoided. In the most of literature, fields fluctuating around 1000V/cm are used. For ease of calculation, the distance of 100 µs between of electrodes was chosen (this distance could have been chosen arbitrarily, as long as correct field-inducing voltage is used). With that knowledge, a custom electroporation device was built that can provide signals between 3 and 33 V, more about it can be learned in Chapter *3. Electroporation device*. In conjunction with designed electrodes, in theory, some 330 to 3300V/cm electrical field can be generated.

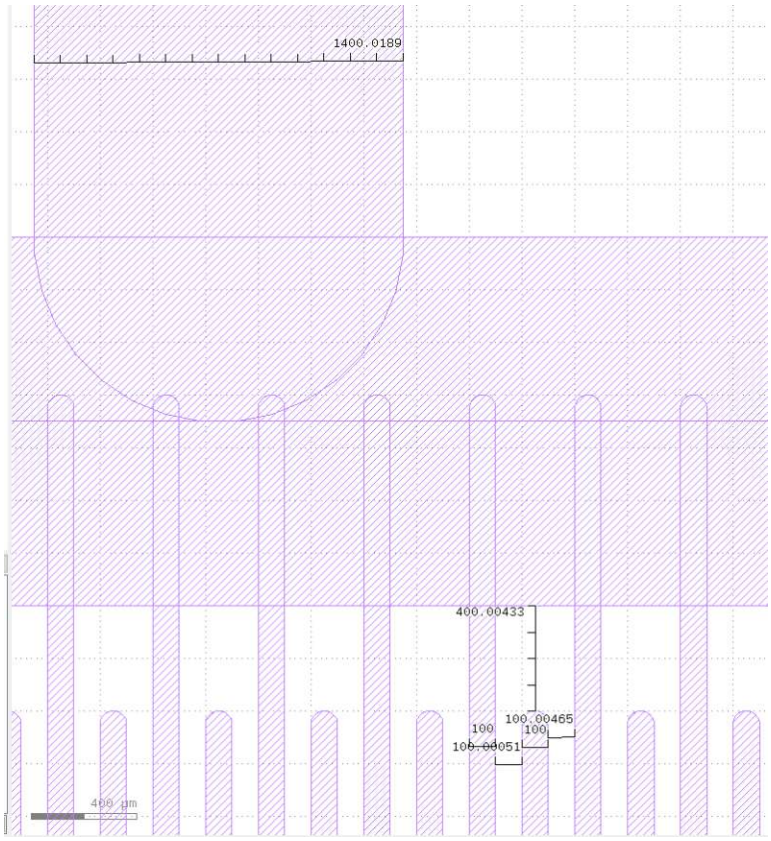

Figure 8 Enlarged section of the Figure 7 chip, focusing on the electrodes and their dimensions

Focusing only on the section of the chip from *Figure 7*, specifically onto the electrodes, and adding measures (for readability), *Figure 8* is created. It shows the expected dimensions of electrodes and can be used to compare with fabricated results. While the distance between electrodes is the most important part of the chip, in regards to electroporation, the dimension of electrodes is important as well. This is due to the relatively high voltages that are being used, which in turn could cause an electrochemical process to take place between gold electrodes and cell media. Due to high voltage, electrons will be kicked out of the positive electrodes, and they

will move toward the negative electrodes (an example of damaged electrodes can be observed in *Figure 65*). Because of that, 100 µm electrodes were designed, since due to their relatively big size, the electrochemical process is less likely to occur. Some papers use even larger electrodes [17], but having too large of electrodes wants to be avoided as well. In the later chapter *4.3 Cell staining*, the effectiveness of electroporation is determined using color staining, and since a light microscope was used, all the data (cells) that are on electrodes is lost (light can't pass through the gold). In the case of this thesis, this leads to the loss of 50% of all data. Circular tips of electrodes were chosen as part of the design since they should provide a more uniform distribution of the electrical field [20]. After that, pads were designed.

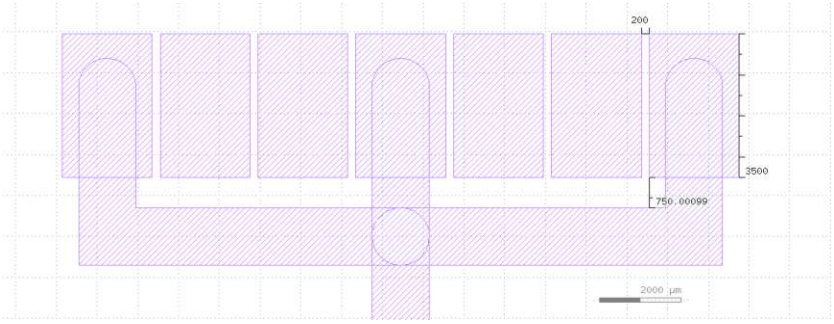

Figure 9 Pads section of the chip in Figure 7

Figure 9 focuses on the pads of the chip whose purpose is so that the electroporation device can be connected (*3. Electroporation device*). These pads are connected to the corresponding electrodes (positive or negative ones). The reason for having three connected pads leading to only one type of electrode is a precaution. In case one of the pads gets damaged (e.g. by a scratch of connecting pins), the other two can still be used, without making the chip obsolete. As well, additional devices can be connected to the chip (like an impedance measuring system), without requiring the electroporation system to be disconnected. Spacing in between electrode pad was chosen in such a way that it can be used in conjunction with *2.3 Chip holder*. Another important component of the design is alignment marks.

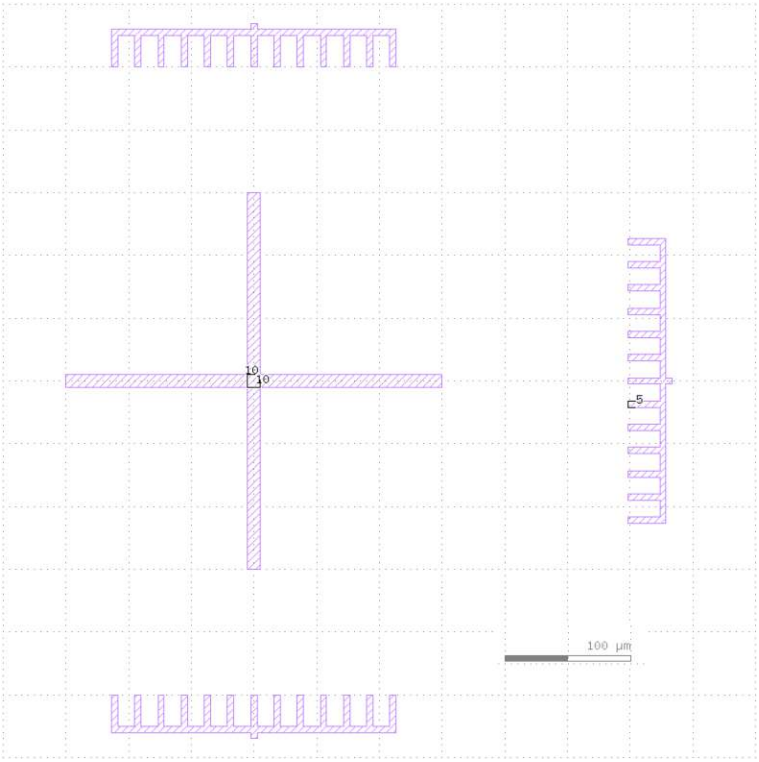

Figure 10 Alignment mark as used for chip shown in Figure 7

Figure 10 shows alignment mark, whose purpose is, as the name suggests, to align the second layer (*Figure 11* and *Figure 13*) with the first one (*Figure 7*). Since the second layer is needed as isolation, pitch-perfect alignment is needed. Otherwise, the isolating layer will cover an area that is not desired. Secondly, due to its, compared to the rest of the chip, very small nature, it can be checked to see how successful the fabrication process was and further calibrations. On the design there are 4 alignment marks in total, spaced equally from each other (7000 µm by X and Y axis), making sort of a square.

Besides the main electrodes, as visible in *Figure 7*, two U-shaped electrodes, that go around the main electrodes are found on the chip. The purpose of these electrodes is to act as a sort of antennas, that will pick up any noise, which is then by pads grounded. On the corners of the chip, L-shaped structures can be found. They don't provide any function besides marking the end of the chip so that potential crashes from the MLA 150 machine (more about in *2.2.2* M) can be avoided. Finally, around the main electrodes, five little strips can be found. Their only function is to assist with accuracy while bonding PDMS well (chapter *2.2.6* Microwell).

Afterwards, the second layer was designed. As mentioned in *1.Introduction*, the second layer is

an insulating layer and two different designs were made. Following [16], a design was made where the space between electrodes was insulated, but the electrodes themself were left exposed.

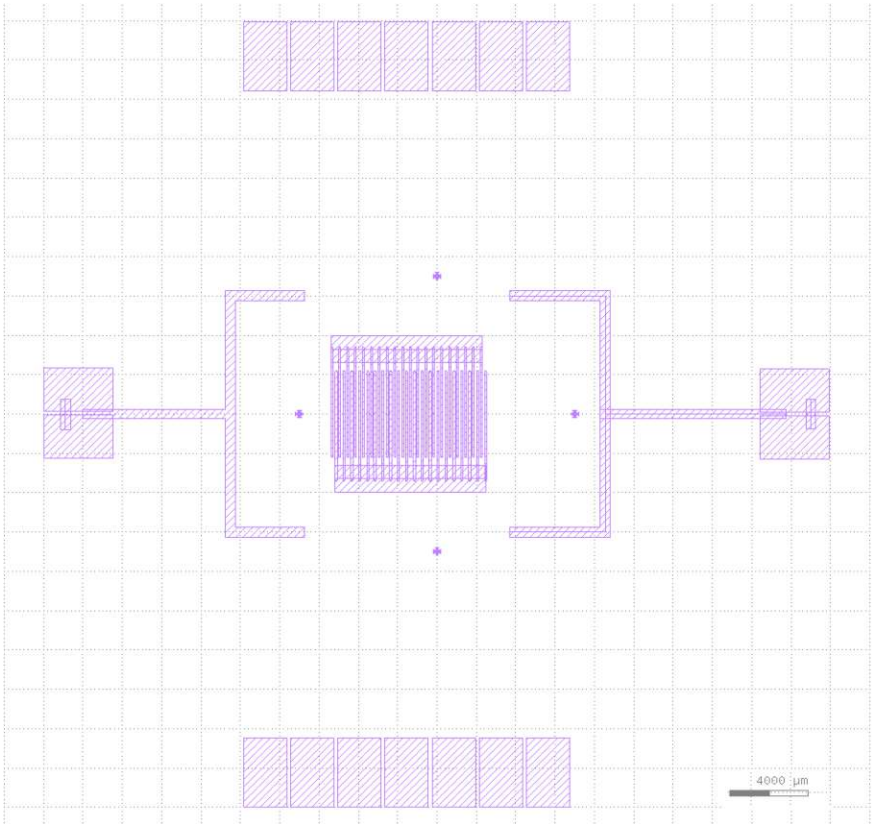

Figure 11 Naked isolating layer as a second layer of the chip, electrodes (Figure 7) are not covered with insulation layer

Figure 11 design for simplicity's sake is called *naked* due to its lack of an isolating layer on the top of electrodes. Everything still marked (purple color) in *Figure 11* will not be covered by the isolating layer. That includes pads (so that 5R0ELA can be connected), electrodes (stimulating and noise canceling), and new alignment marks.

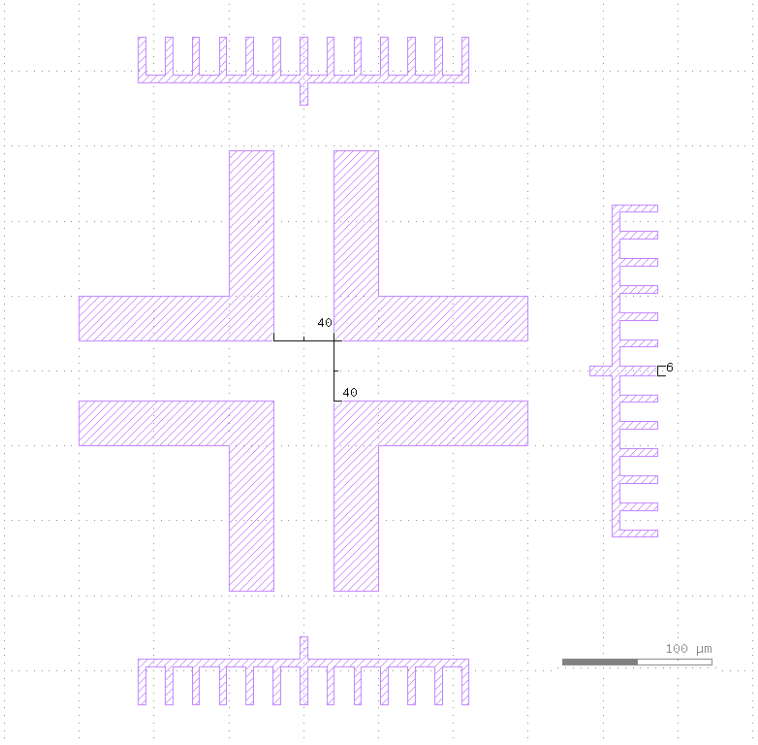

Figure 12 Alignment mark used in the second layer, with Figure 11 and Figure 13 designs

Figure 12 shows the mark used in both second-layer designs (*Figure 11* and *Figure 13*) The second layer alignment mark was designed in such a way that the first layer alignment mark (cross) in *Figure 10* could fit perfectly in the space in between L-shaped structures in *Figure 12*. This means the cross should be exactly spaced 15 µm from L structures. This is used to evaluate the rate of desired overlapping between the first and second layers.

The second design for the insulating layer was made, where electrodes are covered as well with the isolating layer.

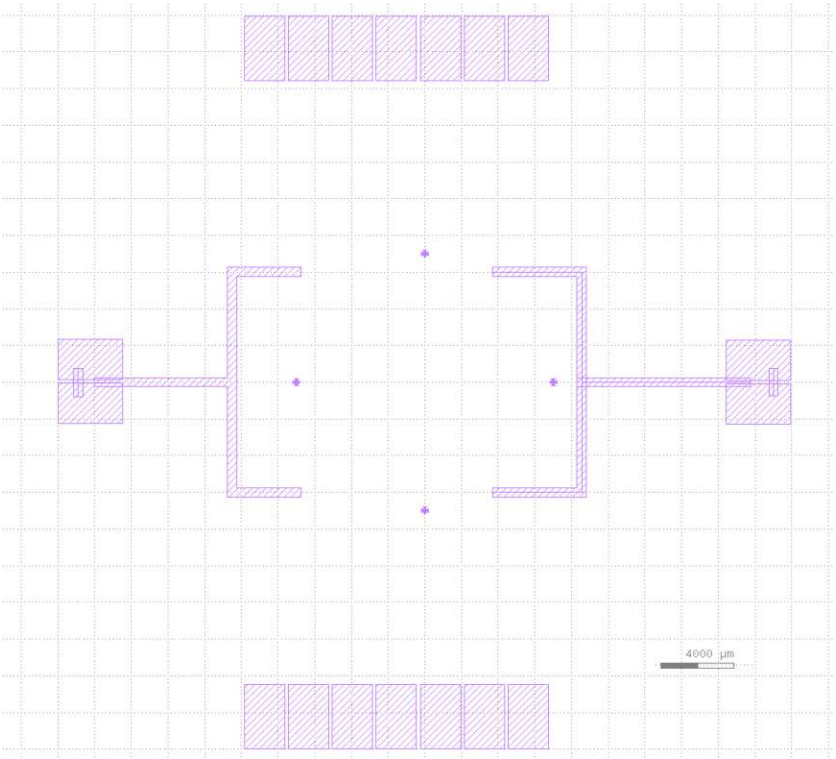

Figure 13 Covered isolating layer as a second layer of the chip, electrodes (Figure 7) are covered with an insulating layer

Figure 13 design is called *covered*, and as the name suggests, electrodes are fully covered (and space in between them) with an isolating layer. Theory suggests [17], that, unlike the design from *Figure 11*, only the electrical field will contribute to the electroporation in *Figure 13*. This is because electrodes are fully covered with an isolating layer, meaning, no current will be able to flow unless breakage of the isolating layer occurs. Alignment marks are the same as in *Figure 12* and both designs from *Figure 11* and *Figure 13* are utilized during *2.2.5 Etching* chapter.

With that, all the necessary design preparations before the fabrication process were finished. The exact process, steps, and results are found within the following *2.2 Chip* fabrication chapter and its corresponding subchapters.

2.2 Chip fabrication

Due to the microchip's small nature, the design was built at TU Wiens, E362 Institute for Solid State Electronics cleanroom. A cleanroom is a controlled environment that filters pollutants, like dust, airborne microbes, and aerosol particles to provide the cleanest area possible.

This fabrication process is called photolithography and has a wide range of industrial applications including microelectronics and micro-electro-mechanical components to thin film patterning for biosensors. The process utilizes ultraviolet (UV) light to expose complex geometric shapes and patterns (in this case microelectrodes, their connections, and pads) onto a light-sensitive photoresist coating and transfer them to the undelaying substrate. All the steps for IDE chip fabrication with their explanation and results are found in the following sub-chapters: *2.2.1 Spin coating*, *2.2.2 M*, *2.2.3 Sputter*, *2.2.4* , *2.2.5 Etching,* and *2.2.6 Microwell*. The spin coating process is the first step in lithography and involves spreading photoresist material uniformly onto, in this case, the glass substrate.

2.2.1 Spin coating

Before the fabrication process starts, the previously mentioned 49 by 49 mm glass substrates are submerged into acetone and then isopropanol. After the drying process, the substrate should be clean and as such it is covered with TI prime. TI prime is an adhesion promoter, increasing photoresist adhesion on substrates such as Si or glass [s7] (in this case, glass). To ensure the TI prime is spread equally, the spin coating method is used. Spin coating starts once the chip is placed into the machine, and secured (to avoid movement) via a vacuum pump.

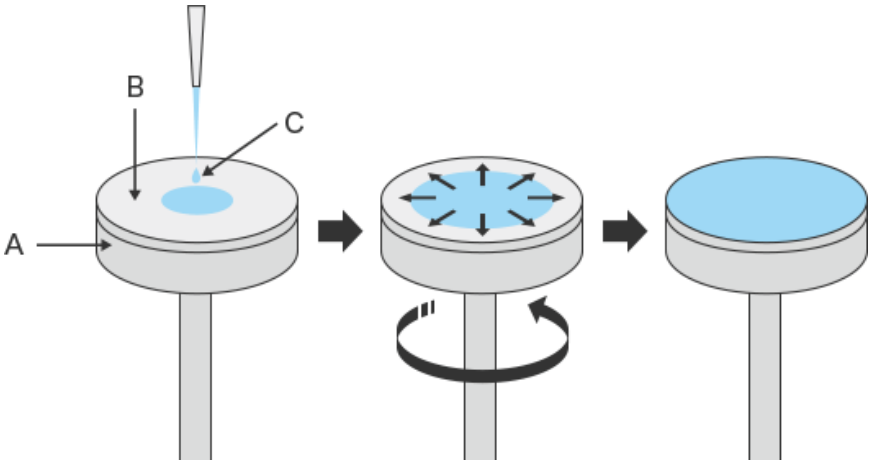

Figure 14 Spin coating process [s8]

Figure 14 demonstrates how spin coating is done. Where C represents TI prime (or photoresist), B is a substrate that wants to be covered (glass), and A is a vacuum pump, that keeps the substrate in place. Uniform coating of the chip is done by using the centrifugal force of rotation. The spin speed of 4000rpm for 60 seconds made sure that the TI prime was uniformly spread. After spin coating, the chip was baked, for 2 minutes at 120 ºC. After letting the chip cool down, it was covered with AZ5214E [s9] (Japanese Version). AZ5214E is a photoresist, a light-sensitive polymer that after being exposed to ultraviolet light, (depending on the method) turns into a soluble material. A photoresist is spread uniformly on the chip again using the spin-coating method (*Figure 14*). To get a photoresist layer height of 1.62 µm, the program with 3500 rotations per minute for 30 seconds was used. This process is again repeated later on in *2.2.5 Etching* as part of the second layer fabrication process.

After that chip is soft-baked for 60 seconds at 105 ºC, followed by UV exposure of the chip so that a pattern can be formed. The pattern is formed thanks to the mask which mimics the desired pattern and is placed between the chip and UV source. Mask fabrication is not a cost-effective process, and as such it is only performed with tried and tested chips. Thus, for the chip that is still in an experimental phase, maskless alignment (MLA) is used which is explained in the following *2.2.2 MLA* subchapter.

2.2.2 Maskless aligner

For a pattern to be formed on the spin-coated photoresist, a mask is used. A mask is an additional lit that is placed between the chip and the UV source. It is designed in such a way, that it mimics the desired pattern, letting the UV light pass on the photoresist only on the desired area. Depending on the type of photoresist used (positive or negative), the desired pattern will be formed by the photoresist. In the case of positive, only the desired pattern of photoresist after the development process will be left. In the case of negative photoresist, the desired pattern without photoresist (photoresist will be intact in the rest of the chip) will be formed after development.

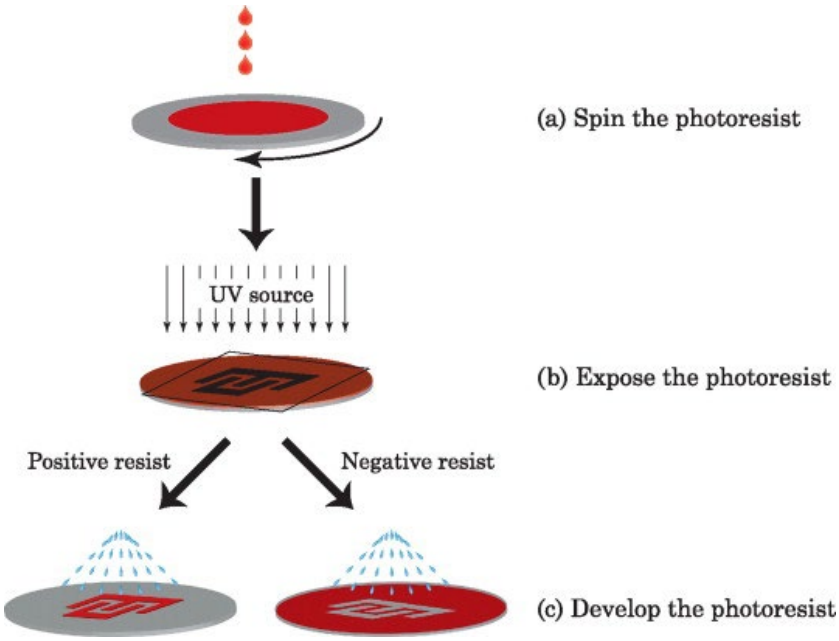

Figure 15 Positive and negative photoresist pattern fabrication [21]

Figure 15 demonstrates how positive and negative patterns are made through a mask onto the photoresist.

Since the chips' current experimental nature, this step was done without the mask. Mask production is an expensive process and it is only produced when it is certain that the chip will be produced on a larger scale. Due to that MLA 150 (Maskless aligner) device was used [24].

Figure 16 Image of Heidelberg Instruments MLA 150, used for maskless pattern formation as part of this thesis[s10]

MLA 150 uses a laser and the design from *Figure 7* to "print" a desired pattern on the photoresist-covered glass chip. After correctly aligning the chip, and selecting the correct exposure parameters desired pattern was drawn. Exposure parameters consist of dose and defocus. Dose is expressed in [mJ/cm^2] and determines the "strength" of the laser's light, while defocus defines where the focus (of laser) is done.

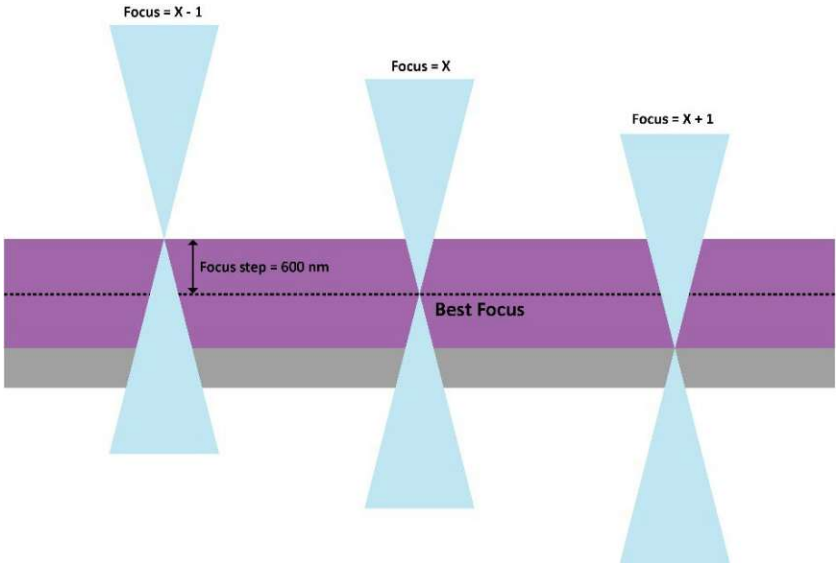

Figure 17 MLA 150 Defocus process [s11]

MLA150 can work in two modes depending on how the focus wants to be done. Optical where the correct focus, as the name suggested is done optically, and pneumatic mode which determines focus via changes in the pressure. Due to the transparent nature of the chip (glass) focusing was done in pneumatic mode. For the first layer, the negative resist process parameter was utilized, meaning following the adjusted datasheet [s12] dose of 40 mJ/cm^2 was used. A defocus of 0 was chosen experimentally (until the best pattern was formed). As a side note, MLA150 was used again later on in the process of second-layer fabrication, more about it can be read in chapter *2.2.5 Etching*.

After the chip was done printing, post-exposure bake at 120 ºC was done for 60 seconds, followed by UV exposure for 35 seconds without the mask (it was "supplemented" thanks to the MLA 150). After that chip was submerged into AZ 726 MIF[developer for about 70 seconds until the desired pattern was formed. AZ MIF developers are ultra-high purity tetramethyl-ammonium hydroxide designed to remove exposed areas of positive-tone resists and unexposed areas of negative-tone resists without leaving any residuals [s13]. Particularly, in this case, unexposed areas of negative-tone photoresist were developed away. The exact duration of development was determined experimentally until the desired results as visible in *Figure 18* and *Figure 19*. All the pictures of the electrodes were captured using a Nikon ECLIPSE LV 100ND [s14] microscope and program.

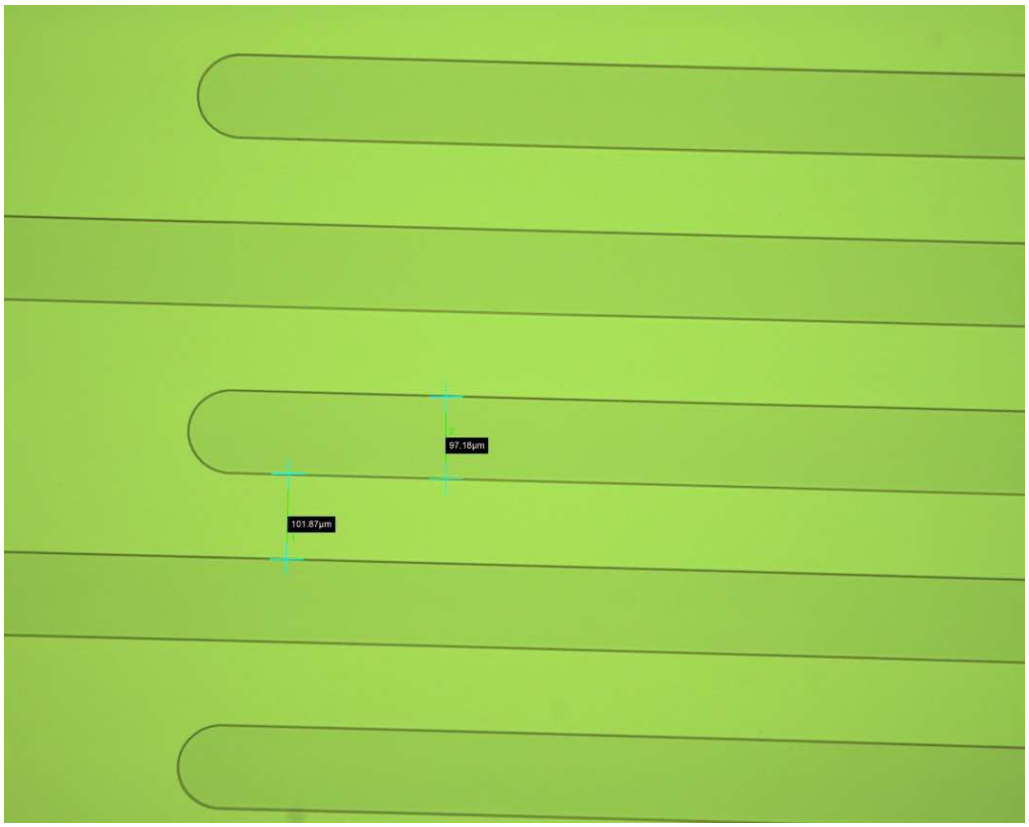

Figure 18 Subsection (760 by 950 µm) on developed electrodes as shown in the design of Figure 8

Observing *Figure* 18, it is determined that the desired result is achieved, where the cut between the future electrodes (one marked with 97.18 µm) and the surroundings (101.87 µm) is clear. At this point, only the border between future electrodes and the environment is observed. Photoresist, due to this layer (1.64 µm) borderline transparent, and contrast is hard to observe. Additionally compared with the design from *Figure 8,* the desired dimensions are achieved. Following that, additional observation can be done on the alignment mark, where *Figure 19*, besides visibly having a clean cut, dimensions are achieved as in *Figure 10*. Note that some deviation (for both *Figure 18* and *Figure 19*), is possibly caused due to measurement since it was done manually (optically).

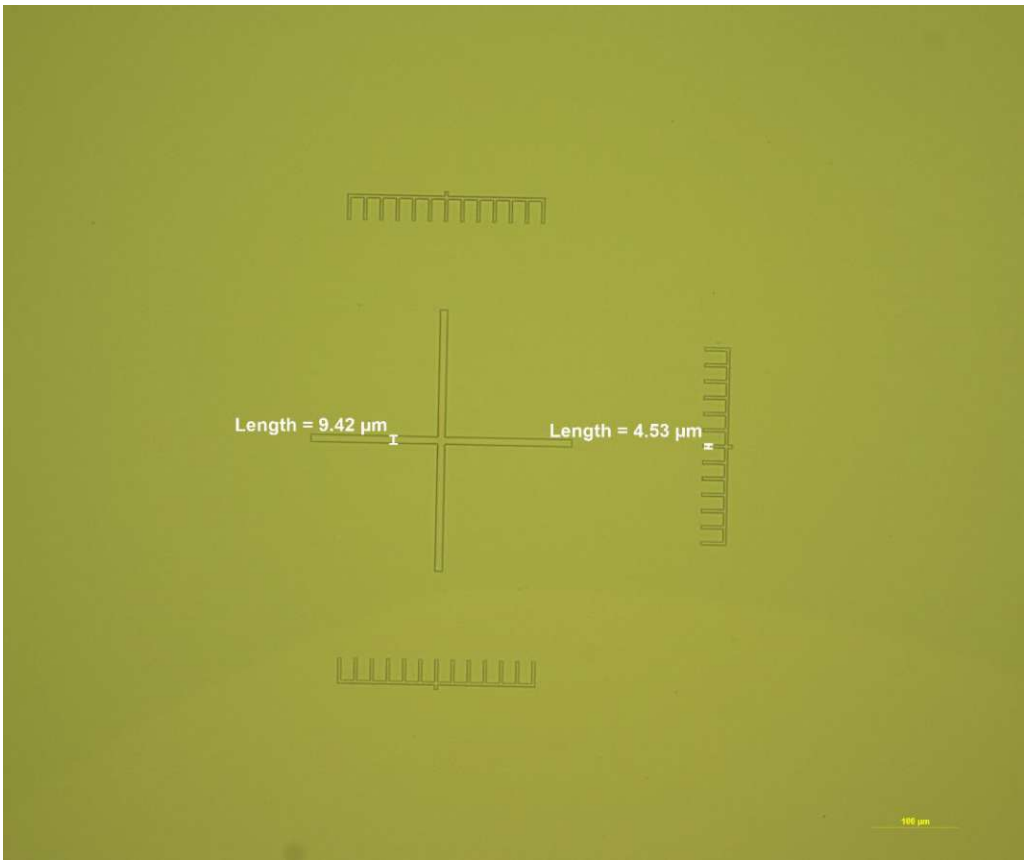

Figure 19 Developed alignment mark for the first layer as designed in Figure 10

Pattern height and spacing were determined using a dektakXT profilometer [s15]. This machine works on the principle that a very light and tiny needle is pressed and dragged against the chip, and thus height profile of the chip can be visualized.

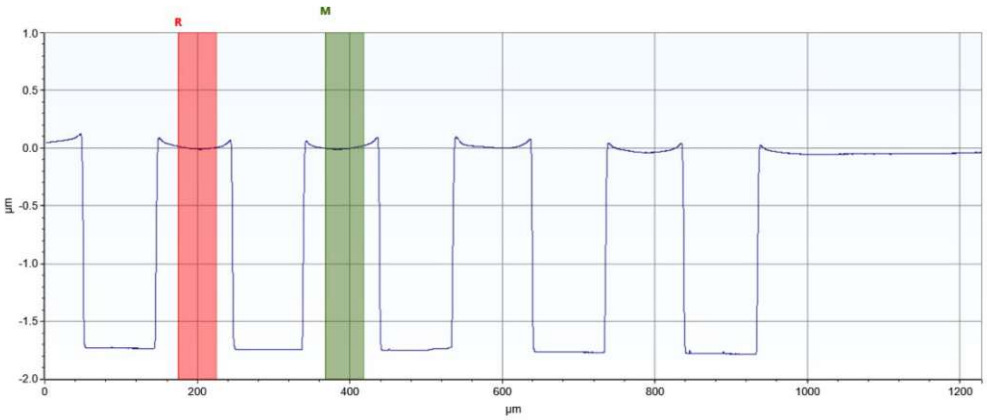

Figure 20 Height profile post-development

Data from *Figure 20* suggests that as chosen during the spin-coating process *Figure 14* difference in height profile is around 1.64 µm. Valleys represent the area that was exposed to the laser

during the MLA process, meaning that there is a lack of photoresist (only glass is left) since it was developed away, while peak represents an "unexposed" photoresist. These valleys represent future electrodes, and they will be filled with gold during a process called sputtering. Sputtering involves ejecting material from a "target" (in this case titanium and gold) onto a substrate (this case glass-covered photoresist with the desired pattern). More about sputtering can be found in the following chapter *2.2.3 Sputter deposition.*

2.2.3 Sputter deposition

In physics, sputtering is a phenomenon in which microscopic particles of a solid material are ejected from its surface after the material is itself bombarded by energetic particles of a plasma or gas. Particularly, for this chip fabrication, particles of gold and titanium were used, which were bombarded with argon ions.

After determining that the chips were well developed (*Figure 18* and *Figure 20*), they were put into the VonArdenne sputter machine.

Figure 21 VonArdenne machine used for sputtering deposition (gold and titanium)

Figure 21 depicts VonArdenne sputtering machine, from the TU Wien clean room, in which, after loading the chips into the machine's chambers, and securing the chamber door, a vacuum was created.

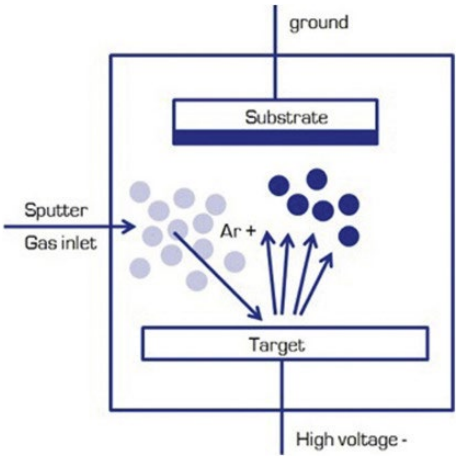

Figure 22 Principle of sputter deposition [22]

Argon is let into the chamber and as *Figure 22* shows, it is ionized. Using a strong electrical field (*1.3.1* Electrical Engineering 101) charged particles, in this case argon ions, are moved around following an electrical field gradient. In this particular case, they are moved onto target (gold or titanium) material. Ions are dragged (bombarded) with such a force, that they, using only physical process, create target vapor, which in turn is deposited on the substrate. Due to the fact that vapor is created using a physical process, this method is categorized as physical vapor deposition (PVD).

An initial run of titanium sputtering was performed on an unoccupied chip slot (100W, 60 seconds). This is performed so that the whole chamber is clean of any possible contamination. After that each chip was fully sputtered first by titanium (50 W, 60 seconds), and then gold (50W, 3x60 or 4x60 seconds). A very thin layer of titanium was used first since it adheres better than gold to the glass, followed by gold deposition. This sputtered gold represents future electrodes, and its sputter duration represents the height of said electrodes. Somewhat "unconventionally" long sputtering duration was used, so that a higher profile of the electrode is achieved. This is done so that electrodes become more "massive" without making them wider (to avoid obstruction for the light microscope). More massive electrodes are more resistant to any electrochemical processes or damage that could be caused by high voltage fields that are required for electroporation.

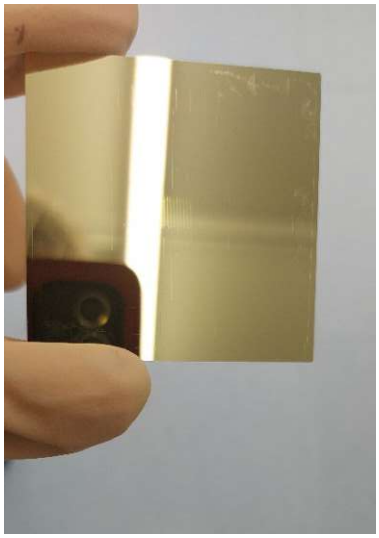

Figure 23 Chip after processing with the sputter deposition process

Figure 23 represents a chip as it is done with a sputtering process, and as it is visible, the chip is fully covered with gold. Electrodes and pads are barely recognizable, as they are slightly lower (for 1.64 µm, due to lack of height of photoresist in their place) situated than the rest of the chip. To remove access gold, chips are submerged into warm acetone (55 ºC, to avoid boiling) for an hour, where lift-off happens. Lift-off is a process, in which the remaining photoresist is dissolved, with it, removing all the gold and titanium layers that were sputtered onto it. Meanwhile, titanium and gold that were sputtered on the glass, remains thus forming microelectrodes, alignment marks, and connection pads.

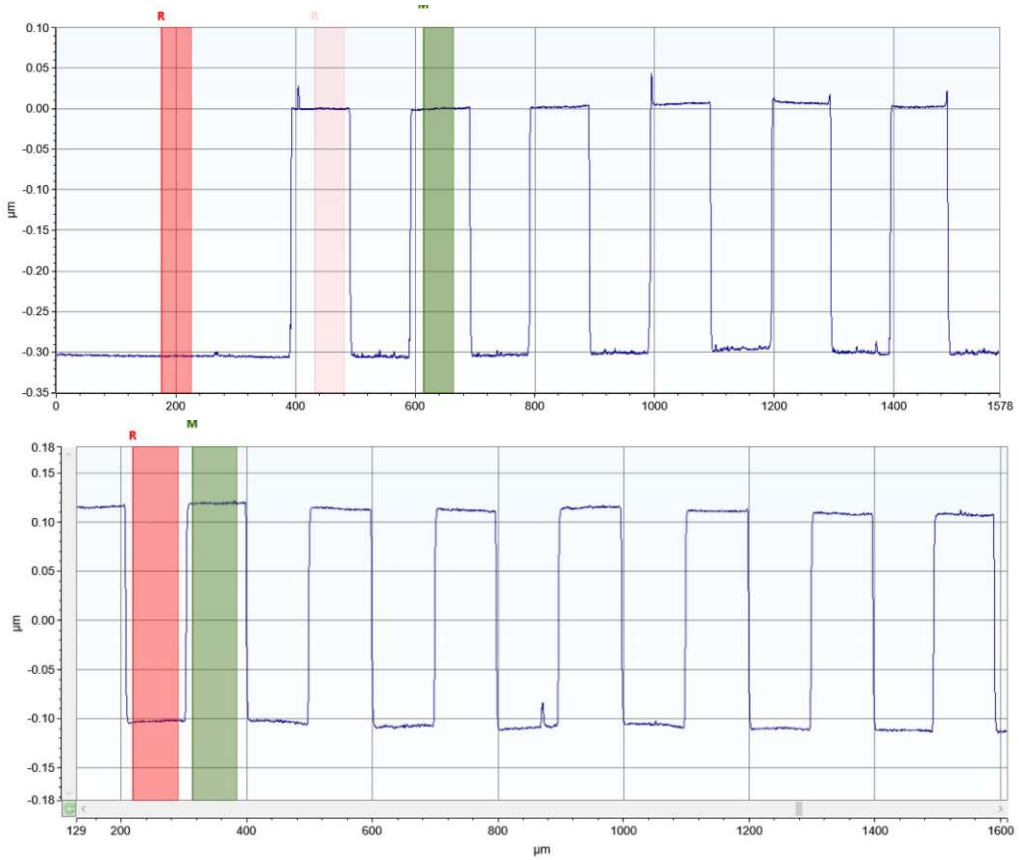

Figure 24 Hight profile of 3x60 s (top) and 4x 60 s (bottom) electrodes after lift-off

Observing *Figure 24* while comparing height differences between 3x60 and 4x60 seconds gold sputtered chips, and making an average of four measurements per height, it is determined that a deposition rate of 0.072 µm for gold and some 0.01 µm for titanium is achieved with used power of 50 W.

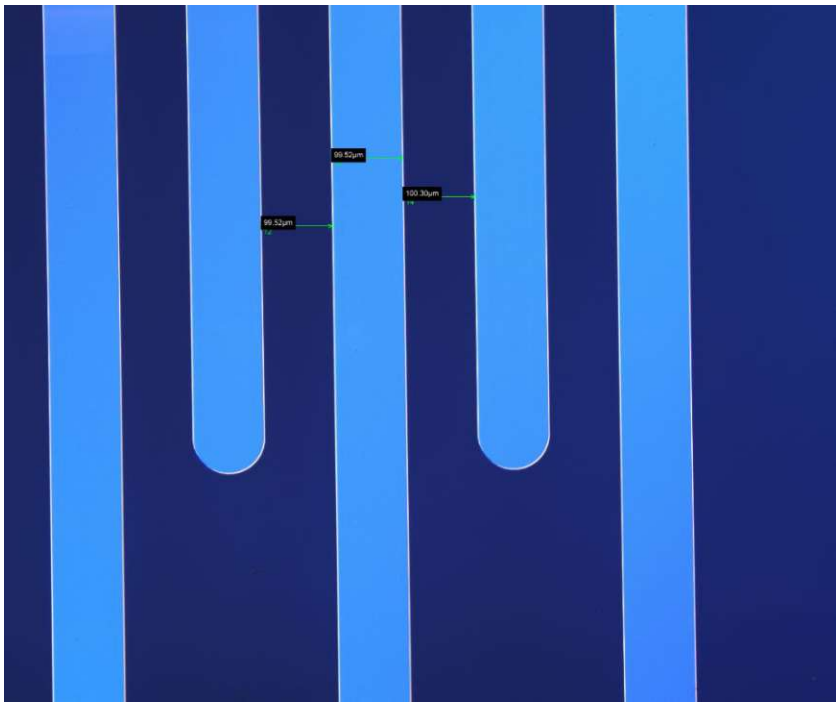

Figure 25 Subsection (1400 by 1200 µm) Gold electrodes with measures, bright blue being gold electrodes, dark blue, glass as designed in Figure 8

Finally, gold electrodes were checked under a microscope (*Figure 25*), to check for possible irregularities or damage. With this step, electrodes were successfully fabricated, but they are still missing the isolating layer as discussed in *2.1 Design*. As the first step of the fabrication for two types of isolating layers (*Figure 11* and *Figure 13*), the whole chip will be covered with an isolating layer, without forming any non-insulating patterns. This was achieved using plasma-enhanced chemical vapor deposition (PECVD) which is different from PVD in the way how deposition vapor is created. PCVD and alongside it, isolating layers are explored further in the following subchapter *2.2.4 PCVD*.

2.2.4 Plasma-enhanced chemical vapor deposition

In chapter *2. Microelectrodes*, it was mentioned that two types of electrodes were designed based on their isolation style (electrodes being fully covered, or just space between them). To build an isolating layer, a PlasmaPro 100 PECVD (Plasma-enhanced chemical vapor deposition) machine was used.

Figure 26 Oxford instruments PlasmaPro-100-PECVD machine used for insulation layer deposition, as part of thesis[s16]

Figure 26 depicts the PlasmaPro 100 PECVD system which is specifically designed to produce high-quality films with excellent uniformity and control of film properties such as refractive index, stress, electrical characteristics, and wet chemical etch rate [s16]. This is done by loading the chip into a chamber, and pumping the pressure down so that a clean environment can be achieved for deposition.

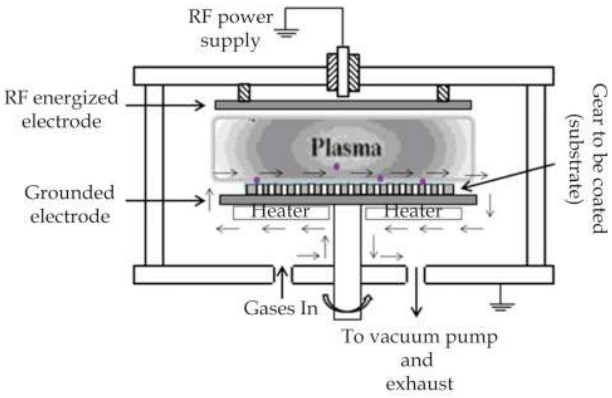

Figure 27 PECVD chamber used for insulation layer deposition [23]

Figure 27 demonstrates a PECVD chamber where a substrate is located, alongside targeted gas which is pumped into the chamber. The benefit of (the plasma-enhanced part of) PECVD is that lower temperatures are required as compared to the chemical vapor deposition to achieve a

reaction between a substrate (chip) and gas. This is achieved thanks to the plasma which is generated by energizing deposition gasses via a radio-frequency (RF) power supply. This new, energized, plasma state of gasses, reacts with the targeted substrate, which is how a PECVD machine covers the whole chip with a layer of SiN. SiN has low electrical conductivity, making it an electrical insulator. PECVD had a deposition rate of SiN of about 9.2 nm per minute so choosing a duration of treatment of 32 minutes, the height of about 295 nm is achieved. Since the whole surface of the chip was equally covered, dektakXT cannot detect any difference, when comparing before and after putting the insulating layer. This is because dektakXT only detects differences in height, and since the whole surface was covered equally, the lack of difference is rather proof of successful SiN deposition.

The difference is visible by the eye since once visibly golden electrodes are now reddish brown colored (copper-like). In the current state, the chip is just a block of a single isolating layer (since it is completely covered), making it virtually useless for any practical function. That means that the isolating layer needs to be etched (removed) in designated areas so that the chip can be functional again and so that correct second layer designs are fabricated (*Figure 11* and *Figure 13*). The process of achieving this is described in the following chapter *2.2.5 Etching*.

2.2.5 Etching

The goal of the etching process is the removal of the isolating layer in certain areas so that the patterns are formed and the chip can be functional again. As previously mentioned in chapter *2.2.1 Spin coating* chip is again covered by the same AZ 5214 E photoresist and spin-coated (*Figure 14*) so that an additional layer of 1.64 µm is built across the insulating layer. Using designs *Figure 11*, *Figure 13,* and MLA 150 (chapter *2.2.2 M*), the desired pattern was imprinted on the second layer of photoresist.

As mentioned in *2.1 Design*, alignment marks play a crucial role here, since the second layer needs to align perfectly with the first layer, otherwise, isolation (or non-isolation) will be found in an area of the chip, where it is not designed to be so. For the second layer, the positive mode of photoresist was used, meaning following the datasheet [s17], a dose of 120 mJ/cm^2 and defocus of 7 was used.

Without post-bake and flood exposure (since the positive process was done), the chip once again is submerged into AZ 726MIF developer for about 70 seconds. In this case, all the photoresists, marked with pink color in *Figure 11* and *Figure 13* should develop away leaving the isolating layer in this area exposed. To demonstrate that, a picture was taken on the borders of the naked design of electrodes (*Figure 11*) due to its greater difference in visibility (as compared with covered electrodes).

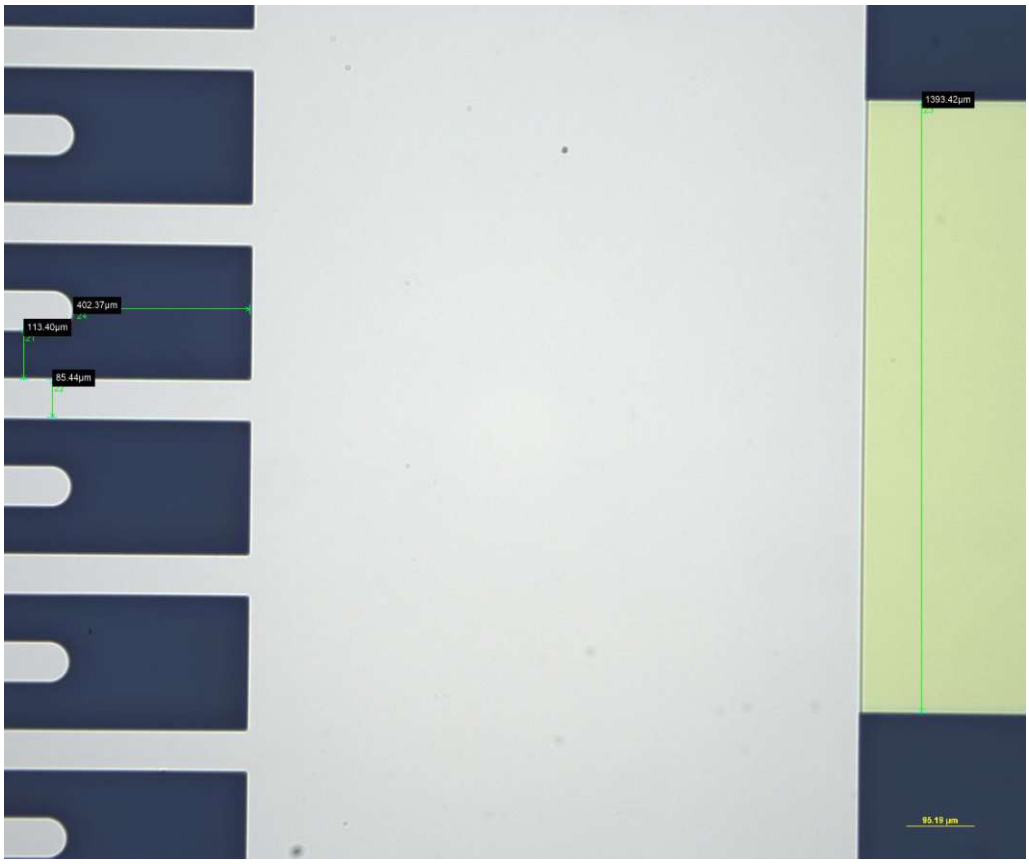

Figure 28 Post development of the second layer, a sharp border between the photoresist-covered connection line (yellow) and photoresist lacking electrodes (white) and semitransparent (glass-covered photoresist+SiN) blue background.

As visible from *Figure 28* and *Figure 29* observing coloring and clear borders, the photoresist was successfully developed away in an area that it was designed to do so (whiteish) compared to where it was not supposed to (yellowish area). Areas that are still covered by the photoresist are "protected" by the etching process since the device will etch away the photoresist, leaving the isolating layer untouched. Likewise, an area in which photoresists develop away leaves the isolating area unprotected, and as such, the isolating layer will get removed (etched).

Figure 29 Post development of second layer, pads(white) without photoresist, sharp border, connection line(yellow) covered with photoresist, and semitransparent (glass-covered photoresist+SiN) blue background.

In both designs, photoresists from pads were developed away, so that the isolating layer could be removed, and the electroporation device successfully connected to the chip. Using dektakXT, there is no clear difference between *Figure 20* and *Figure 30* since electrode height is negligible compared to the photoresist height.

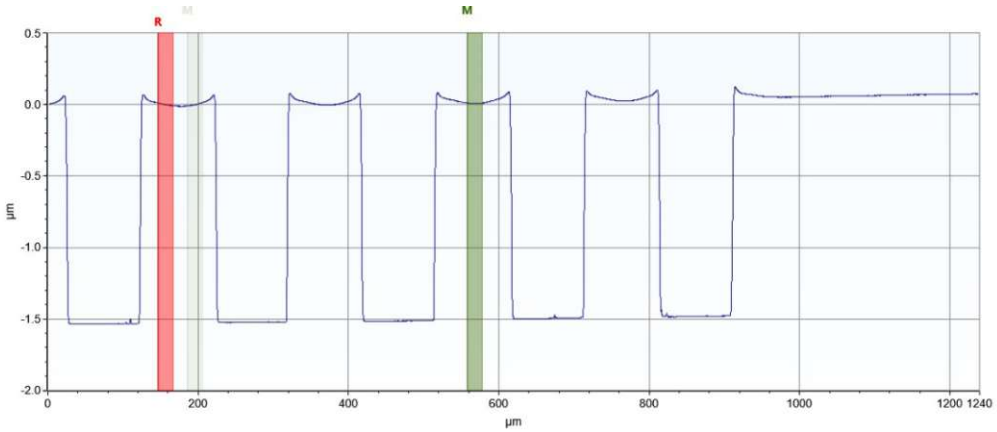

Figure 30 Height profile of the developed second layer, naked electrodes

Meanwhile, this difference is visible in the covered electrode design when comparing *Figure 20* and *Figure 31*. This is due to the design *Figure 13* where electrodes (this case 4x60 second) and

space between them are covered with an isolating layer equally leading to the difference of height of only electrodes themself. The sinus looks of *Figure 31* are achieved due to slow photoresist build-up on the sides of the isolation-covered electrodes.

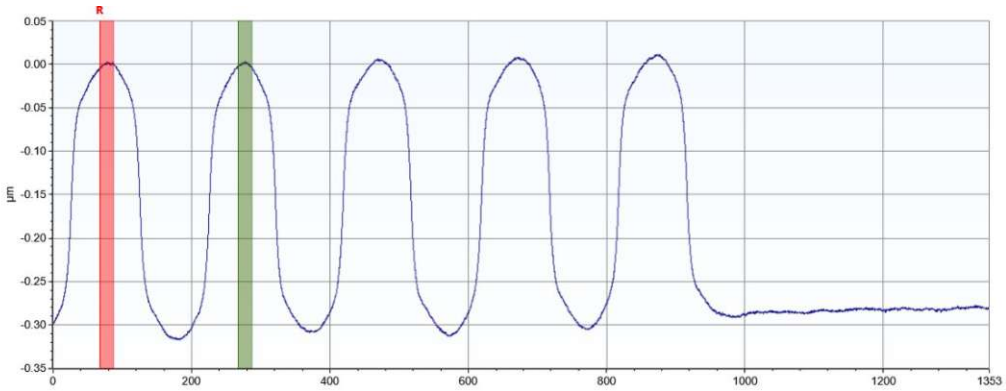

Figure 31 Height profile of developed second layer, covered electrodes

Etching was done using a ZMNS RIE-ICP machine and Sulphur Hexafluoride (SF6). RIE stands for reactive ion etching and works on a similar principle to the *2.2.3 Sputter* by employing strong electrical fields.

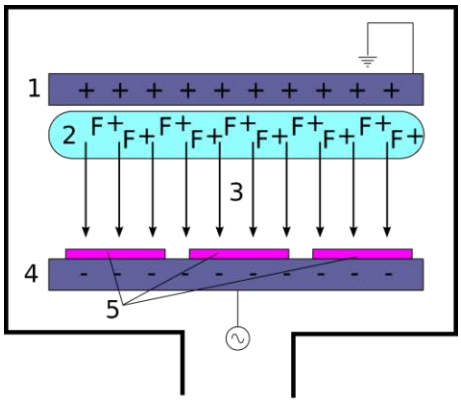

Figure 32 A diagram of a common RIE setup, with 1) and 4) being electrodes, 5) being a substrate, and 2) ions that are being accelerated by electrical field 3) [s18]

Figure 32 describes the working principle of a RIE setup, where a difference of potential between two electrodes "plates" (1 and 4 in *Figure 32*) creates high voltage, and with it electrical field (covered in *1.3.1 Electrical Engineering* 101). Plasma is created via an RF source by generating said electrical field which in turn accelerates ions toward the surface of a substrate (2 and 5 respectively in the *Figure 32*), which in turn chip away layers of the substrate.

Figure 33 ZMNS RIE-ICP (PlasmalabSysem100) used for insulation layer etching

Figure 33 depicts the ZMNS RIE-ICP system from the TU Wien cleanroom, in which the substrate was placed so that etching can commence. The duration of the etching process (5 minutes) was chosen so that in that time frame, the isolating layer is etched away, which in this case is 295 nm of the SiN. Since the photoresist is much thicker and not so reactive, it didn't get etched away.

Due to this chip was once again put into acetone so that the remaining photoresist could get dissolved. After each used ZMNS RIE-ICP needs to be cleaned using SF6 and oxygen gasses. With this step, the fabrication of the microelectrode is finished.

Measuring the height difference once again of covered microelectrodes after the etching, the sinus looks of *Figure 31* are gone and are replaced once again with a "pulsed" shape (with only height difference being the height of the electrodes themself).

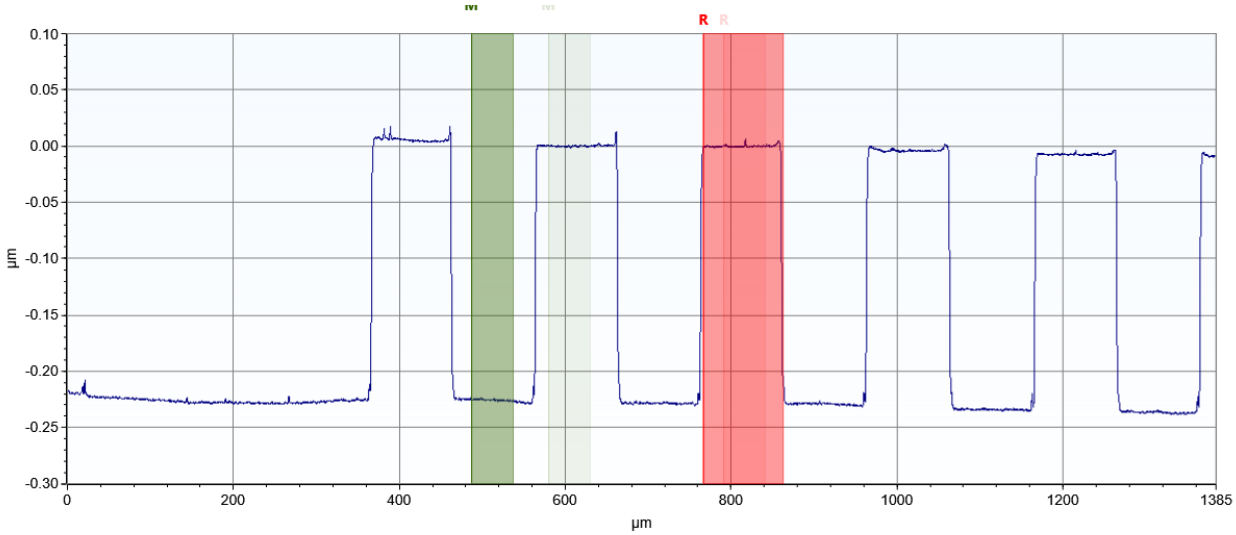

Figure 34 Height profile of covered electrodes (3x60), after etch

As for naked electrodes, there is only a height difference of about 0.07 µm due to gold electrodes (3x60) having height of about 0.230 µm and the isolating layer being 0.300 µm.

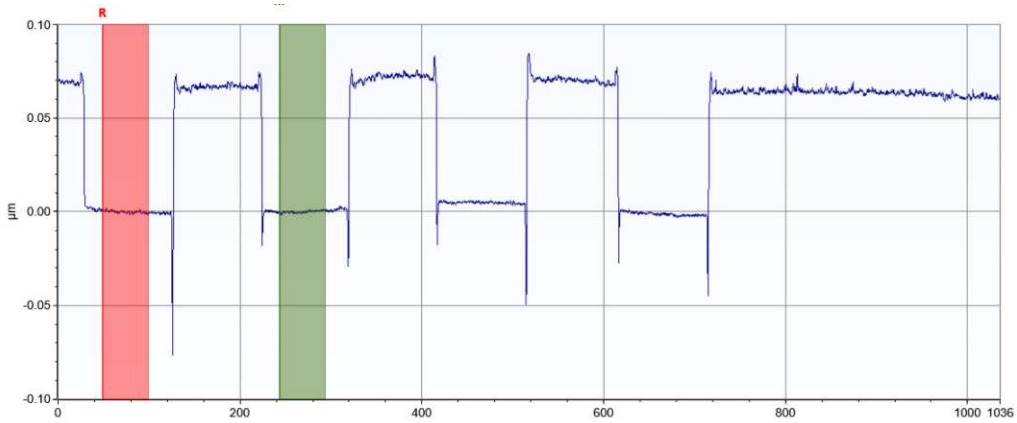

Figure 35 Height profile of naked electrodes (3x60), after etch

Observing electrodes (naked version *Figure 11*) under the microscope, there is still a clear difference between the area that is without layer (gold electrodes) and isolating connection leading to in (copper color).

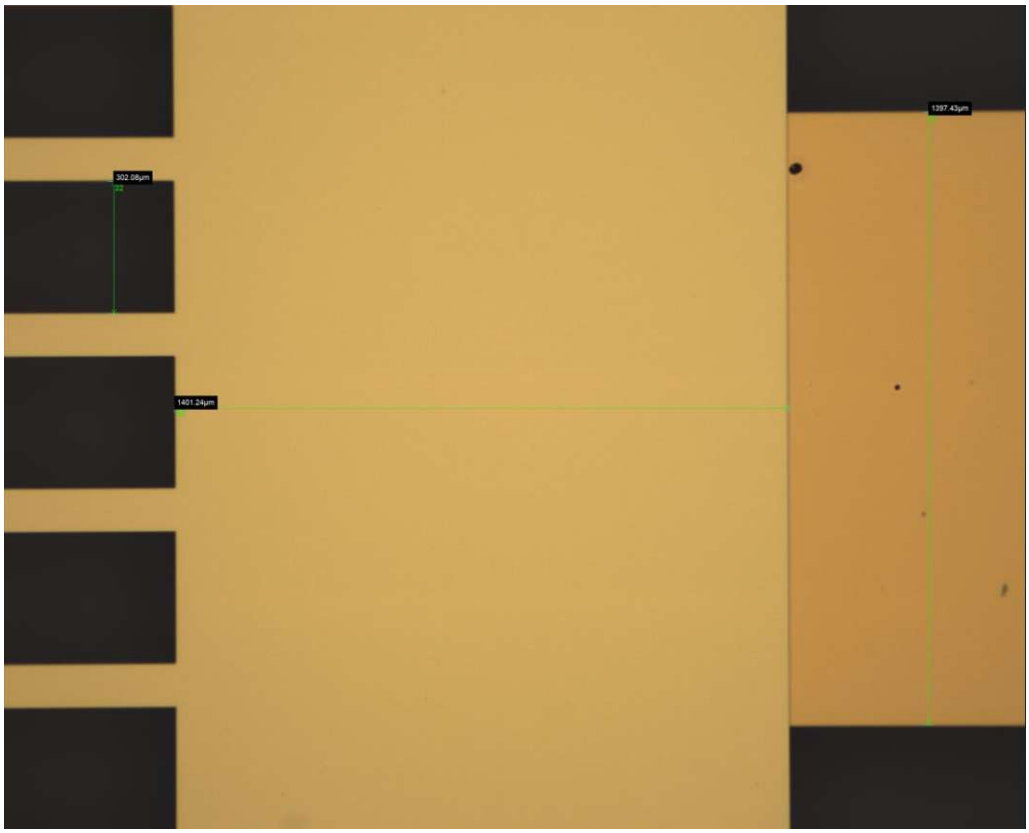

Figure 36 Sharp border between isolating (right), and non-isolating (left) parts of the chip alongside a "semi-transparent" glass background (2550 by 1900 µm picture)

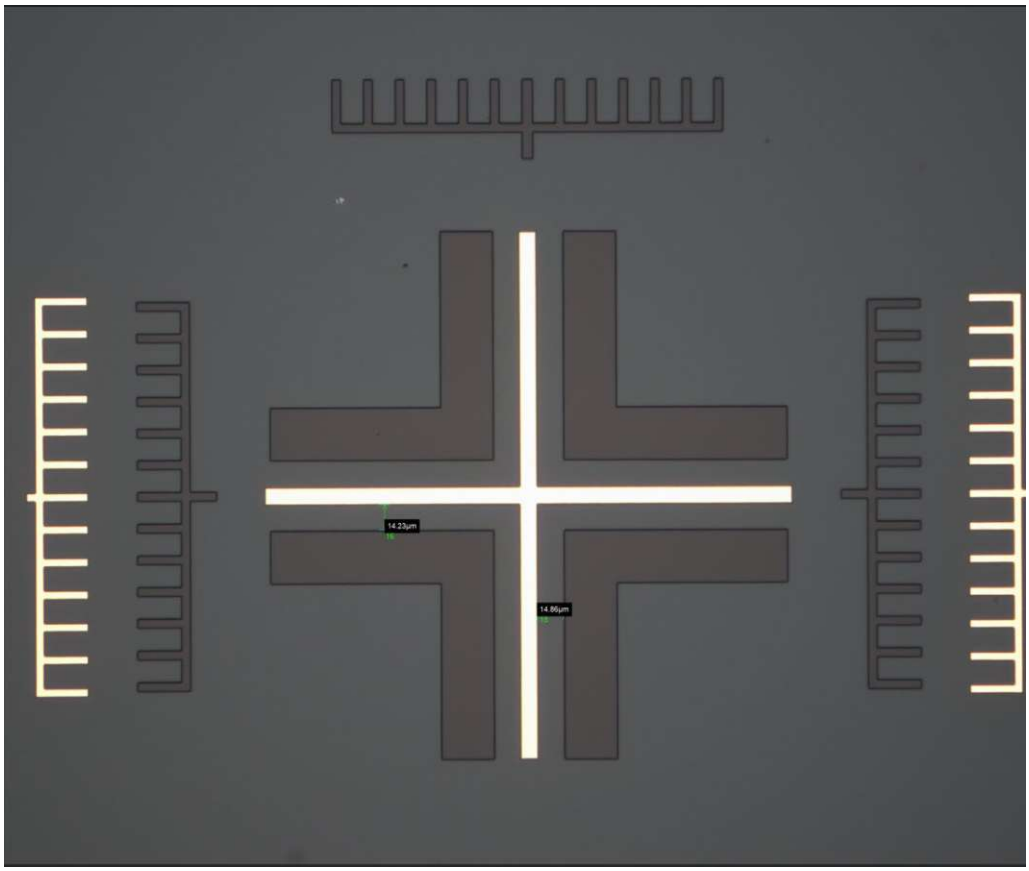

Figure 37 Alignment mark after etching, combining Figure 10 and Figure 12 alignment marks

Finally observing *Figure 37* (comparing with a combination of *Figure 10* and *Figure 12*) the alignment mark, it is clear that even finer parts (compared to electrodes) of the chip were well fabricated.

For the definite answer, if the isolating layer was successfully implemented, additional measurements were done using a Fluke 116 true RMS multimeter [s19], in short circuit detection mode.

Throughout this whole chapter (*2.2 Chip* fabrication), observing different figures (result) of electrodes via microscope, or dektakXT it is noticed that the thickness of layers is always continuous. Concluding it via numbers (dektakXT) or by observing the color intensity (microscope) of the structures. This is always a sign of a successful fabrication process.

While electrode fabrication was successfully finished, a well for the chip was still needed. Well is a small structure that is added on the top of electrodes, so that cells can be kept concentrated (atop of electrodes), and not spill around the chip. Fabrication of this part is described in the following chapter *2.2.6 Microwell*.

2.2.6 Microwell

Said microwell was built out of a block of custom-made PDMS (Polydimethylsiloxane) using a silicone base and curing agent in a mixed ratio of 10:1 (measured by the weight). After removing all air bubbles from the PDMS and baking it for 35 minutes at 120 ºC, a block of PDMS was removed from the mold and cut into 9 equal square pieces. In the middle of said square, circular holes were made, thus making a well. Said well was attached to the chip using O_2 plasma binding (etching).

Figure 38 Low-pressure plasma system V10-G, used for PDMS (microwell) and chip binding [s20]

Figure 38 shows plasma system used for microwell binding. Placing both chip types and microwell into a PINK V10-G etching machine (*Figure 38*) for 5 minutes at 200W and after that on top of each other, binding was successful. In addition, the final version chip was afterward placed on a hot plate for 20 minutes, at 100 ºC, securing the bond between the chip and the microwell.

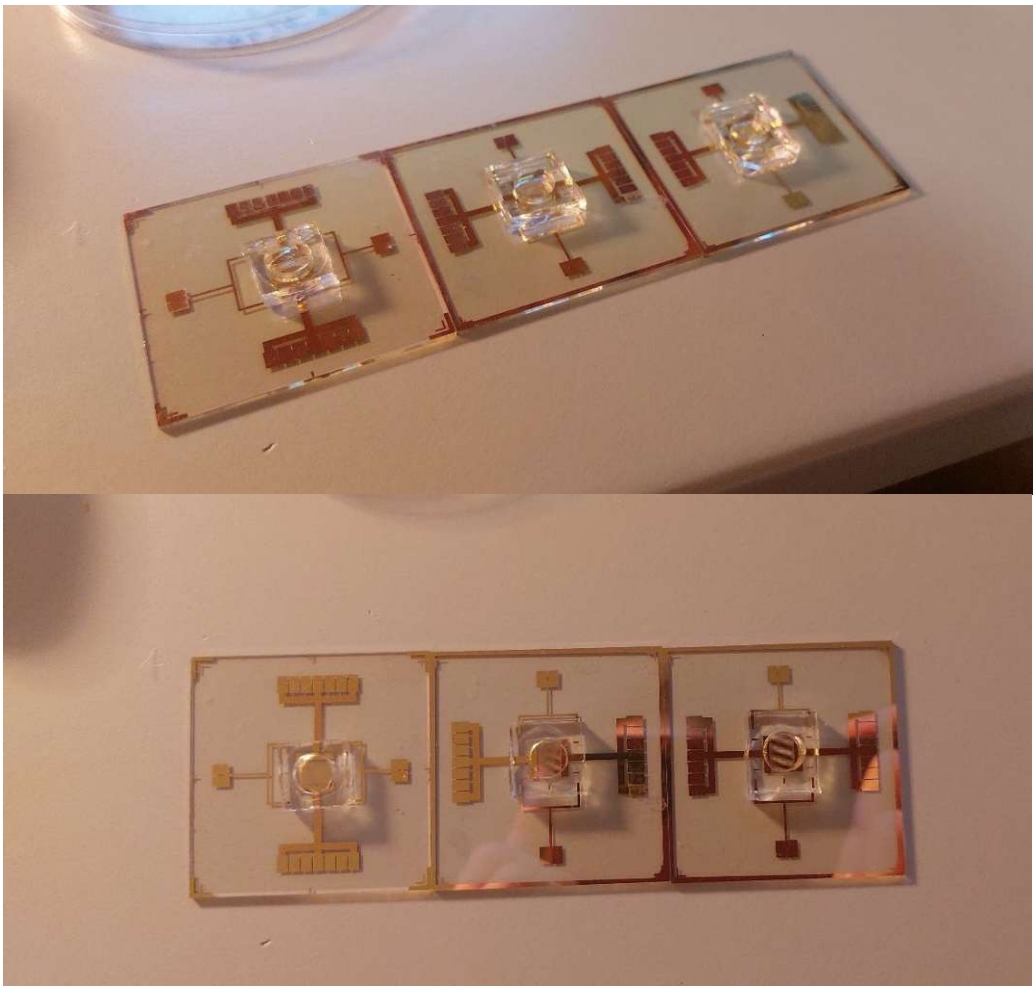

Figure 39 Final chip product, naked (left) and two covered (middle and right) electrodes from different angles

Figure 39 shows the final product of the chip fabrication process, with both types of electrodes (naked-left, middle, and right-covered) and their wells. PDMS well fabrication and binding process was the same for both types of electrodes. With that, the chip fabrication process is finished.

During the thesis work for the sake of speeding up the electroporation process, and out of fear of possible chip damage, 12 chips were fabricated.

Due to the small nature of the chip, a custom chip holder (*2.3 Chip holder*) was created which allows interfacing between microelectrodes (*2.* Microelectrodes) and "5R0ELA" electroporation device (*3. Electroporation device*). More about a self-fabricated chip holder can be learned in the following chapter.

2.3 Chip holder

The chip has a dimension of only 49 by 49 mm and has an even smaller electrical pad, being only 3.5 by 2.2 mm (*Figure 9*), it is somewhat difficult to connect the electroporation chip with the electroporation device. For that purpose, a custom chip holder was built that can keep the chip stable in a place while at the same time, providing an easy way to connect the electroporation device with the chip (or any other chip that has the same dimensions as other devices). The spacing of the pads for the chip (*Figure 9*) was chosen so that it complements proto-board hole spacing. Out of this thick plastic square, a 50 by 50 mm inner square was cut out, so that the chip could be inserted. On the sides of a square, two half circles are found which are used for easier insertion of the chips and as well as drainage, in case there is accidental cellular (or media) spillage. This structure was placed on top of 4 spacers to give the structure electrical insulation from the ground and to avoid scratching. The upper structure is made out of 2 parallel protoboards, which are screwed onto a metallic board covered with an insulating layer. On each protoboard, 15 pogo pins and 5 three-way wire sockets were soldered.

Figure 40 Spring containing pins called pogo pins, used as pins in self-fabricated chip holder [s21]

Figure 40 depicts pogo pins that are made out of gold (for good electrical conduction). Pogo pins differ from regular pins since they contain springs inside of them. This allows for the whole upper part of the chip holder structure to be lowered onto the chip, and screwed into place while providing good contact (compressing the spring part of a pin) between pins and pads, without

scratching the pads. Each of the soldered wire socket outputs corresponds to the one of pogo pins and allows a device to be easily connected to any pogo pin of choosing. This allows a lot of control over which pads are currently in use and easy switching between different pads. The connections between pogo pins and sockets are done with insulated wire but can be easily improved by designing and building a custom PCB board.

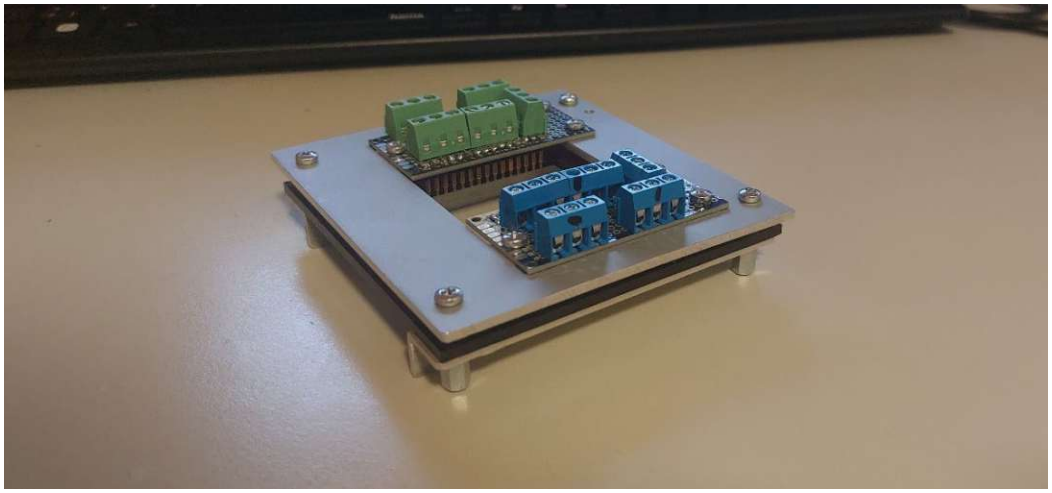

Figure 41 Custom pogo-pin chip holder

Figure 41 depicts the look of a custom-made chip holder, which is opened up by unscrewing the 4 corner screws visible in the figure. By opening the chip holder, a new chip can be inserted or an old one removed. The pogo pin setup was chosen over other solutions (like belts, or hinges) due to its simplicity, efficiency, and small size.

This chip holder was used during all the electroporation experiments.

While the microelectrode chip is an important part of the electroporation setup, the most important part is the "5R0ELA" custom electroporation device, which provides the signal for electroporation. Its fabrication, functionality, and user guide are described in the following chapter *3. Electroporation device*.

3. Electroporation device

As mentioned in *1.3 Electroporation*, to achieve electroporation, an electrical field is needed. Electroporation devices are widely available and functional, but they are somewhat pricey. According to Fisher Scientific [s22], prices for a capable device range from 10000 to 25000 Euros. And even then, since they are intended to work with a cuvette (due to electrodes being far apart), they can only output high voltages (from 10V to 3000V). Likewise, due to the huge size of the cuvette, more cells are needed, for each experiment. Thus, it was decided that a custom, cost-effective, electroporation device would be built, which produces an excitation signal, which in combination with IDE (2. Microelectrodes) creates an electrical field, which in turn causes reversible electroporation of tumor cells.

This custom electroporation device is named 5R0ELA. While it does not have (EU)2017/745 [s23] medical device certificates, all the safety rules were followed. These rules include two separated fuses, mains indicator and separation, an isolated h, battery system and a buffer.

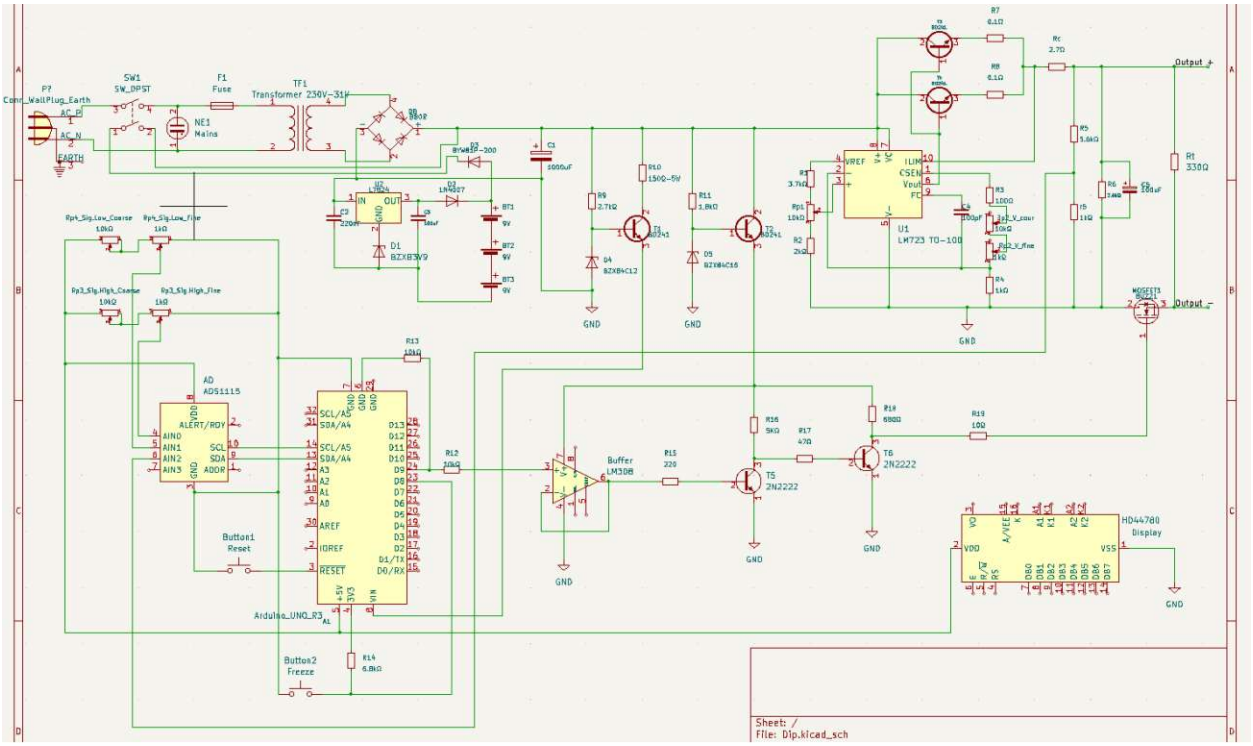

Figure 42 The Electrical schematic of 5R0ELAousing electroporation device

device depicts the electrical schematic of 5R0ELA, but due to its relatively big size, it is somewhat hard to read it. For that reason, another one is found in the *Appendix- Schematic*

(*Figure* 66) where it can be studied properly.

All of the pictures from the following chapter, that describe the working principle of the electroporation device, were captured using a Rigol DS1074ZPlus oscilloscope [40]. An oscilloscope is an instrument that graphically displays electrical signals and shows how those signals change over time.

The device was working under normal (expected) conditions, and all pictures were captured while the electroporation device was outputting the same signals (Square signal, DC, 1Hz, 10, 15, and 20 V amplitude, with a duration of a high state of 100 µs).

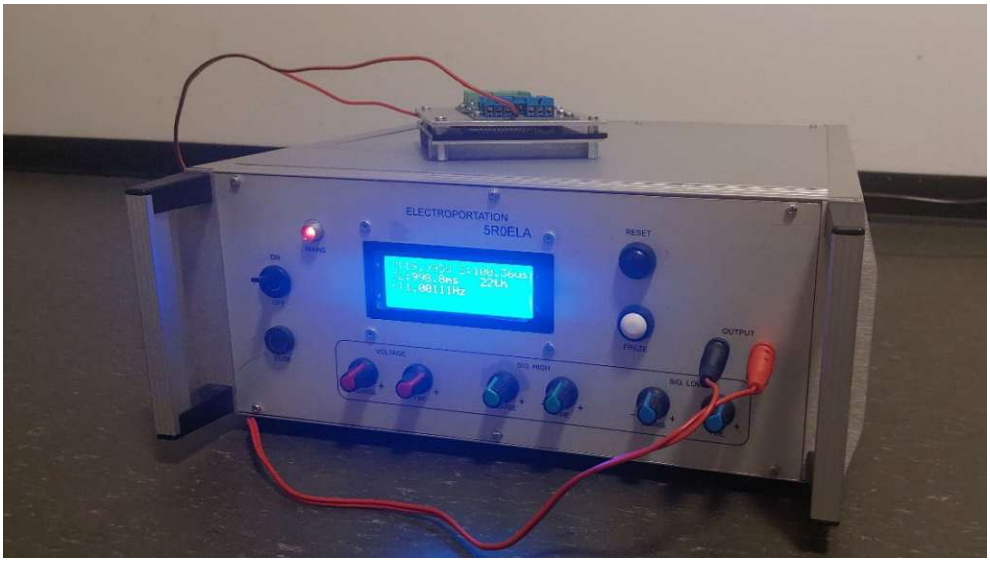

Figure 43 Interface(box) of 5R0ELA electroporation device with the 2.3 Chip holder on the top of it

Figure 43 depicts the front part of the 5R0ELA case. The box is made out of semi-hard aluminum which is hard anodized. Hard anodizing is a surface treatment process that provides corrosion resistance to the aluminum. At the same time, as an accidental byproduct of the process, aluminum is covered with an isolating layer. While it is a good isolator, due to its relatively thin layer it is not reliable as the only method of protection.

5R0ELAs interface consists of three pairs of color-coded knobs (potentiometers) that are used for setting signal parameters. The interface also includes an LCD, the mains indicator, an off-on switch, fuse access, a reset and freeze button, and wire sockets for output. A more detailed explanation of an interface can be found at the end of *3.1 Device design and function.*

3.1 Device design and function

Since 5R0ELA's main function is to provide a stable excitation signal, the voltage regulator is a central component of the device. The voltage regulator outputs stable, continuous voltage, no matter what voltage it receives at its input (as long as it follows the power class and the input voltage is higher than the output). Due to the experimental nature of the thesis, the adjustable voltage regulator LM723, TO-100 version [s25] was used. It can output between 2 and 37 V (in contrast to the common regulators which only output a single certain value) which, in combination with microelectrodes (equates to a field of 200V to 3700V/cm), is more than enough for reversible electroporation. As mentioned before, a voltage regulator needs to be supplied with a voltage equal to or higher (in addition to LM723 voltage drop of 2V) than what it outputs.
All the components with their names, abbreviations, and their position during the phase of explanation of 5R0ELA functionality, can be found in *Figure 65* or *Figure 41*.

The 5R0ELA system has two different ways of being powered-up options and each works independently. The first and that being the main one is supplied from the mains power grid (230V, 50Hz AC), which is, by using a transformer (TF1), transformed to 31V AC (effective).

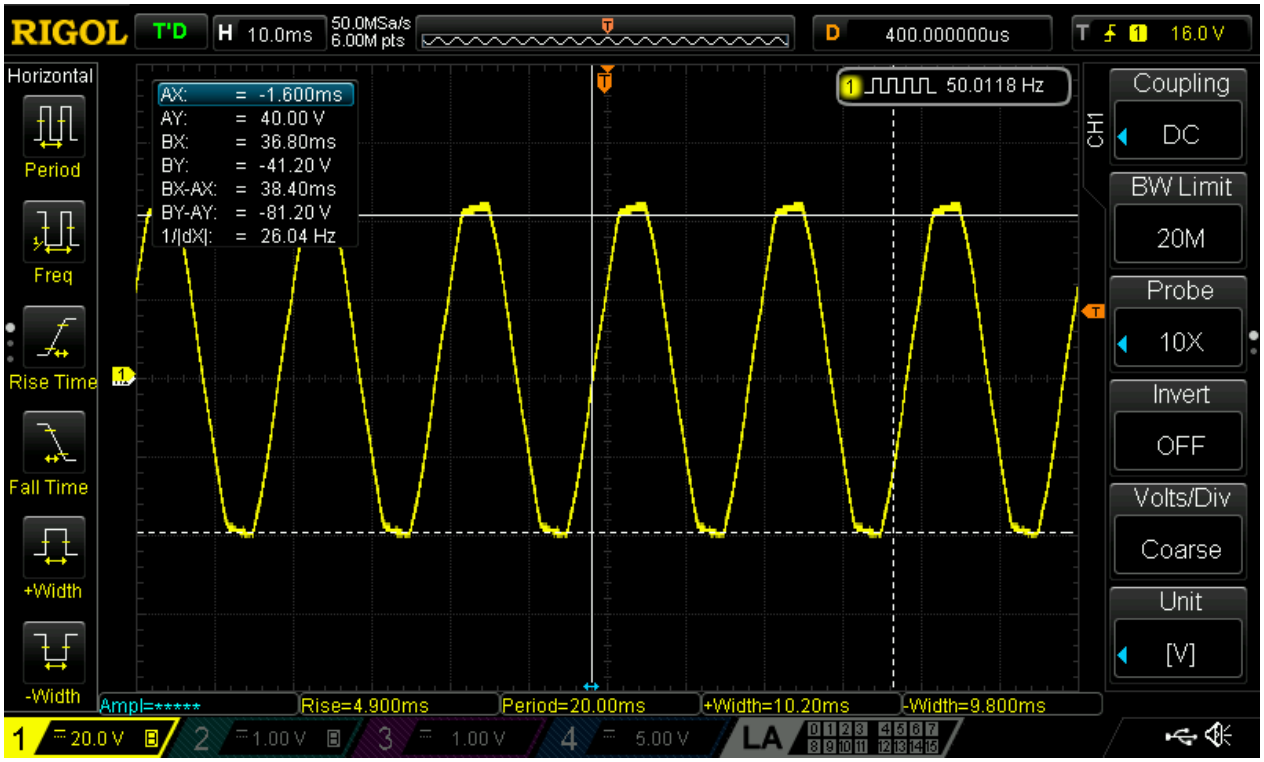

Figure 44 Sinuous signal on the secondary of the transformer

In *Figure 44*, a little yellow arrow, numbered with 1, represents zero volts. The yellow parallelogram (later on, blue one will be used as well) on the bottom left represents how many volts each square (division) on the oscilloscope represents (in *Figure 44,* 20V for each square following the Y axis). It is visible from *Figure 44* that a sinuous signal, with an effective value of circa 31V (peak circa 43 V) was generated. The little rectangle and the top left with white numbers indicate (in *Figure 44,* 10 ms, following X axis) how much time each square (division) represents. After that, the signal goes through the B80R full bridge rectifier [s26] (DB). The purpose of this component is to rectify the signal from AC to DC (it does not go below zero value again).

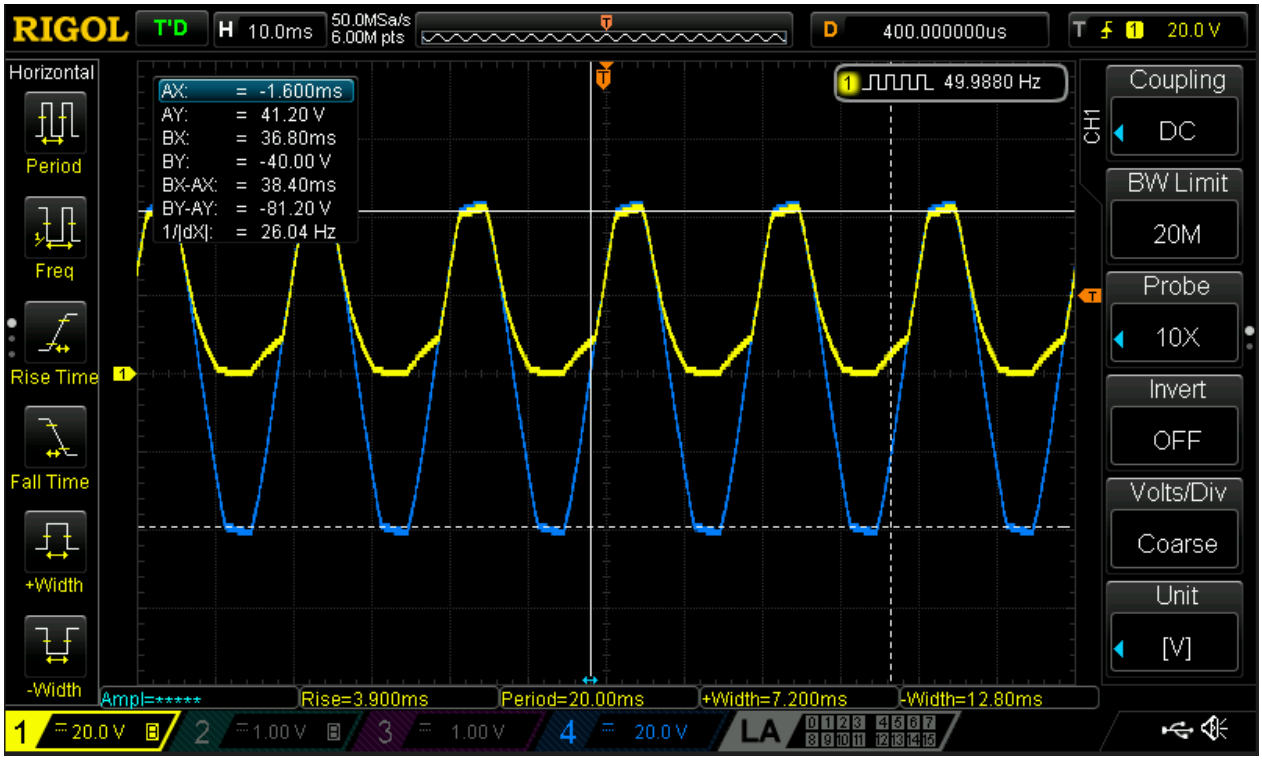

Figure 45 Signal being rectified (yellow) compared to non-rectified (blue) from Figure 44 as signals phase is preserved

In the case of *Figure 45*, for comparison's sake, the blue signal represents the signal before the rectifier, while yellow, is the new (rectified and 100% overlapping) signal of interest. While there is only a DC component present now, using a C1 (1000uF) capacitor, the signal (yellow from *Figure 45*) is being smoothed out to get a continuous voltage. The capacitor was chosen experimentally. If the too-small capacitor is selected, the signal will not be able to smooth out. While selecting too big a capacitor, would not harm the signal, but it is more expensive and take up more space.

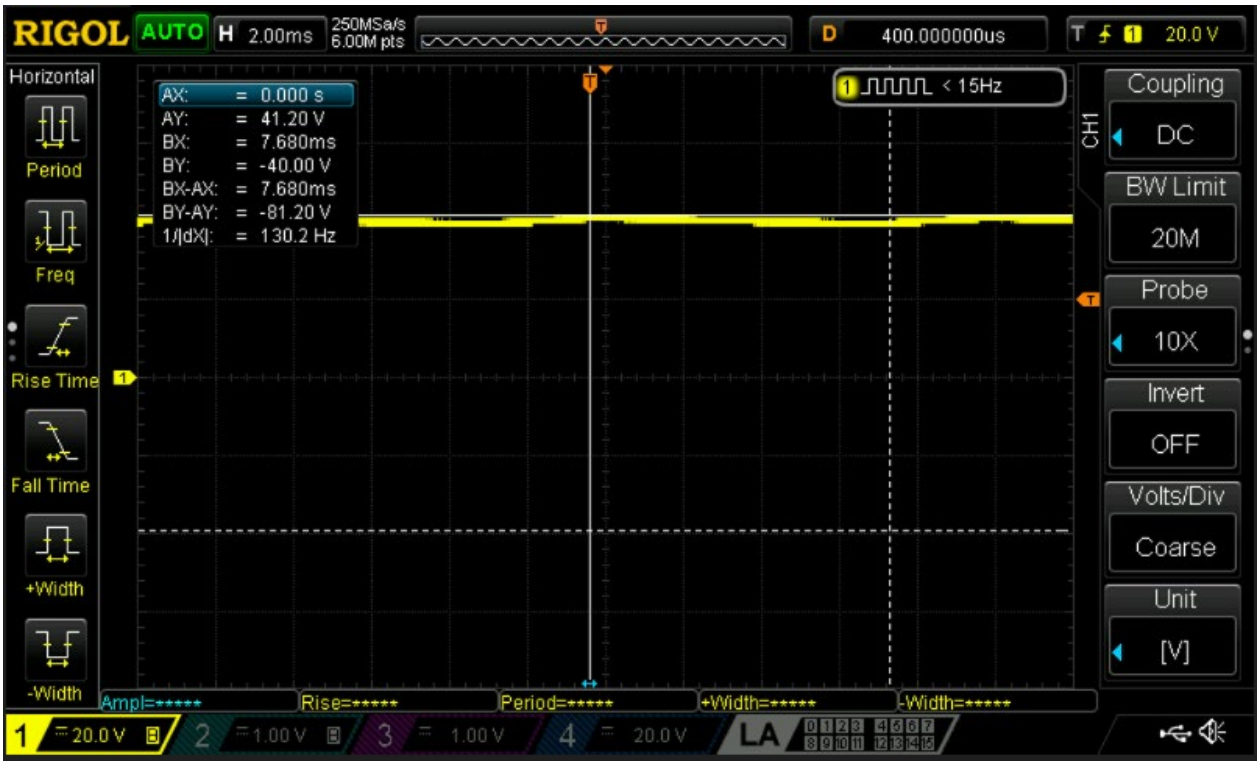

Figure 46 The Rectified signal (blue from Figure 45) becomes a continuous signal after the C1 capacitor

From *Figure 46* it is visible that a continuous signal (after the C1 capacitor) was successfully generated and this signal is being used to supply the LM723 voltage regulator (U1). For future reference, this point will be called a power line.

In case of sudden (or selectively) loss of power from mains, the device is undisrupted and seamlessly switches to a secondary power supply. The secondary system is powered by 3 sets of rechargeable 9V batteries (27V). This battery system consists of an LM7824 voltage regulator (U2) [s27] and two capacitors (C2 and C3) for stabilization with one BZX 3.9 V Zener diode (D1) [s28] connected between ground and U2 to artificially rise a ground level. In this mode, U1 will output 27.9 V (24V+3.9V=27.9V) in comparison to the common ground. On the output of U2, one 1N4007 diode (D2) [s29] is found to prevent backflow of current since this output is connected to the said three 9 V batteries (BT1, BT2, and BT3). At the same time, these three batteries are connected to the power line, just behind the output of DB, with only BYW81P-200 (D3) diode [s30] between them, to prevent the flow of current from the main power line toward the batteries. While 5R0ELA is being supplied by the main power grid, U2 is as well (via power line), and in turn, provides a constant voltage (27.9 V) with which batteries are being

automatically charged. If 5R0ELA is connected to the main power grid, and the power switch is on, the voltage of the power line will always be higher than three batteries, thus batteries do nothing in this case (and they are protected via D3). In case the power switch is on, but 5R0ELA is disconnected from the main power grid, the power line will be at 0 V meaning the rest of the device will be powered by the battery system (as it has a higher potential now). It was calculated and concluded that in the worst-case scenario, 5R0ELA can work for about an hour, before the battery system needs to be recharged again.

While working with the main power grid, it is always important to consider that it never actually provides 230V AC but rather it varies, up to some + 10% and as low as - 15% (253V and 196V respectively). This is due to the load of the main power grid. For example, at 3 am, when nobody is using electricity, the voltage will go up and there will be closer to 253V, compared to early evening, when everybody is back from work and cooking/watching TV, and more power is being consumed, it is closer to 196V. These values were considered while the device was being designed.
If the maximum aimed voltage that is being outputted from the U1 (LM723) regulator is 35V, losses of the regulator and rectifier have to be considered. This should amount to about 3V, thus at the very least 38V peak value has to be generated at the secondary winding of the transformer (in worst case - 196V out of the power grid). Calculating values for the transformer, effective values are used and they are obtained by dividing the peak value with the square root of 2. Meaning the transformer has, in the worst-case scenario output (at secondary) at very least 26 V AC. This is 85% of 31 V, and thus 31V secondary winding was chosen.

All components in the device were chosen so that they don't overheat/get damaged in case the device is used when the power grid is at 253V. The thermal image was taken using Fluke TiS55+ Thermal Camera [s31]. It was concluded that after 2 hours of continuous work, the 5R0ELA device, the maximal achieved temperature of certain components was 52 ºC. This is well below the critical temperature value for semiconductor technology (usually around 150 ºC).

For the sake of safety, there is a fuse before the transformer on the primary wiring. As well there is also a lamp (visible in *Figure 43* as mains) identifying whether a device is currently being

supplied by the power grid or battery system. A simple dual on/off switch (SW1) controls whether the device is powered up or down.

The continuous voltage that is outputted by LM723 is controlled by the two Rp2_V potentiometers (10 and 1 kΩ for course and fine and voltage changes, respectively). They are visible as two red knobs (the last two on the left) in *Figure 43*

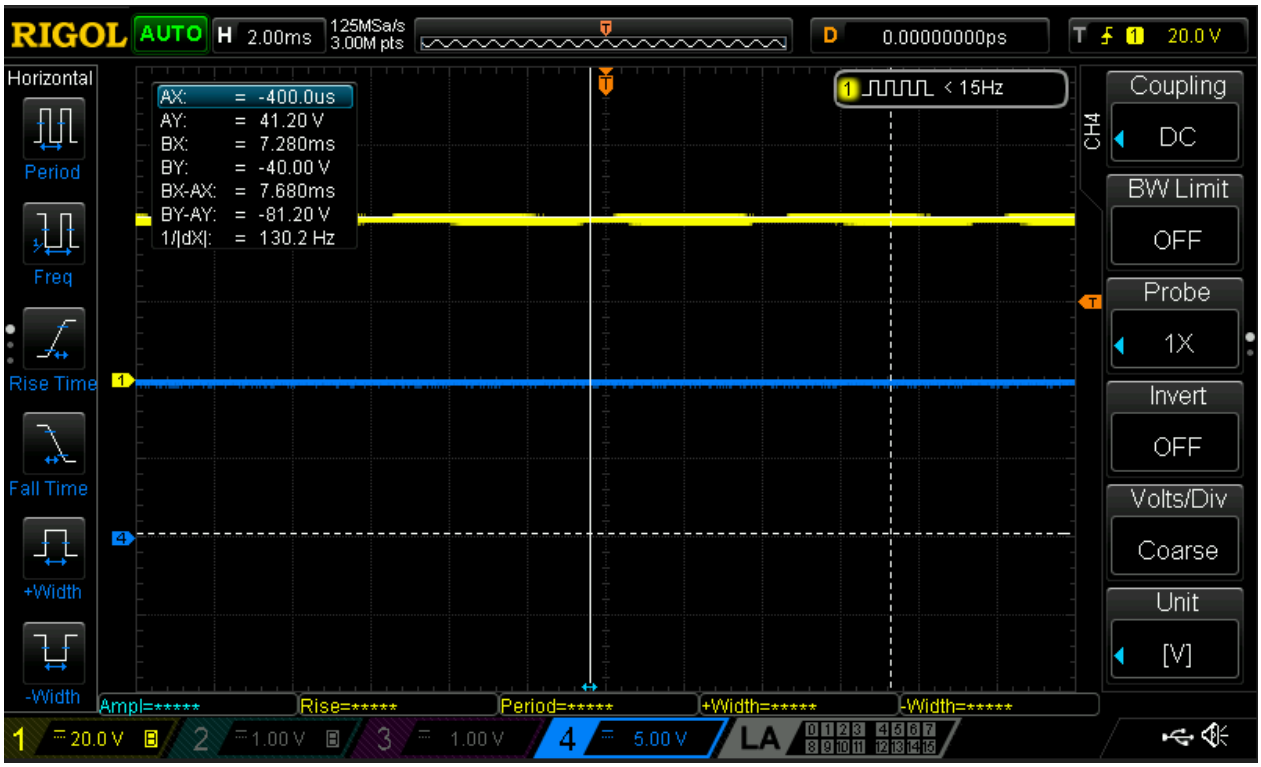

Figure 47 Continuous LM723 10V output signal (blue) compared to the 41V (yellow)input

Figure 47 depicts two signals, one the input of LM723, which in truth is a signal from *Figure 46*. The blue signal is the output LM723, and 10V was chosen by turning two Rp2_V potentiometers (for coursed and fine settings). Rp2_Vs were selected in relation to Rp1, which sets up the minimal voltage, that LM723 can output. This relation works in such a way that the maximal voltage that this device can output is 10 times the value of voltage that is found at Rp1 (minimal output voltage of LM723), which is 3 V.

As mentioned during the introduction of this chapter, all the signal figures were captured while producing 10V, DC, 1 Hz, with a duty cycle of 0.01%. From Figure 47 it is visible that a 10 V continuous signal, was successfully produced. Turning two (red) Vout knobs from the front of the device, any value from 3 to 33V can be selected.

Vout (pin 8) from LM723 controls the gates of two BD241 transistors (T3 and T4). Two transistors (instead of one) are used to spread the heat dissipation and they work in gain mode. Ri resistor is used to protect against "over current" (in case of a short circuit). With 2.7 Ohm current is limited to 0.3 A. In case it is surpassed, there will be a voltage drop at the Vout to compensate, and the current will be lowered.

As previously mentioned in *1.3 Electroporation* about electroporation, signals used are usually with small frequency and duty cycle. LM723 provides continuous voltage meaning there is no duty cycle or frequency to control. For this purpose, the ArduniUno [s32], a programmable microcontroller, is used. Using Arduino, square signals are produced.

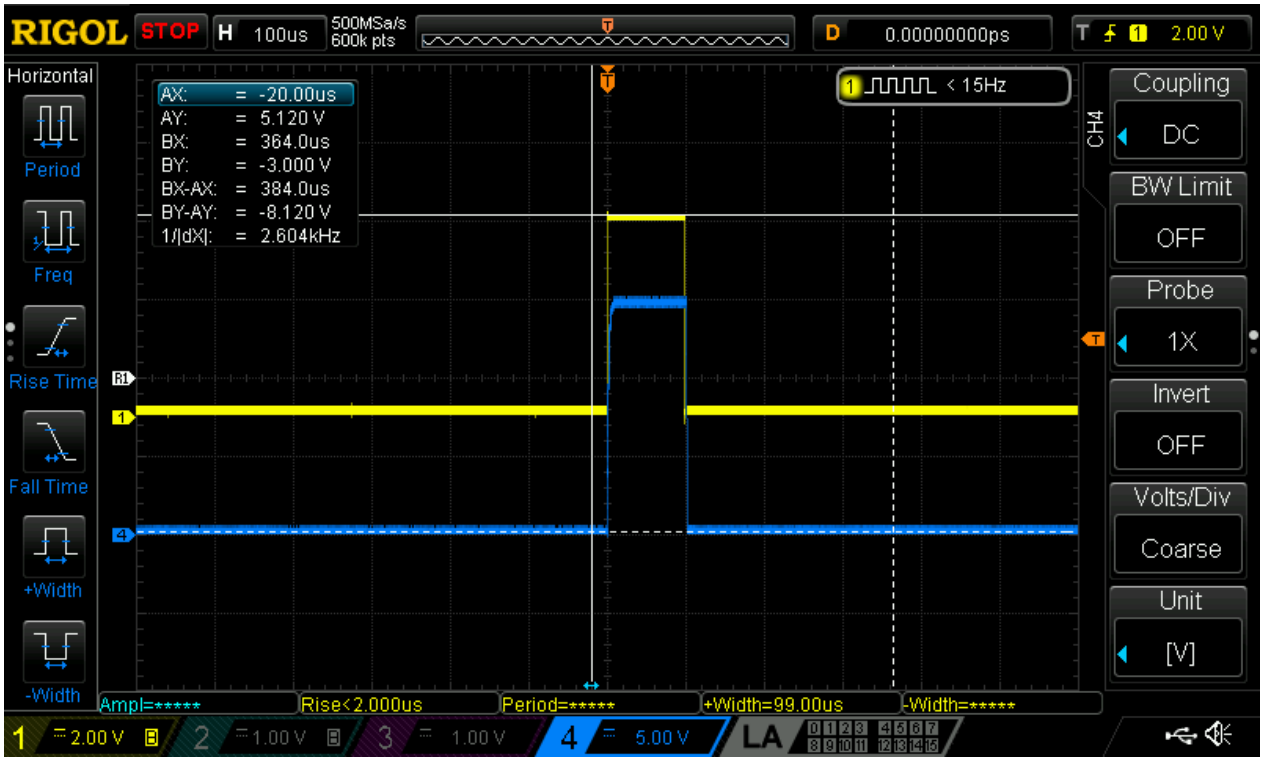

Figure 48 Arduino signal (yellow) and BUZ21 drive (blue)

As visible from *Figure 48* highly accurate (timing-wise, in this case 100 µs) signal (5V yellow) can be produced. Using two pairs of Rp3, Rp4 (blue and green knobs, middle and rightmost on the front of the device *Figure 43*), and ADS1115 16-bit [s33] analog-digital converters, the duty cycle (duration of signal in 5V) and frequency of the Arduino signal are controlled (both of them have fine and coarse adjustment).

Arduino operates an LCD (liquid crystal display) [s34] where current voltage, frequency, signal number, and duration of high and low states are displayed. LCD is found at the front end of the device (*Figure 43*).

At the input pins, Arduino can receive a maximum of 5 V without causing any damage to it. Thus, information about current voltage output is received from the R5 and r5 voltage divider (and ADS). Values of them were chosen in such a way that the maximal output (33V) measures 5V at Arduino.

Usually, Arduino is powered by 9V via a USB cable from a PC. To avoid unnecessary wires and bulk caused by PC, a voltage regulator is needed that will power Arduino. The same power that is powering LM723 (*Figure 46*) is used to power Arduino. Sadly, there are no regulators that can change 35 V to 12 V (Arduino can operate to up to 12 V without heating up) without getting damaged over prolonged use. Thus, a custom voltage regulator was built using a 12V Zener diode (D3) and BD241 transistor (T1)[s35]. This should provide 11.5 V (some 0.5V loss due to the operation of a transistor) to Arduino pin 8 (Vin).

LCD is via an I2C adapter (to avoid unnecessary wiring) connected to the Arduino. Like LCDs, ADS1115 SCL and SDA are connected to the Arduino pins 14 and 13. Inputs 0,1 and 2 from ADS collect data about, low-high state (their durations), and voltage status (respectively) for the main output signal.

Visible on the front of the device are two buttons, named reset and freeze (colored black and white). The purpose of the reset button is to reset the whole system and the freeze button is to stop the functionality of the Arduino (no outputs) until it is pressed again. To avoid an accidental restart, a 5-second delay between freezing and de-freezing was added. Reset and freeze buttons are connected to the pins 3 and 8 of Arduino.

Square signal, generated by Arduino with the attributes assigned by pairs of Rp2, Rp3, and Rp4 is outputted at pin 9. All of the explained functions were written with custom C code and can be found at the end of this thesis via *Appendix-Code*. The whole code is explained via comments.

The output signal (after R10) goes through the LM308 [s36] buffer (op-amplifier that has an amplification of 1) whose purpose is to protect Arduino from feedback signals and keep the integrity of the control signal. The signal was attenuated so that it could be used as a base signal in 2N2222 [s37] signal transistors. Signal transistors are very fast and precise but sadly cannot handle high-value signals. Thus, later on, BUZ21 [s36] MOSFET was used, where its gate is driven by T5 and T6 2N2222 transistors. The purpose of the dual signal transistors is to "amplify" the initial 5V output (Arduino can only provide a fixed 5V) signal from Arduino as 5V is not enough to drive BUZ21. The signal is double negated via T5 and T6 and amplified via a similar custom-made (D5+T2) voltage regulator that is supplying Arduino (in this case it outputs 15V). The reason for using two separated voltage regulators is due to heat dissipation, as otherwise they would overheat.

15 V signal drives (blue signal *Figure 48*) the gate of the BUZ21 in the "rhythm" of the signal provided by Arduino. The source of the BUZ21 is connected to the output of the LM723, and the drain is connected to the ground. Thus, only when BUZ21 is driven, the circuit, connecting LM723 with the output and ground is closed.

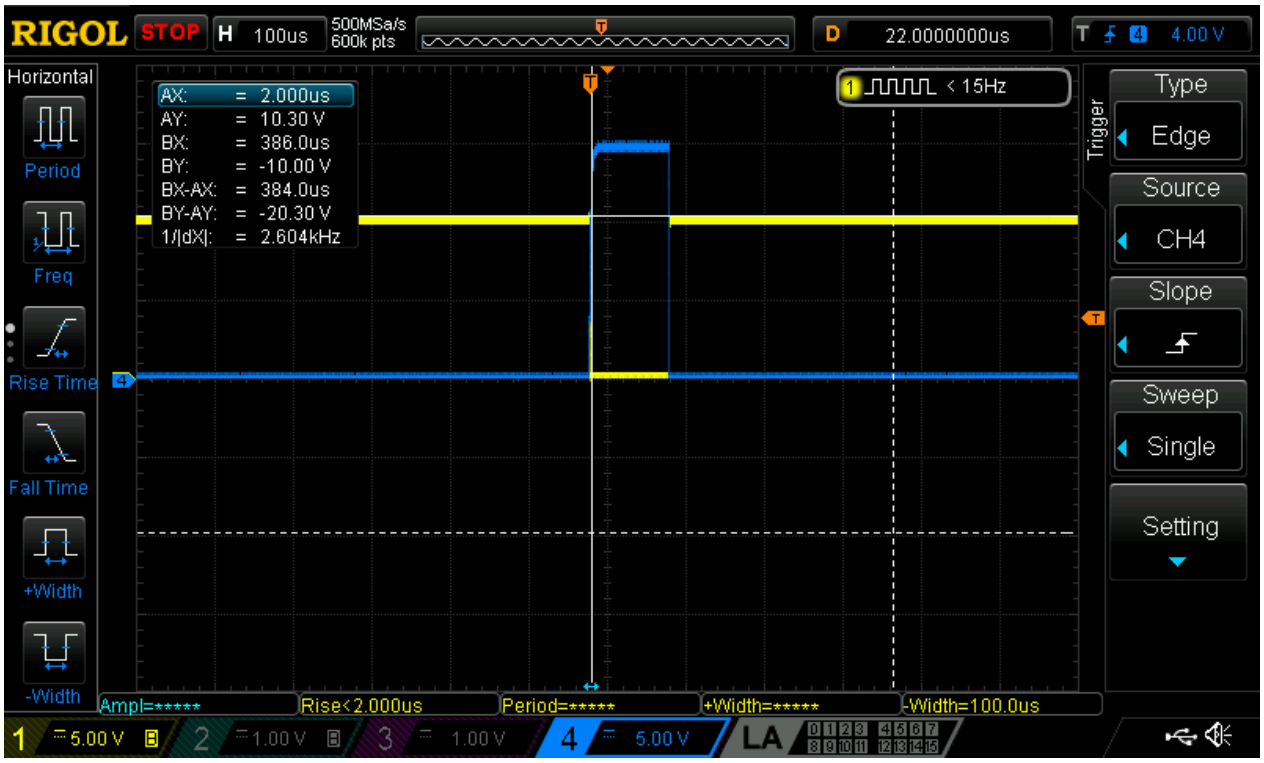

Figure 49 BUZ21 drive (blue) and voltage drop of LM723 (yellow)

As visible from *Figure 49*, the moment BUZ21 is driven (blue), there is a voltage drop (10 V) on the output of LM723 (yellow). This happens due to the circuit being closed (connected to the ground) via the main output of the device, which provides electroporation to the chip. The main output of the device (black and red circles on the front of the device *Figure 43*) is connected in parallel between the output of the LM723 and the source of BUZ21.

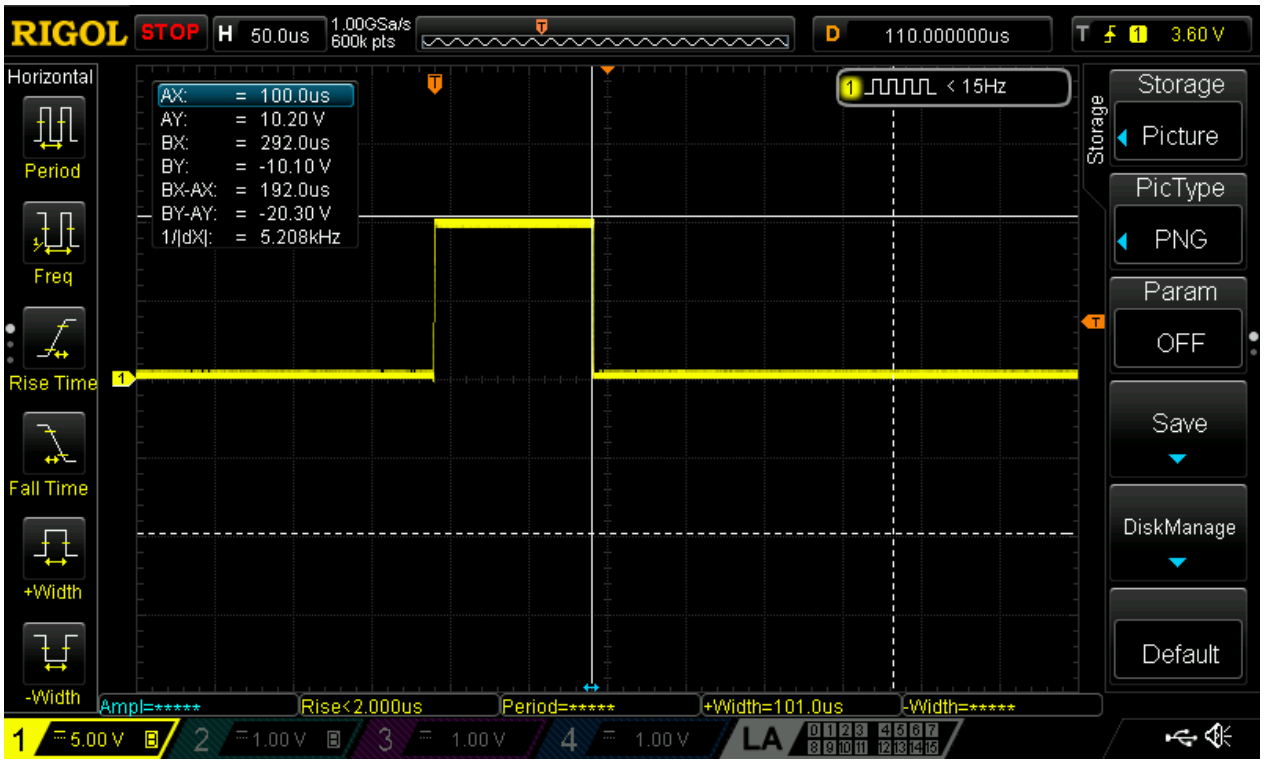

Figure 50 Electroporating signal at the main output used for the electroporation

Figure 50 provides, s promised at the beginning of the chapter, a square 10V signal with a frequency of 1 Hz and duty cycle of 0.01% (100µs) was generated at the output of 5R0ELA. Due to the extremely short nature of the high state in comparison to the rest of the signal, it is somewhat hard to capture the true nature of the signal via an oscilloscope. An attempt at it was made in *Figure 51.*

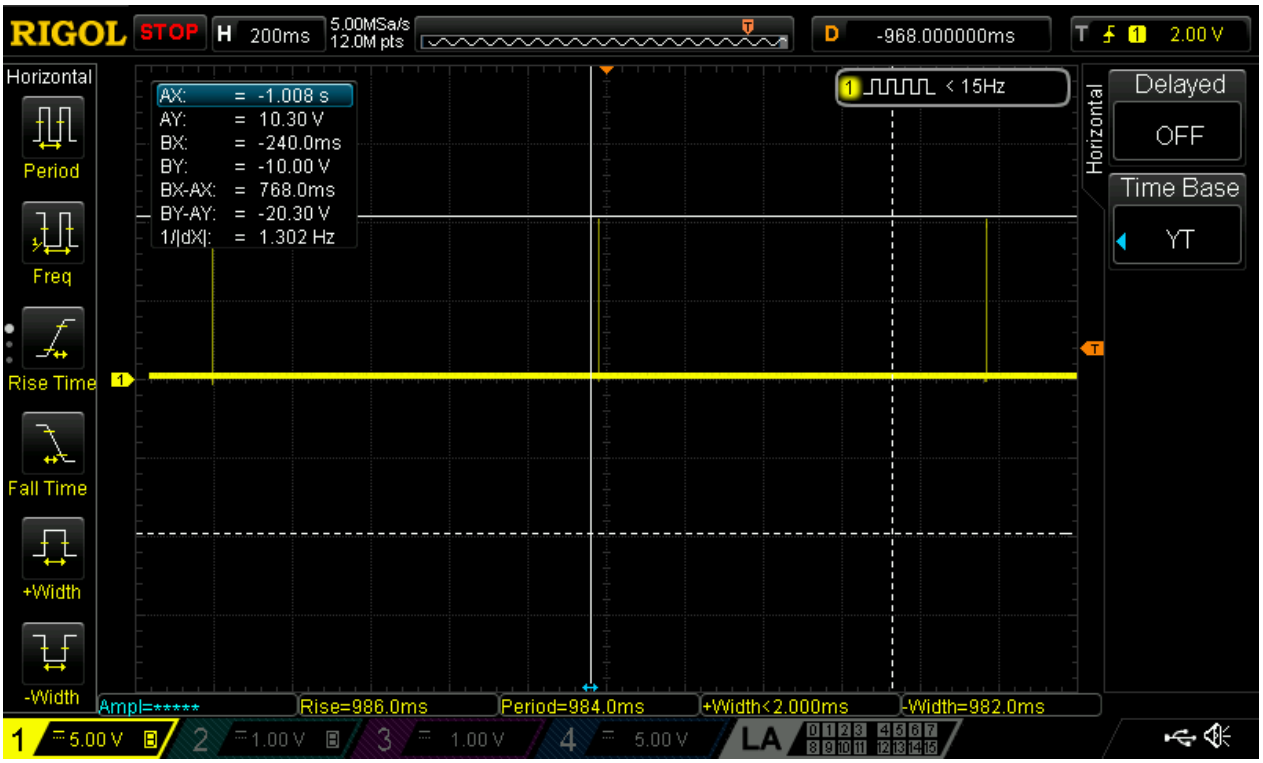

Figure 51 Electroporation signal at the main output, on 200ms time scale

While an oscilloscope is a great tool for observing the nature of the signal, it is not a measuring instrument. A small error is visible in *Figure 51*, where the signal period instead of 1 second is calculated to be 984 ms. This could be due to an error in oscilloscope calculation since it cannot truly calculate high signal duration (due to low resolution) or due operating system of Arduino. Nonetheless, error (if there even is any) is only in the range of 1-2% which is more than acceptable.

Via two (red and red with black line) wires signal is further taken to the custom chip holder (*2.3 Chip holder*), which in turn is connected to the IDE chip(*2. Microelectrodes*). Additional resistors and capacitors are found in the device whose purpose is to filter and smooth out signals. The device is placed in a custom-built case whose purpose is to protect the circuit and the operating person from possible harm. The front interface contains an LCD, an ON-OFF switch, a mains indicator, easy access to replace the fuse, potentiometers for signal settings, reset and freeze buttons, and wire connection points for the output signal. Additionally, the purpose of the case is to provide ventilation while at the same time protecting the device against dust. The connection point for supplying the device with the main power grid is found at the back of the case. Since 5R0ELA generates signals as electroporation theory demands, it is ready to be tested on cells.

4. Experiment

Combining microelectrode (*2.* Microelectrodes), 5R0ELA electroporation device (*3. Electroporation device*), and custom chip holder (*2.3 Chip holder*), a setup for electroporation experiments on tumor cells was prepared. HT-29 tumor cells were chosen for the initial experiments. HT-29 is a cell line with epithelial morphology that was isolated in 1964 from a primary tumor obtained from a 44-year-old, White, female patient with colorectal adenocarcinoma. [s39]. HT-29 is extensively used in biological and cancer research. HT-29 cells were kept and cultivated during experiments in fetal bovine serum. It is derived from the blood drawn from a bovine fetus and it is used since it contains a large amount of nutrients, growth factors, and antibodies for protection from contamination.

4.1 Experiment Setup

2D HT-29 tumor cells were kept in fetal bovine serum that was exchanged every two days, to keep the pH value of serum in optimal value (between 7.0 - 7.6) for cells. Initial passage number 58 of the cell was used, and once cell coverage reached 80% of the flask, cells would be either divided into two new flasks or used in experiments.

HT-29 cells were electroporated using the signal that is referenced in the most current literature [11], which generates a pulsing electrical field of 1kV/cm, frequency of 1Hz, and duty cycle of 0.01%. 1kV/cm, with fabricated microelectrode (spacing of 100µm) corresponds to generating a pulsing signal of 10V, while 0.01% duty cycle corresponds to a signal being in a high state for 100µs. Besides 10V, 15 and 20 V signals (corresponding to 1.5 kV/cm and 2kV/cm respectively) were used as well with both electrode types. Each electroporation value was replicated at the very least 2 times on each type of electrode for the sake of accuracy of the experiment.

While the main point of this thesis is to prove that electroporation is possible with such a setup, different voltage values were used, to observe if changes in cell viability/electroporation rate are noticeable.
Two methods were used to check cell electroporation, that being the CASY (*4.2 CASY*) and cell

staining (*4.3 Cell staining*) with different fluorescent colorings.

Before the experiment, old cell media was removed, while cells remained in a flask due to their adhesion to the surfaces. Trypsin is an enzyme that was added (5ml) to the flask, and incubated for 10 minutes at 38 ºC, which ceased the adhesion of cells to the surface of the flask. Adding fresh (5ml) media, the activity of the enzyme was stopped since it is harmful to the cells over prolonged exposure. After that vial with cells was put in a centrifugal machine, where it was centrifuged for 5 minutes at 1300 rotations per minute.

With that cells are found at the bottom of the vial (pellets), while the media-enzyme combination is found at the surface, which allows for their easy removal. Finally, fresh media was added once again, where the amount depended on the desired cell concentration and cells were ready for experiments.
IDE chip (*2. Microelectrodes*) was placed into chip holder (*2.3 Chip holder*), after which cells were added into the well (*2.2.6 Microwell*) which is located on the top of electrodes. Depending on the method used, cells were electroporated right away or after adding initial staining (PI), after which the detection process started. More about said processes in the following chapters.

The impedance counting method (*4.2 CASY*) of detection was decided to be performed first since it is a great indicator of whether electroporation is possible at all with the current setup.

4.2 CASY

Casy is a cell counter and analyzer device produced by OMNI Life Science. It works on the principle that it measures conductivity between two electrodes. A sample of the cell is placed into a cup filled with 10 ml of CASYton, a defined buffer solution. A cup with cells is placed into a device slot where said electrodes are found.

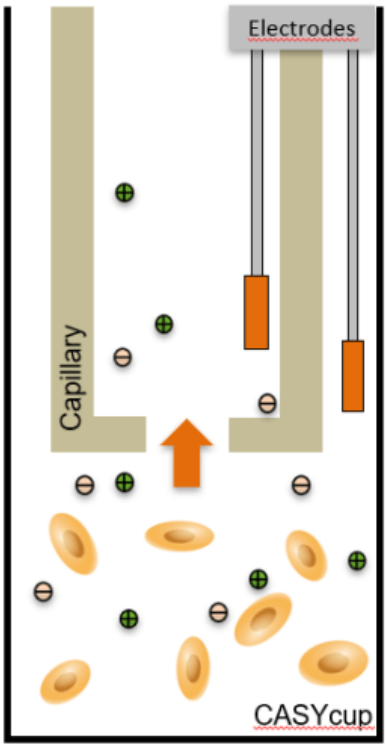

Figure 52 CASY electrodes [s40]

Figure 52 CASY electrodes [s40] illustrates a cup with cells and CASYton in which cell counting is performed. Cells counting and their viability are done by sending a signal from the electrode and then measuring how did initial signal transformed. Basically, measuring the bioimpedance of cells in the cup. During chapter *1.3.2 Electrical model of the cell,* it was said that the cell can be represented with an electrical model, where the cell membrane acts as a capacitor and ICF and ECF (CASYton in this case) as resistors. Sent signals will have many different frequencies, and depending on this value, and formula (2) signal will only travel in ECF or ECF, membrane, and ICF. From the whole impedance spectrum, cell count is determined.

Up to a certain frequency value of the signal, the cell membrane will "block" the flow of the signal. When a cell dies, its membrane becomes porous and the signal will be able to pass it at any frequency, thus a device determines total cell viability in a cup.

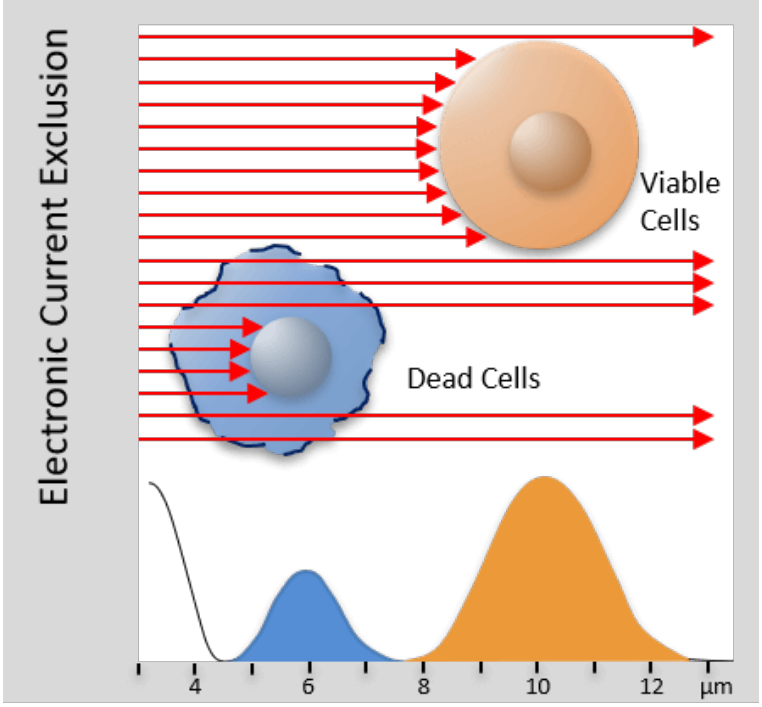

Figure 53 Work principle of CASY[s40]

Figure 53 depicts the working principle of the CASY system in a correlation of bioimpedance which was discussed in *1.3.2 Electrical model of the cell.* This effect was interesting for this thesis since electroporation causes cells to become porous and thus can "trick" the CASY system into counting alive cells as dead. Observing cell viability, it can be concluded whether cells got successfully electroporated.

Sadly, as mentioned in *1.3 Electroporation*, electroporated cells are only electroporated for a few seconds, before resealing again. This causes problems since electroporated cells need to be removed from the electrodes, placed into a vial filled with CASYton, and placed into a CASY whose measurement takes a minute or so. Due to that, CASY can't be used to determine the success rate of the electroporation signal. On the other hand, while most cells reseal almost instantly (after electroporation), not all of them will, but rather depending on the signal value it might take up to a few minutes. So, it was decided that this CASY method would be only used as initial testing whether the electroporation device in combination with the chip can even successfully electroplate.

Non-electroporated cells were placed into CASY, just to determine initial cell viability and concentration from the initial sample.

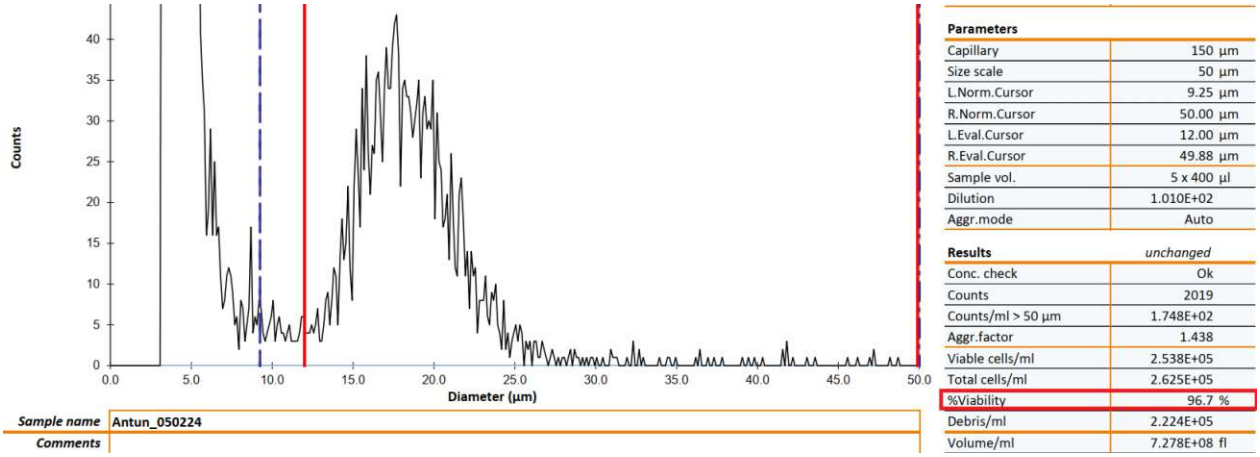

Parameters	
Capillary	150 µm
Size scale	50 µm
L.Norm.Cursor	9.25 µm
R.Norm.Cursor	50.00 µm
L.Eval.Cursor	12.00 µm
R.Eval.Cursor	49.88 µm
Sample vol.	5 x 400 µl
Dilution	1.010E+02
Aggr.mode	Auto
Results	*unchanged*
Conc. check	Ok
Counts	2019
Counts/ml > 50 µm	1.748E+02
Aggr.factor	1.438
Viable cells/ml	2.538E+05
Total cells/ml	2.625E+05
%Viability	96.7 %
Debris/ml	2.224E+05
Volume/ml	7.278E+08 fl

Figure 54 Initial cell counting

From *Figure 54* it is visible that initial cell viability (marked with a red rectangle) was 96.7 %. Additionally, a control positive test was done where cells were kept in ethanol for 30 minutes, just to make sure the viability of the cell would be as low as possible, and CASY concluded that cell viability was 0%.

While the most of literature suggests using 8 pulsed signals of 10V 1Hz and 100µs, for this initial experiment 20V 1Hz and 200µs pulsed signals were used instead. These parameters are four times higher than recommended values which will in turn cause both reversible and irreversible electroporation, decreasing the overall viability of the cells. At the same time, this will cause cell membranes that were electroporated reversibly, to reseal a bit slower, so that it can be captured on CASY.

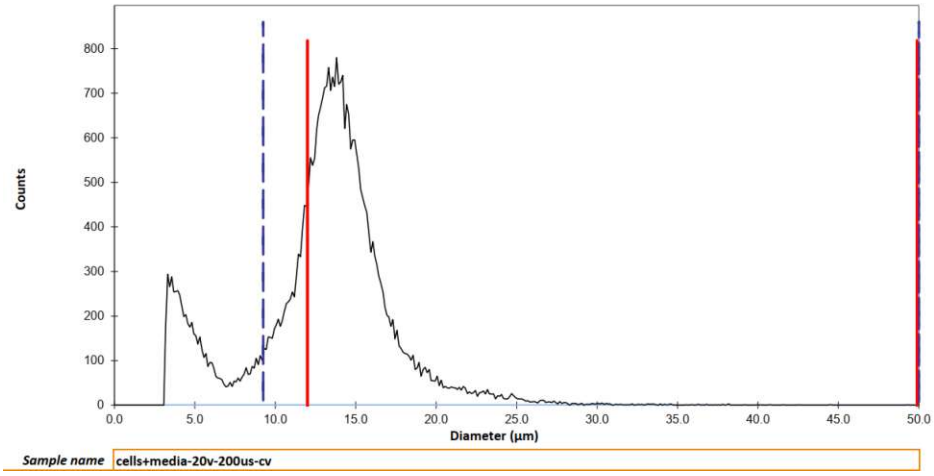

TT-2HB-1440	07/03/2024
bGRZ	13:12
Parameters	
Capillary	150 µm
Size scale	50 µm
L.Norm.Cursor	9.25 µm
R.Norm.Cursor	50.00 µm
L.Eval.Cursor	12.00 µm
R.Eval.Cursor	49.88 µm
Sample vol.	5 x 400 µl
Dilution	1.010E+02
Aggr.mode	Auto
Results	*unchanged*
Conc. check	Ok
Counts	25873
Counts/ml > 50 µm	3.147E+02
Aggr.factor	1.537
Viable cells/ml	2.086E+06
Total cells/ml	2.362E+06
%Viability	88.3 %
Debris/ml	3.220E+05

Figure 55 Viability 1 minute after electroporation

As *Figure 55* suggests, viability decreased from 96,7 % to 88.3 %. This is a promising result

since there is an 8.4 % viability change, present even 1 minute after electroporation meaning electroporation was successful. The exact percent of successful reversible electroporation can't be concluded since most of the viability was restored within this time frame, as the cell membrane resealed. As well it can't be concluded whether irreversible or reversible electroporation was performed. For that reason, the sample was left for 15 minutes, with the expectation that some of the cells had not yet been resealed due to the higher energy signal used.

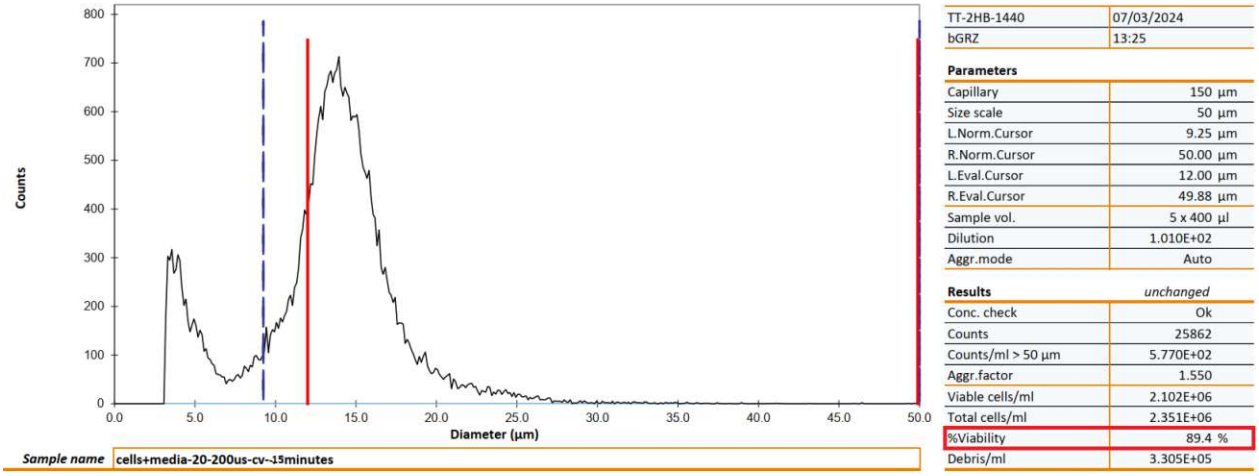

TT-2HB-1440	07/03/2024
bGRZ	13:25

Parameters	
Capillary	150 µm
Size scale	50 µm
L.Norm.Cursor	9.25 µm
R.Norm.Cursor	50.00 µm
L.Eval.Cursor	12.00 µm
R.Eval.Cursor	49.88 µm
Sample vol.	5 x 400 µl
Dilution	1.010E+02
Aggr.mode	Auto

Results	*unchanged*
Conc. check	Ok
Counts	25862
Counts/ml > 50 µm	5.770E+02
Aggr.factor	1.550
Viable cells/ml	2.102E+06
Total cells/ml	2.351E+06
%Viability	89.4 %
Debris/ml	3.305E+05

Figure 56 Viability 15 minutes after electroporation

Figure 56 suggests that cells are being "revived" since after 15 minutes viability increased by 1.1%. This is because some cell membranes were still resealing (most of them resealed after a few seconds) in *Figure 55*. This is definite proof that by using a 5R0ELA device (*3. Electroporation device)* and IDE chip (*2. Microelectrodes*), reversible electroporation is possible. It has to be noted that CASYton is not a natural environment for the cell, but rather it is poisonous, further decreasing cell viability during this 15-minute wait. Suggesting that more than 1.1% of cells had a slower membrane resealing process. The experiment was performed for additional time, with the same signal parameters, on the fresh set of cells, yielding a cell "revival" rate of 1.8%.

Due to the time delay between electroporation and measurement, it is impossible to determine with the CASY system the total percentage of successful RE cells. Nonetheless, "reviving" cells is excellent initial proof that reversible electroporation is indeed possible.
To determine (approximate) a percentage of successful RE cells, cell staining method was used.

4.3 Cell staining

Cell staining is a technique that is used to better visualize cells and their current states under a microscope, using a different fluorescent agent to achieve so.

During the experimental phase, both naked and covered electrodes (named after their isolation layer type) were used, in combination with PI, DAPI, and Calcein staining, all of them being fluorescent staining. Fluorescent staining uses special dyes called fluorophores (PI, DAPI, and Calcein in this case) to stain cells. After cells are exposed to the light of a specific wavelength, they will emit different colors depending on the type of stain (and exposed light) [24]. For initial experiments, a combination of DAPI and PI was used. DAPI (4′,6-diamidino-2-phenylindole) is a blue-fluorescent DNA stain. It fluoresces blue (405 nm) when bound to double-stranded DNA and excited by exposure to 345 nm light [s41]. Stock DAPI solution stored at -20 ºC was used and 1µl of it was with cells before electroporation and checked under microscope after 5 minutes of incubation at room temperature. With it, PI was added as well before electroporation. Propidium iodide (PI) is a popular red-fluorescent nuclear and chromosome counterstain. Since propidium iodide is not permeant to live cells, it is also commonly used to detect dead cells in a population. [s42].

PI binds to DNA by intercalating between the bases with little or no sequence preference. In an aqueous solution, the dye has an excitation/emission maxima of 493 / 636 nm. Adding 1.5 µl of PI, it can determine if electroporation was successful since PI binds to dead cells. This is done by passing the cell membrane which, in case of cell death, is compromised. Cell membranes become compromised as well during electroporation and as such can be used to determine if electroporation took place while the cell still being alive. Before electroporation cells, control positive (CP) and control negative (CN), experiments were done. During CP cells were incubated for 15 minutes with ethanol, (after removing ethanol) followed by adding PI and DAPI to cells which were incubated for an additional 5 minutes. The mixture was placed on an empty glass slide on which the PDMS well was attached (*2.2.6 Microwell*). The following cell figures in this chapter were produced using Nikon ECLIPSE TE200 [s43], an attached camera, and a mercury lamp (used to produce excitation wavelengths).

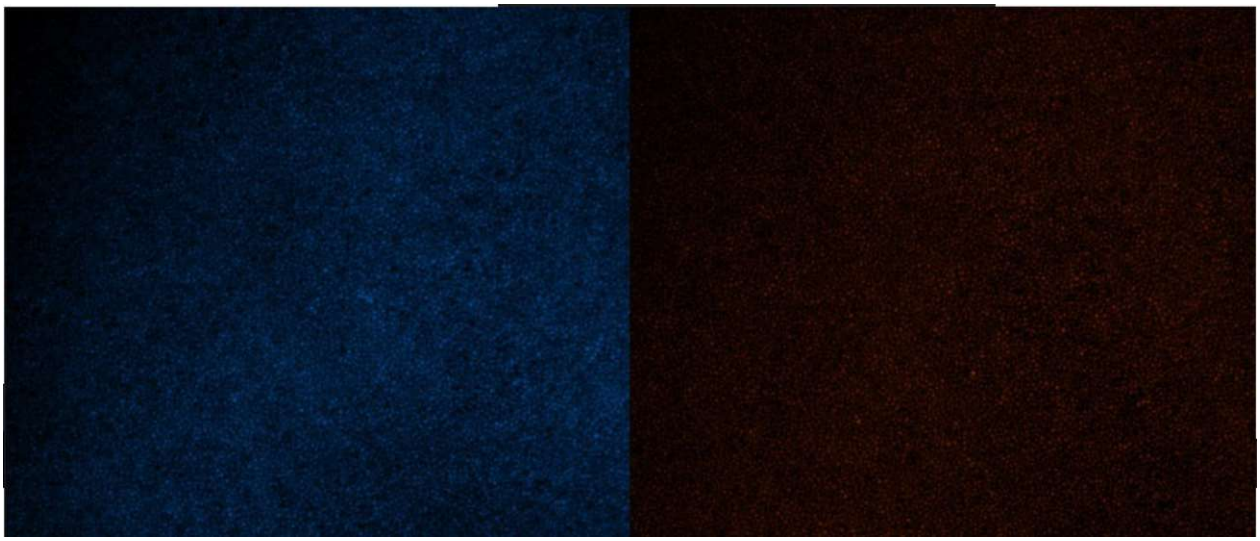

Figure 57 CP DAPI (left) and PI (right)

Following that, CN was performed where healthy and uninfluenced cells were mixed with DAPI and PI and observed under a microscope after a 5-minute incubation period.

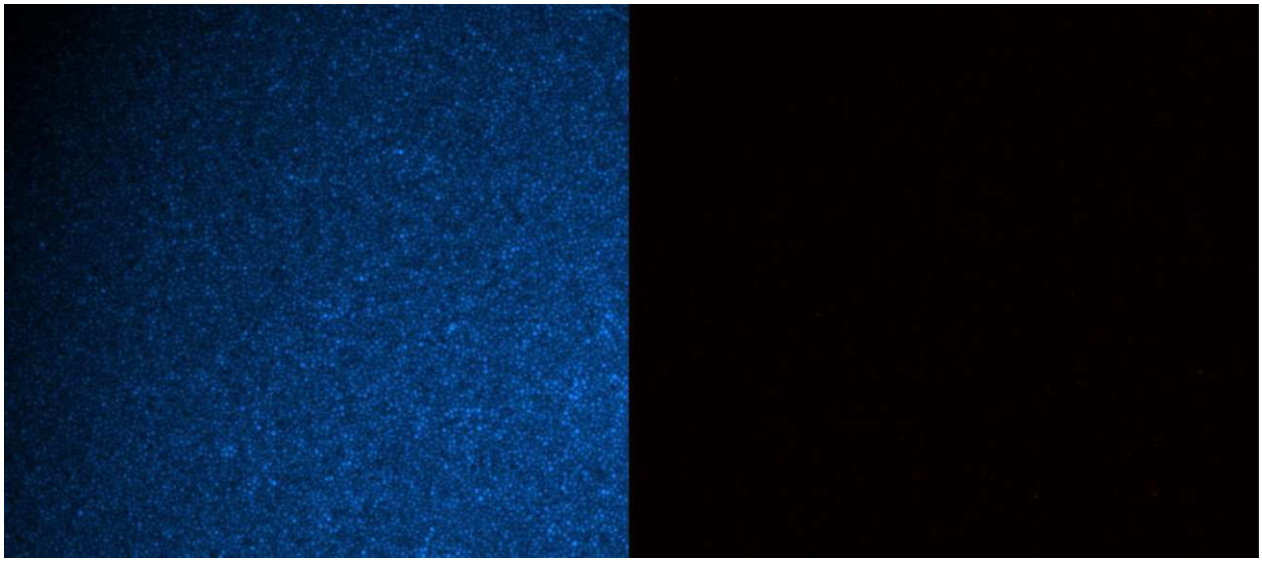

Figure 58 CN DAPI (left) and PI (right)

Comparing *Figure 57* and *Figure 58* difference between CP and CN is visible. In case when cells are dead (CP), PI (red) coloring is visible, unlike in the case of CN, where most of the cells are alive, and PI is not visible. In both cases DAPI is visible, but it is of a much stronger intensity in the CN case.

With knowledge of how a sample of cell staining looks look before electroporation (*Figure 58*), cell culture was added to both types of electrodes.

First, cells were added with the combination of PI, onto both types of microelectrodes (naked and covered from *2. Microelectrodes*), and incubated for 5 minutes. Afterwards, they were electroporated using 5R0ELA (*3. Electroporation device*) with 8 pulse signals of amplitude of 15 V, 1 Hz, and duration of 100 µs. Afterward, DAPI was added, and incubated for an additional 10 minutes. Separated pictures were taken of both PI and DAPI with corresponding exciting wavelengths and then superimposed, using the ImageJ program.

ImageJ is public domain Java-based software for processing and analyzing scientific images developed at the National Institutes of Health and the Laboratory for Optical and Computational Instrumentation. While taking pictures, it was important not to move the camera even for a µm, since then overlap between pictures would not be possible.

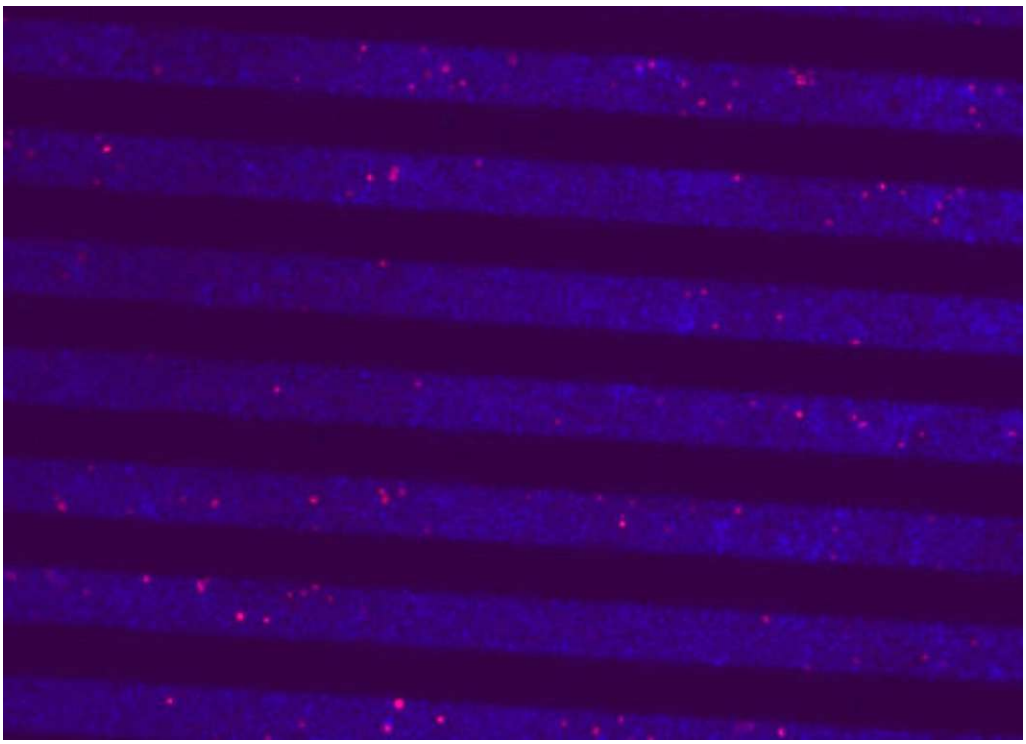

Figure 59 Electroporated monolayer of HT-29, on section (1800 by 1300 µm) of naked electrodes, with blue (DAPI) and red (PI) staining

Comparing *Figure 59* with *Figure 58* it is visible that red dots started to form. Red dots represent PI which means electroporation happened. Blue is stained by DAPI and represents cells, staining them all, regardless of whether they are dead or alive. Following that, electroporation was done on a covered type of electrode, and the results are visible in *Figure 60*.

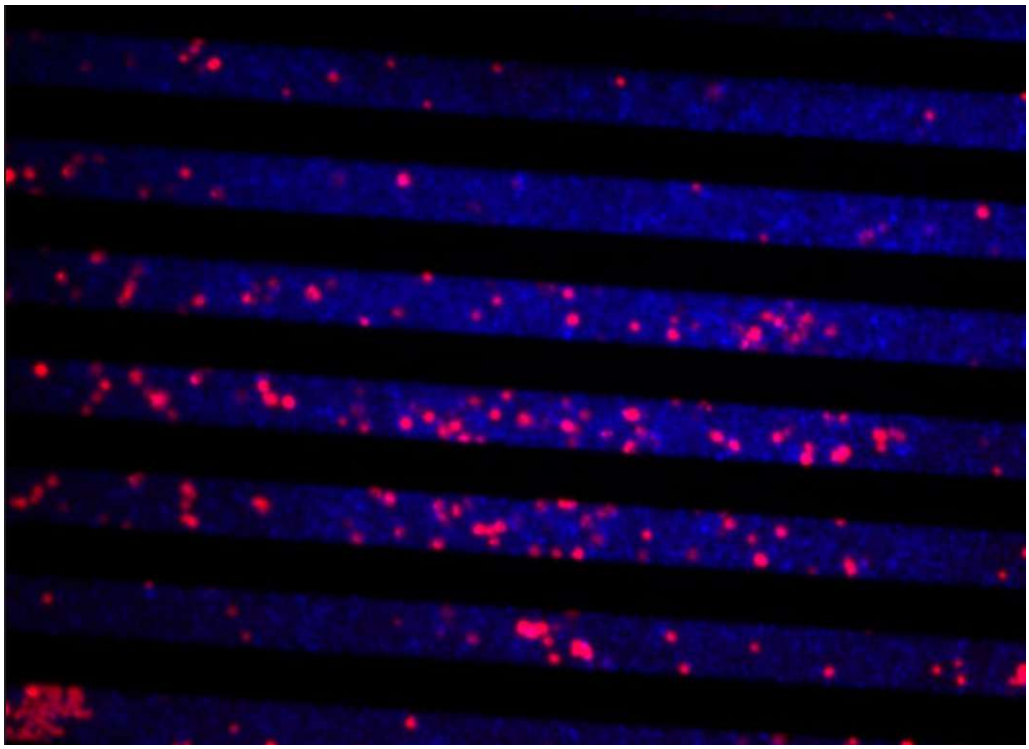

Figure 60 Electroporated monolayer of HT-29, on section (1800 by 1300) of covered electrodes, with blue (DAPI) and red (PI) staining

Comparing *Figure 59* and *Figure 60* it is clear that electroporation was more successful on the type of electrodes that were isolated (covered type) since there is a higher amount of red dots. The reason for this outcome is not clear but a theory within this thesis was developed.

This theory suggests that due to the presence of an isolating layer, no current flow can be achieved between electrodes, but rather only an electrical field. This correlates with the theory of electroporation, where electroporation is caused by an electrical field. On the other hand, the majority of research papers on the topic of electroporation on microelectrodes use electrodes that are not fully insulated. This causes pure current flow between electrodes. In such a state, electrodes are more prone to get destroyed (*Figure 65*), but more importantly, current will flow around the cell, through the media. This is because in electroporation, relatively low frequencies (1Hz) are used. Following formula (2) this leads to the high reactance of the cell (as discussed in *1.3.2 Electrical model of the cell*). In other words, due to low-frequency current won't be able to penetrate the membrane, so current will flow around the cells. Nonetheless, according to the Ampere law [s44] the magnetic field formed by an electric current is proportional to the magnitude of the current passing through. Following this, according to the Faradays Law of

electromagnetic induction [s45] a changing magnetic field in turn produces an electrical field. This electric field in the end will cause electroporation, but due to its secondary (product) nature, it is much smaller compared to the electrical field produced by insulated electrodes.

With this experimental setup, it was proven once again, that custom electrodes and 5R0ELA devices can cause electroporation. With the addition of DAPI and PI staining, it was visualized as well. Sadly, it can't be determined whether reversible or irreversible electroporation happened since DAPI stains all cells regardless of their current status. Observing *Figure 58* it is noticeable that alive cells, stained by the DAPI, are outputting a much more intense blue color compared to *Figure 57* where cells are dead. With intensity analysis, conclusions about electroporation type can be made, but it is somewhat difficult. That's why DAPI was switched with Calcein AM.

Calcein AM is a cell-permeant dye that can be used to determine cell viability in most eukaryotic cells. In live cells, the nonfluorescent Calcein AM is converted to green fluorescent Calcein, after acetoxymethyl ester hydrolysis by intracellular esterases [s46]. Calcein is excited by 494 nm blue light and it emits 517 nm green light. Unlike DAPI, Calcein emits green light, only if cells are still alive. With that, it is expected, that if at the same spot, both green and red lights are found that means that the cell got reversibly electroporated. Calcein is here to signal that the cell is alive, while red light signals that PI could pass the membrane, due to electroporation. In case the cell only emits green light, that suggests that the cell didn't get electroporated while only red light signals that either the cell was irreversibly electroporated, or was dead even before the experiment.

The setup was done in a way that 100 µL of media with cells (approximately 10000 cells) were placed on the electrodes and 2µL PI was added. After incubation of 5 minutes, a picture was taken, followed by 5R0ELA electroporation with different voltages, while keeping other signal parameters the same (8 pulsed signal, 1Hz, 100 µs). After electroporation, 1 µL Calcein was added and incubated for an additional 10 minutes after which pictures of both PI and Calcei were taken again. Like previously, PI and then Calcein images were superimposed. Starting with 10V as most of the literature suggests, the following picture was made.

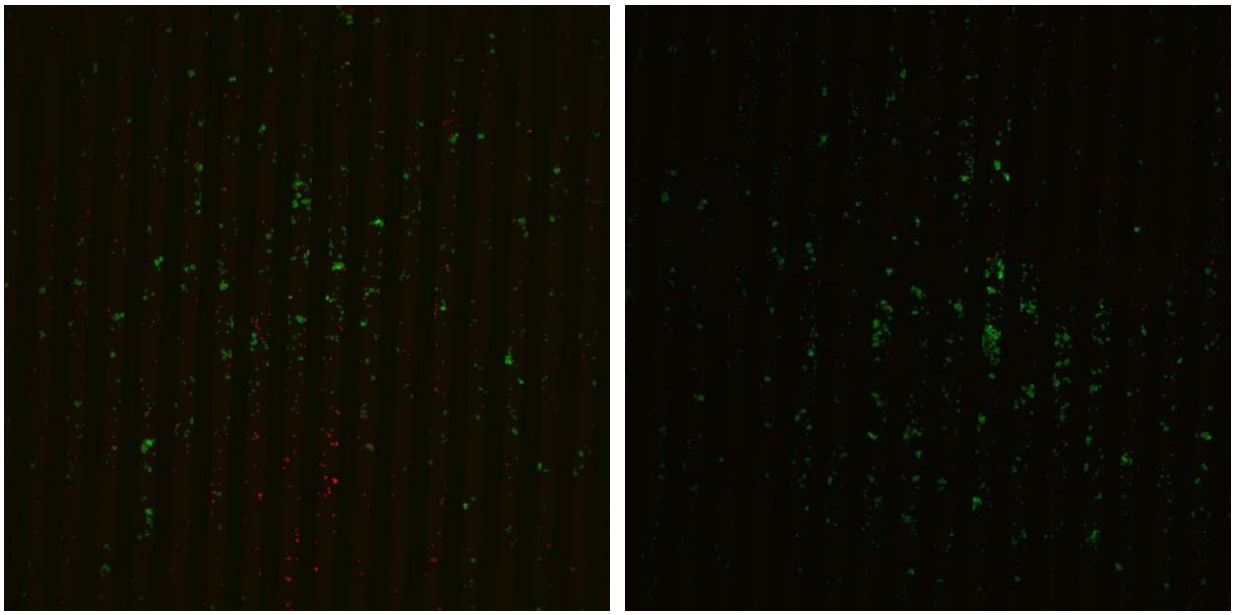

Figure 61 Section of electrodes (3200 by 3200 µm), pictured after electroporation 10V, PI(red)+ Calcein(green), with covered electrodes(left) and naked electrodes (right)

Visually *Figure 61* proves a theory, from *Figure 59* and *Figure 60* which suggests that electrodes with an isolating layer will electroporate better, as it has more red spots (dead and/or electroporated cells).

To discern between irreversible electroporation and previously dead cells, the image of PI from before and after electroporation was taken. Comparing the number (before and after) of red-stained cells exact value of irreversible electroporated cells can be calculated. Instead, an interesting phenomenon was noticed. Cells changed position when comparing from before and after electroporation, especially ones that were not bunched together. This phenomenon is called dielectrophoresis. Dielectrophoresis (DEP) refers to the movement of a neutral but polarizable particle when it is subjected to a nonuniform electric field due to the interaction of the particle's dipole and spatial gradient of the electric field [25]. DEP is used in science for particle sorting and is a current subject in different scientific studies. In this particular thesis, it is an unexpected and unwanted side effect of electroporation, since this complicates things, as IR from previously dead cells cannot be discerned.

Meanwhile, to calculate the exact number of reversible electroporated cells, 10x zoom with a microscope was made on the section of the electrodes.

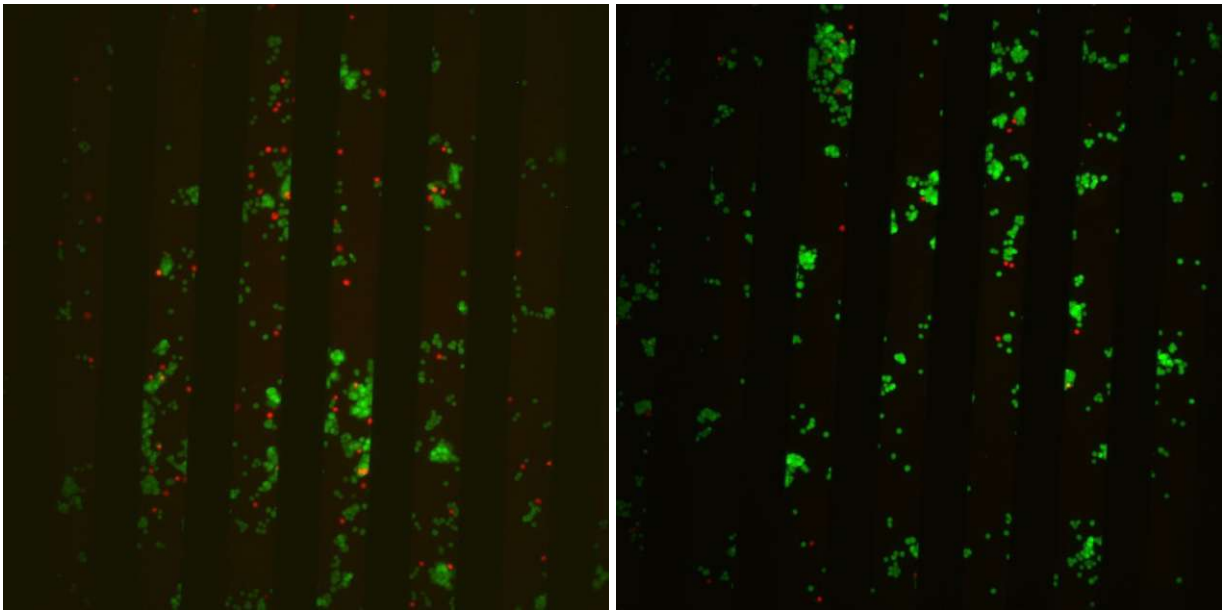

Figure 62 Section of electrodes (1300 by 1300), pictured after electroporation 10V, PI(red)+ Calcein(green), with covered electrodes(left) and naked electrodes (right)

Figure 62, was made with 10x zoom with a microscope, on the section of the electrodes, so that the exact number of RE cells can be calculated. For each electroporation, 2-3 differently positioned images with 10x zoom were taken on each electrode setup.

Due to the high number of cells, it is somewhat hard to count the exact percentage of successful reversible electroporation. It was calculated by counting cells in different zoomed-in images from the same electroporation and averaging it, making a success rate between 5-10%. For more accurate calculation the relation between previously dead, irreversible, and reversible electroporated cells was made, which is visible in *Table 1, Table 2, Table 3, and Table 4* from *Appendix- Cell count* part of the thesis.

With the data from *Appendix- Cell count*, it is visible that as voltage increases, the ratio of the number of all PI-stained cells (dead + reversible and irreversibly cells) and the number of reversible electroporation cells decreases. This coefficient is named the PI ratio. With that, it is concluded that the number of successfully reversibly electroporated cells increases with the

voltage, while the PI ratio decreases. Of course, at some voltage point, the PI ratio will start to increase again, as with increased voltage, there is a higher chance for irreversible electroporation to occur. Likewise, the PI-ratio is much higher in non-insulated electrodes, as compared to insulated electrodes, due to the previously mentioned developed theory (due to initially dead cells as well).

Since theory says that cell density influences (negatively) electroporation success rate, one measurement with 10V was made where the cell density was much higher than compared to the previous measurements.

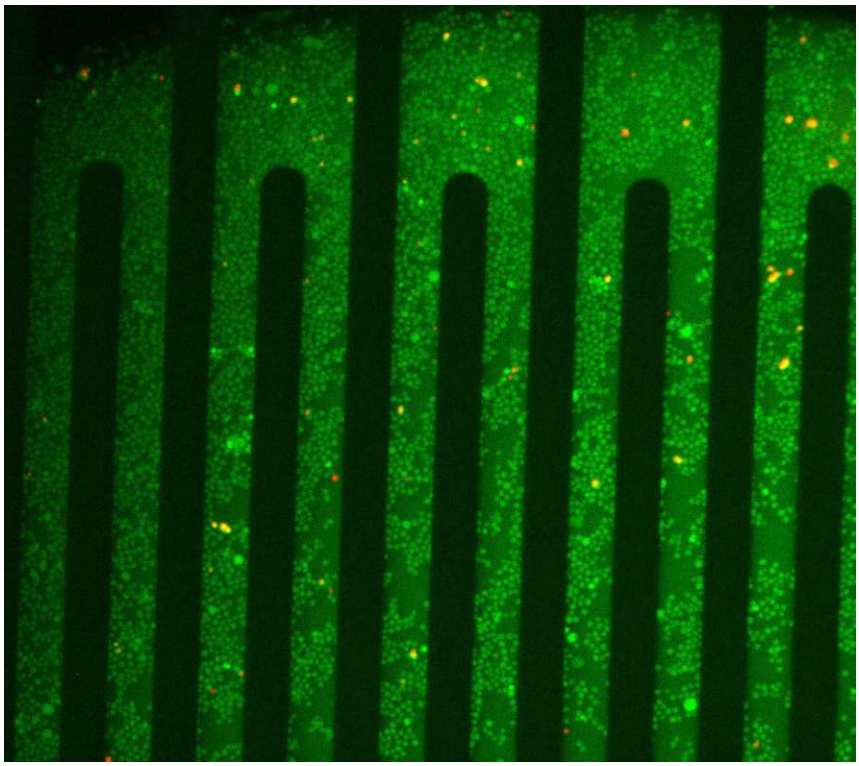

Figure 63 Section of electrodes (1900 by 1700 µm) High cell density, 10V, PI(red)+Calecin (green) insulated electrodes

Comparing *Figure 63*, with previous measurements (*Figure 61*) it is observed that the electroporation rate decreased (due to cell density), but the number of irreversibly electroporated cells decreased drastically as well. To overcome this problem, the best solution would be designing, a new nanoscale-based electroporation chip. Nanoscale- or nanochannel-based electroporation (NEP) is a novel single-cell resolution transfection approach in which strong but nanoscale-focused electric fields result in transfection efficiencies and cell viabilities of nearly 100% [26]

In this thesis electroporation success rate is determined visually, by counting the cells, which is not the best solution as this method is tedious and prone to error. To avoid that, it is recommended to use a flow cytometry system. Flow cytometry is a laser-based technique used to detect and analyze the chemical and physical characteristics of cells or particles. Sadly, during the experimental phase, access to this system was not achieved as it requires special training to operate.

While electroporation was achieved, the overall success rate was not that good (2-10%). This can be due to a lack of optimization of the used signal, thin isolating layer, and cell density, but it is suspected that it is mainly due to the cell medium. All the electroporations were made with cells being in FBS. FBS provides nutrients for the cell, but due to its high conductivity, it is not the best option for electroporation. Most of the papers, use a so-called electroporation buffer as it is a formula that is used to improve electroporation by minimizing cell mortality while ensuring highly efficient delivery of staining or other particles [27]. Sadly, during the experimental phase said electroporation buffer was not available. As a replacement Phosphate buffered saline (PBS) was used for a few measurements just to test a theory, as it is more similar to electroporation buffer than FBS, but at the same time much more unfavorable environment for the cells.

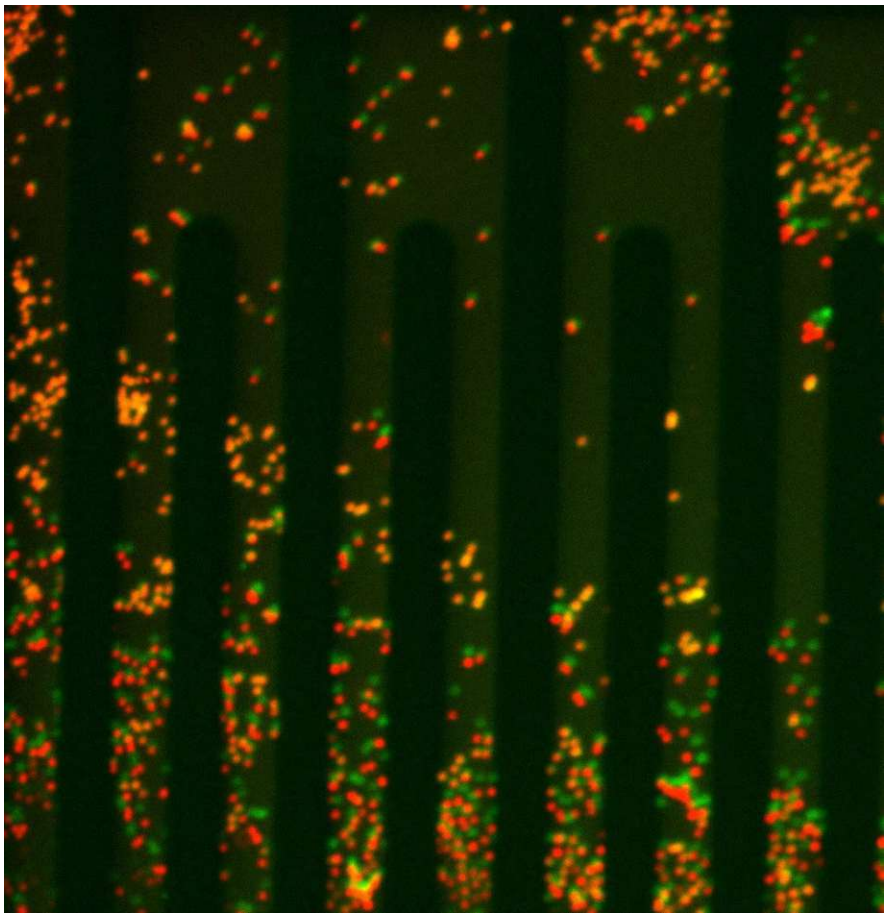

Figure 64 Section of electrodes (1600 by 1600 µm)15V isolated electrodes, PBS as media

While it is visible from *Figure 64* that the success rate of reversible electroporation drastically increased (to around 80-90%), a small shift between cell images was caused (around 1µm) due to microscope handling error. Reversibly electroporated cells are those that emit bright white/orange light and those that should do it, but if a 1 µm shift is ignored.

An additional possible reason that could cause a lower electroporation success rate is that due to prolonged usage of electrodes (due to repeated measurements), the isolating layer degrades, especially on the covered electrodes. The check was done using the same Fluke 116 true RMS multimeter. Interestingly enough, it started to detect some faint short-circuit points on the isolating layer over the electrodes.

Additionally, as it was mentioned in *2.1 Design* 50% of data is lost, since electrodes obstruct the view (microscope light can't pass through them). As the electrical field damps over the distance,

it is expected the best results success rate of electroporation would be found at the electrodes. This can be circumvented by decreasing the size of electrodes, but they can't be too small, otherwise, they will get destroyed by an electrochemical process. Unrelated to current measurements, an example of it is the electroporation of HT-29 spheroids (three-dimensional cell aggregates that can mimic tissues and microtumors), where higher voltages are required. For electroporation of spheroids, 30 V signals were used.

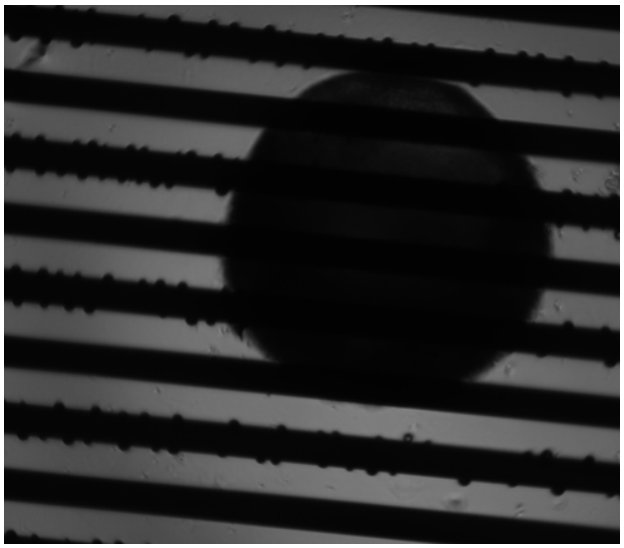

Figure 65 Electroporated HT-29 spheroid, with destroyed electrodes

This destroys the electrodes as it is visible in *Figure 65*. Every second electrode (black line) is ribbed, meaning as expected, destruction was caused on positive electrodes (moving electrons from positive toward negative electrode). For that reason, thicker electrodes were designed and fabricated, where it is considered that 50% visibility is a good compromise.

Conclusion

The main goal of this thesis work was to prove, that reversible electroporation of tumor cells is possible with a micro electrode chip. This work is of interest to the current scientific community since, electro-chemotherapy is a novel method used in cancer treatment, which still requires a lot of optimizations.

During the thesis, three different objectives were set, that needed to be fulfilled. Only with all three of them, working together, the main goal of the thesis could be achieved.

The first objective was to design and fabricate two types of custom microelectrode chips. These two types differ in their isolation layer plating, with one having their interdigitated microelectrodes completely covered, by a thin layer of insulating material and the other, where the isolation layer is only present between the interdigitated microelectrodes and not on them. Chips were, by all accounts (height, size, equal material distribution, etc.), successfully fabricated.

The second objective is focused on electroporation devices. Commercial electroporation devices can be somewhat expensive, and not everybody can afford them, which is a problem, as a lot of optimizations (testing) in tumor electroporation is still required. For that reason, as and second objective, it was decided that a custom, cost-effective electroporation device would be fabricated. It was named “5R0ELA”, and using an oscilloscope it was determined that it indeed produced signals that are being used in commercial (and electroporation theory) electroporation devices. Concluding that the second objective was fulfilled as well.
Alongside 5R0ELA, a custom chip holder based on pogo-pins was designed and successfully fabricated. Its purpose is to interface 5R0ELA (or any other electrical device), with a microelectrode chip from the first objective (or any other, with similar dimensions).

The third objective relates to tumor cell cultivation, the experimental setup, and its execution. Successfully cultivated tumor cells were placed on a fabricated microelectrode chip, which was inserted into a chip holder allowing to electroporation be performed via 5R0ELA. Two methods

(CASY and cell staining) for electroporation detection were proposed, each with its own set of drawbacks. Both of them were performed successfully, providing results of cell electroporation. The drawback of the CASY method, which is based on bioimpedance, is that it takes a long time for measurement, during which most of the cell membranes are already resealed again. The cell staining method requires for analysis for each cell to be counted individually, and compared which is especially problematic if cell density is high or there is a movement of a cell due to the dielectrophoresis effect. This problem can be circumvented by using flow cytometry, but this method was not available during this thesis work.

While both methods confirmed, that reversible electroporation is indeed possible with this setup, the success rate was not that good (between 2 and 10%). There are several reasons why this could occur: the main perpetrator could be the FBS media within which tumor cells were electroporated. Usually, electroporation testing is done as tumor cells are in an electroporation buffer, which was not available. Replacing cell media with PBS whose structure is more similar to electroporation buffer, a success rate increased (to around 80%).
An additional improvement that could be done is by performing electroporation with different isolation layer thicknesses on the microelectrodes. It is possible that during the experimental phase, due to high electrical fields used in electroporation, a thin isolating layer was breached on the micro/nano level. This can also cause a lower reversible electroporation success rate since it was determined during the experimental phase, that non-isolated electrodes have a much lower success rate as compared to the isolated electrodes.

In conclusion, all three main objectives were accomplished, while at the same time providing promising results. However, experiments showed that more optimization (of excitation signal parameters) needs to be done, as it is a current scientific topic worldwide.

Appendix- Schematic

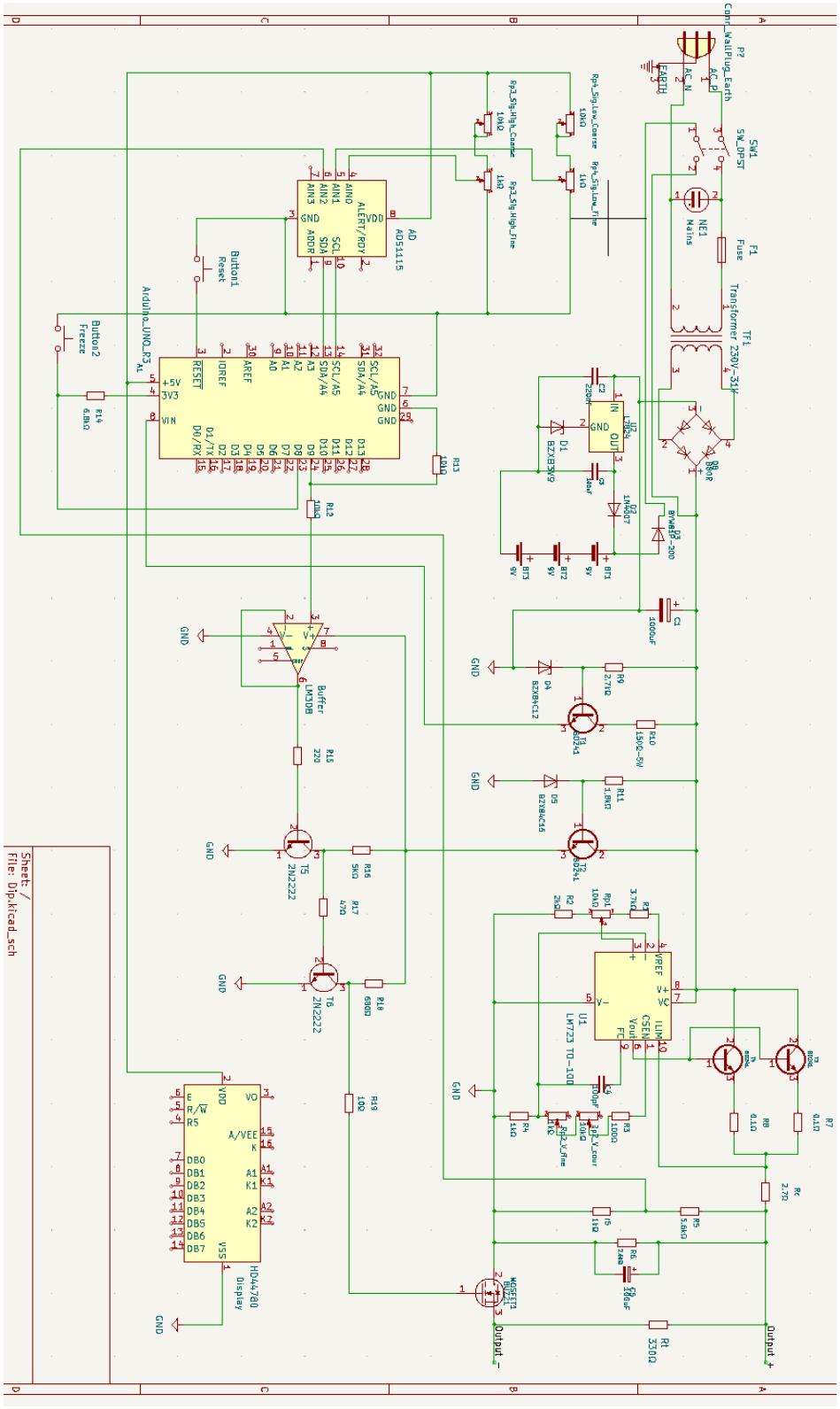

Figure 66 Schematic diagram of 5R0ELA electroporation device

Appendix-Code

C++ code used to generate control signal (and all additional functions) with ArduinoUno:

```
#include <LiquidCrystal_I2C.h>
LiquidCrystal_I2C lcd(0x27,20,4);
#include <ADS1X15.h>
ADS1115 ADS(0x48);
int but;
int buts=1;
int i=0;
void setup() {
  Serial.begin(115200);
  lcd.init();
  lcd.backlight();
  ADS.begin();
  ADS.setGain(0);

  pinMode(9, OUTPUT);
}

void loop() {
  int b=9;
  //i++;
  buts=1;
 // ADS.setGain(0);
  double v0= ADS.readADC(0); //read v0 from potentiometer, used to determn signal lenght
  double v1=ADS.readADC(1); // read v1 from potentiometer, used to determen signal period
  double v2=ADS.readADC(2); // read v2 from voltage divider, it is used to diplay current voltage
  float f=ADS.toVoltage(1); //  f from  ADS library, used to convert digital signal to coresponding voltage
  double sig=v0/100; // float takes up same memeory as double, double 15 digits, float 6-7
  double rst=v1/10;
  double freq=1/((sig*0.000001)+(rst*0.001));
  double DC=(sig/(sig+(rst*1000)))*100;
  double V=v2*f*6.65; // 6,56 used to translate 0-5 Volts to represend 0-cca 35 volts
  //Serial.print(i);
 // Serial.print("\tAnalog2: "); Serial.print(v2); Serial.print('\t'); Serial.println(V, 3);
 // Serial.print("\tAnalog0: "); Serial.print(v0); Serial.print('\t'); Serial.println(v0 * f, 3); Serial.print('\t');
Serial.println(sig);
 // Serial.print("\tAnalog1: "); Serial.print(v1); Serial.print('\t'); Serial.println(v1 * f, 3); Serial.print('\t');
Serial.println(rst);
 // Serial.print("\tDuty cycle[%]: "); Serial.print(DC,7);
 // Serial.print("\tFreq[Hz] "); Serial.print(freq,7);
  ///Serial.print(f,9);
  but=digitalRead(8); // following loop was used to have a button that will freeze the program
  if(but!=1){
    lcd.setCursor(12,2);
    lcd.print("FROZEN");
    lcd.setCursor(13,1);
   lcd.print(i);
   lcd.print("th");
    delay(5000); // safety delay of at very least 5 seconds to avoid accidental double press of freeze button
```

```
  while(buts==1){
    buts=digitalRead(8);

  }
  }

 Serial.println();
 uint32_t t1=millis();
 lcd.clear();
 lcd.setCursor(0,0);
 lcd.print("V:");
 lcd.print(V,3);
 lcd.print("V"); // disp voltage
// lcd.print("DC:");
 //lcd.print(DC,10);
  //lcd.print("%");
  lcd.setCursor(10,0);
  lcd.print("S:");
  lcd.print(sig+10); // disp lenght of signal
  lcd.print("us");
  lcd.setCursor(0,1);
  lcd.print("SL:");
  lcd.print(rst,1); // disp time in between signals
  lcd.print("ms");
  lcd.setCursor(13,1);
  lcd.print(i); // display how many signals was sent
  lcd.print("th");
 lcd.setCursor(0,2);
lcd.print("f:");
 lcd.print(freq,5); // disp current freq of signal
 lcd.print("Hz");
   //lcd.print("DC:");
 //lcd.print(DC,8);
 // lcd.print("%");
 uint32_t t2=millis();
 //Serial.print("t1:\t");
 //Serial.println(t1);
 //Serial.print("t2:\t");
// Serial.println(t2);
 uint32_t T=t2-t1; // some additional delay is caused due communication with display, it is compensate here
 //Serial.print("T=");
// Serial.println(T);


 digitalWrite(b, HIGH);
 //Serial.println(b);
 delayMicroseconds(sig);//max value ->16383 can only take int value if double it will round it down, delay
Microsecond actually works with steps of 4 microseconds, it rounds down
 digitalWrite(b, LOW);
 //Serial.println(b);
 delay(rst-T-30); // Wait for 1 second before repeating, max 49 days
 i++;  // counter used to count how many signals were sent
```

Appendix-Cell staining

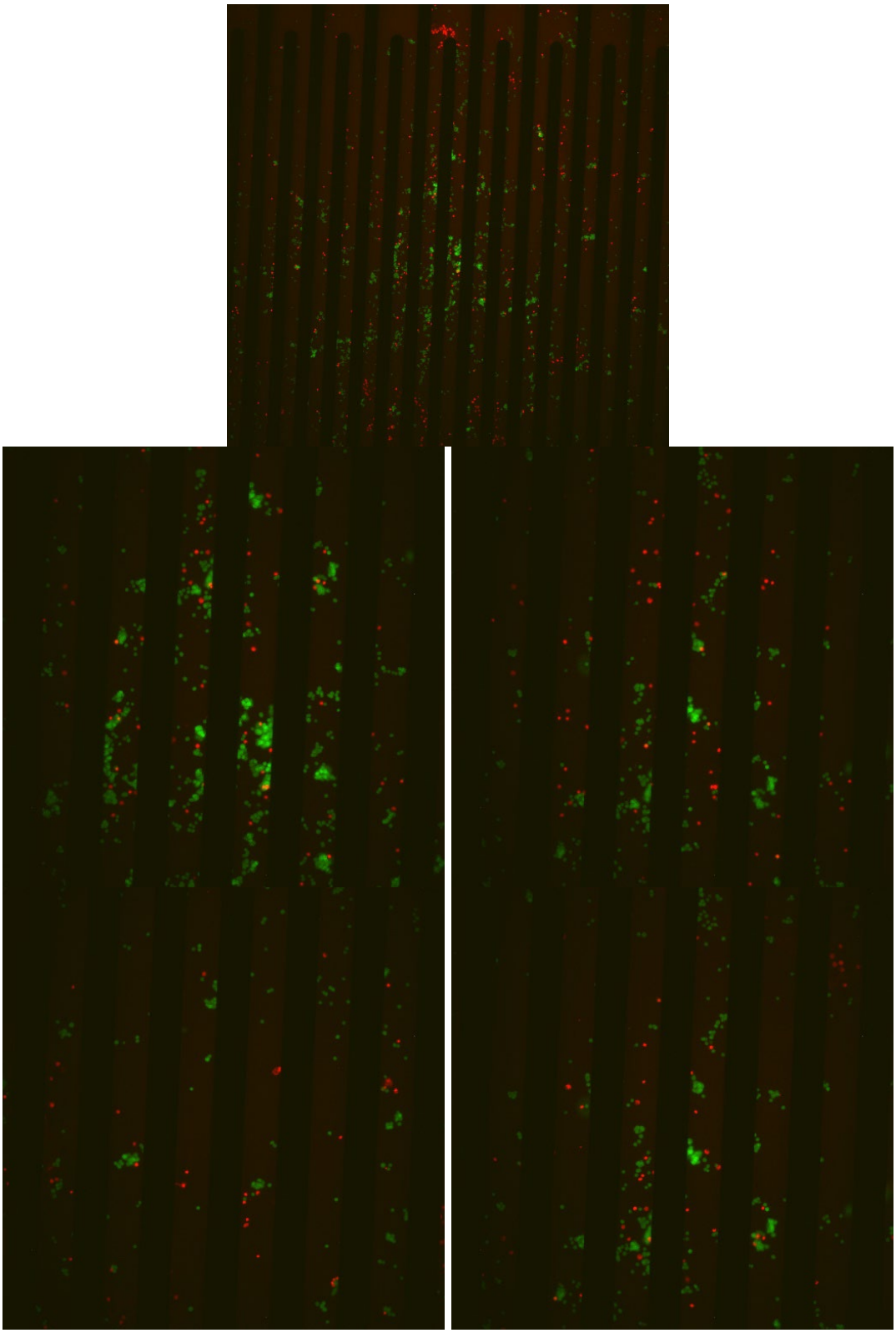

Figure 67 10V-covered 4x followed by 10x zoom:#1-1,#1-2,#1-3,#1-4 (clockwise), PI+Calcein, count in Table 1

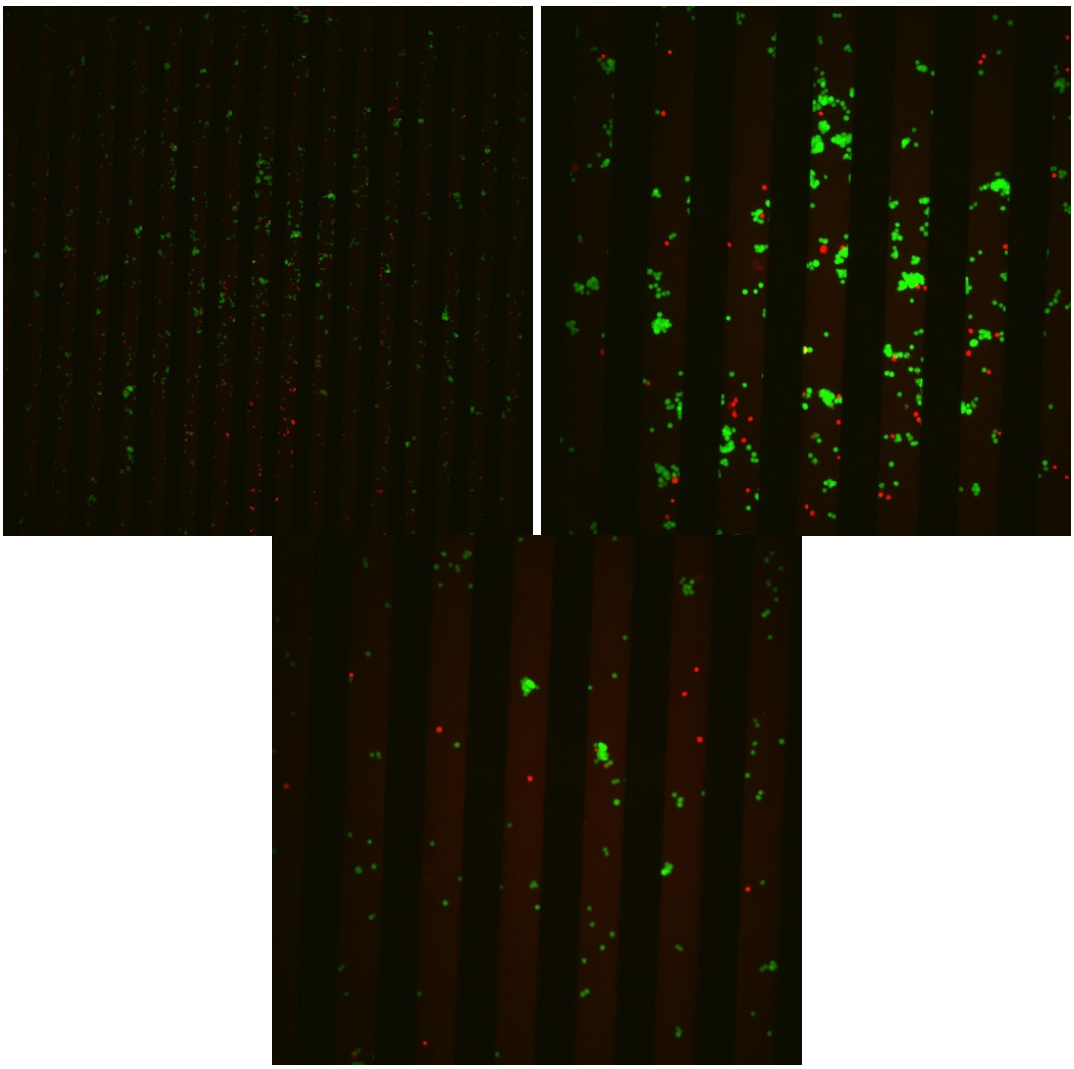

Figure 68 10V-covered 4x followed by 10x zoom:#2-1,#2-2 (clockwise), PI+Calcein, count in Table 1

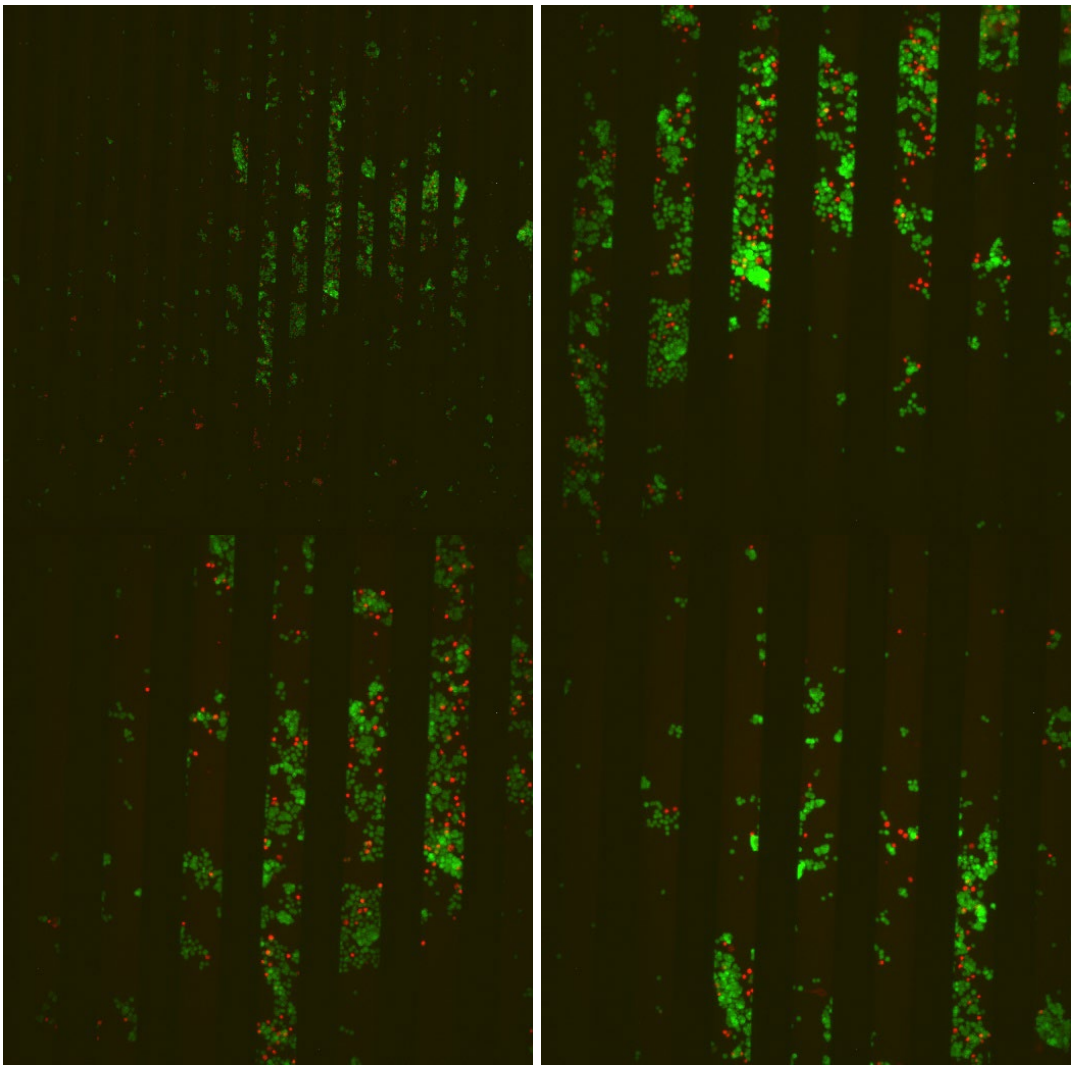

Figure 69 15V-covered 4x followed by 10x zoom:#1-1,#1-2,#1-3 (clockwise), PI+Calcein, count in Table 2

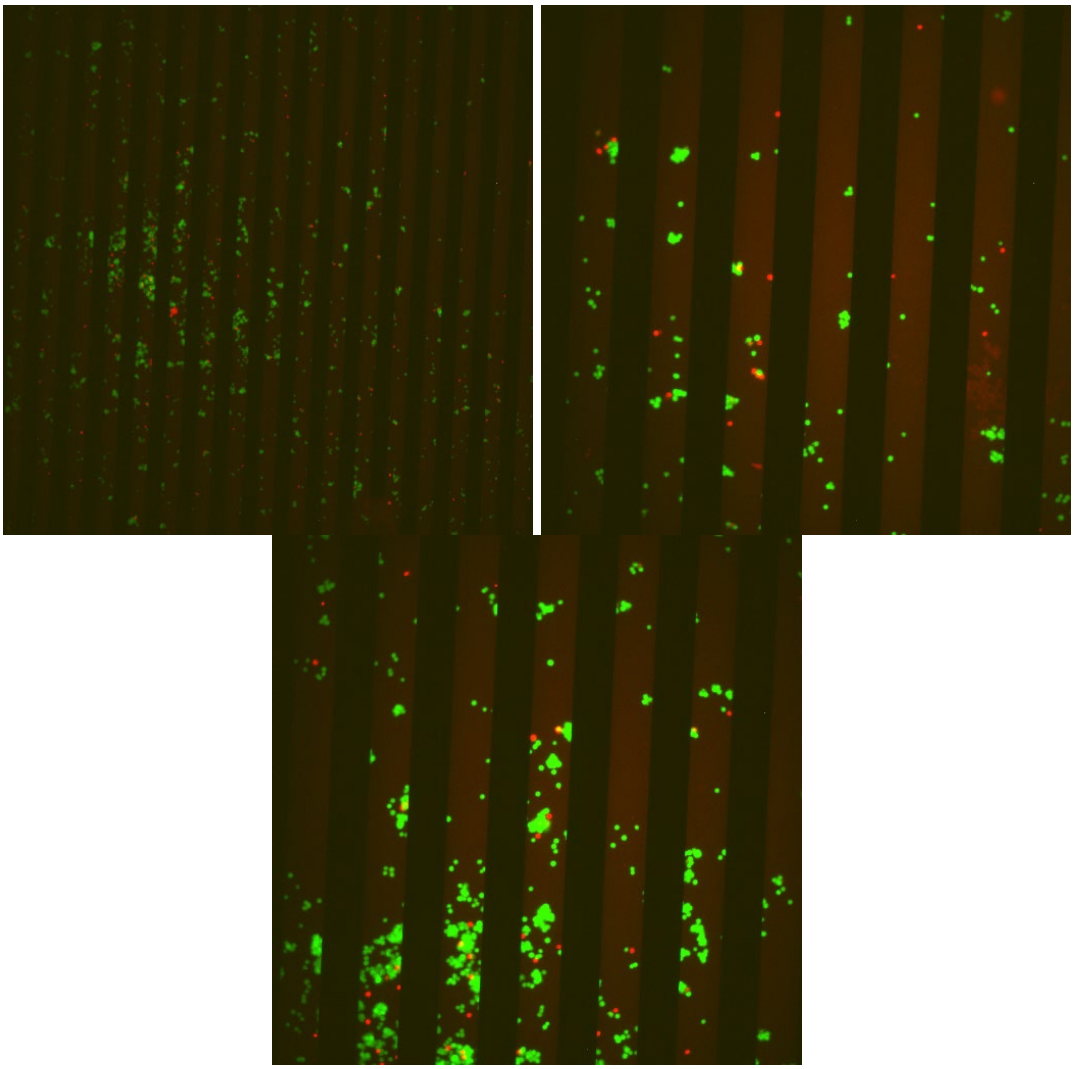

Figure 70 15V-covered 4x followed by 10x zoom:#2-1,#2-2 (clockwise), PI+Calcein, count in Table 2

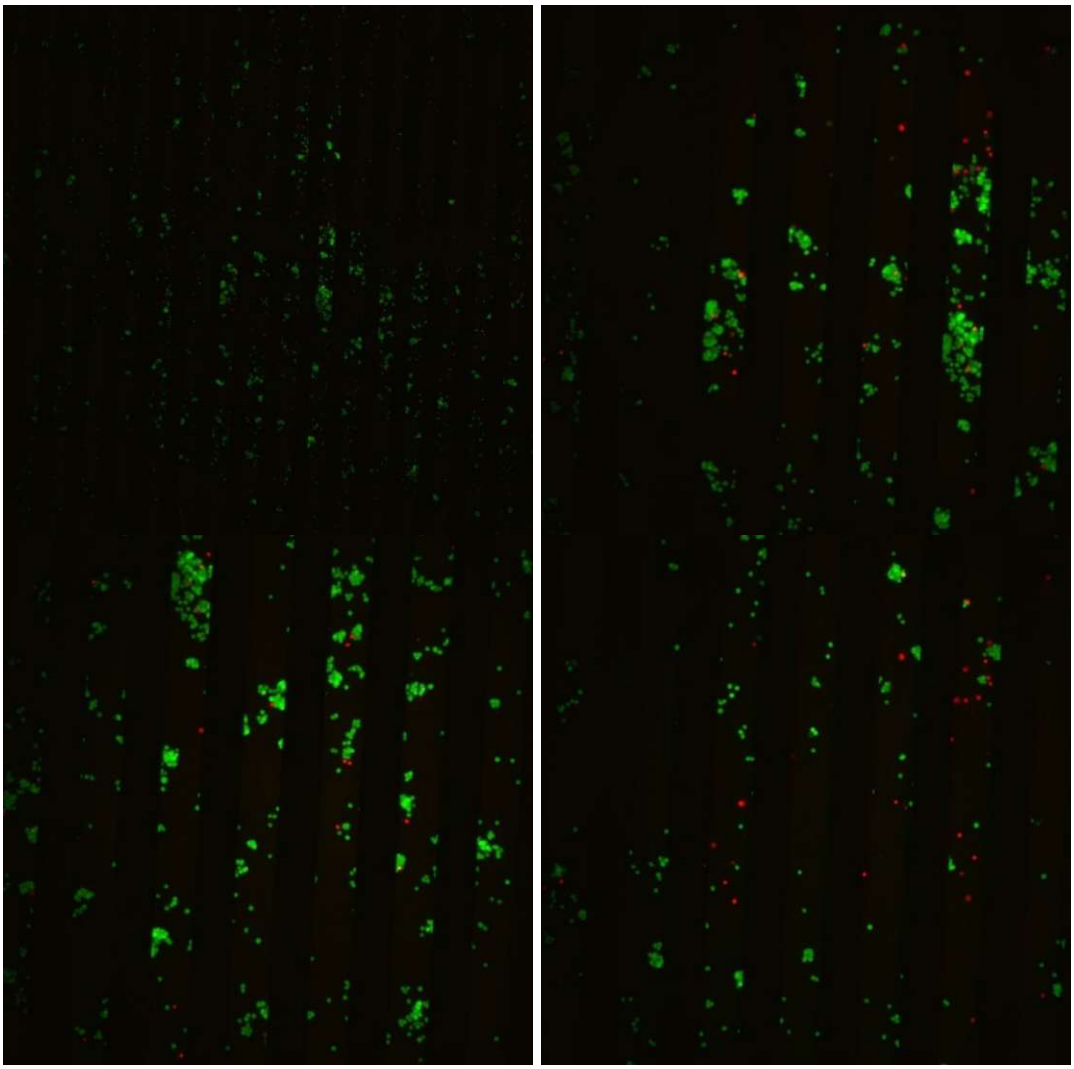

Figure 71 10V-naked 4x followed by 10x zoom:#1-1,#1-2,#1-3 (clockwise), PI+Calcein, Count in Table 3

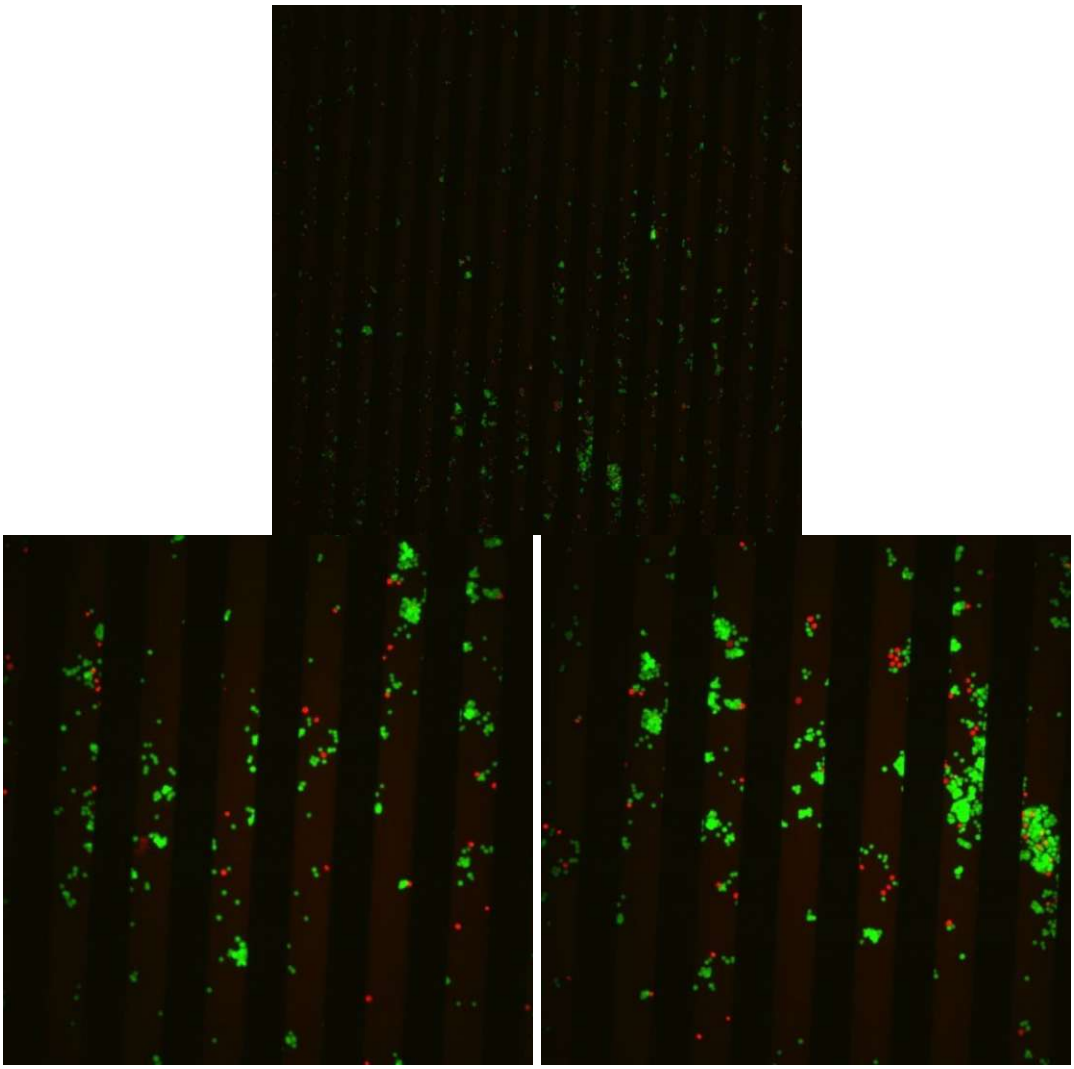

Figure 72 10V-naked 4x followed by 10x zoom:#2-1,#2-2 (clockwise), PI+Calcein, count in Table 3

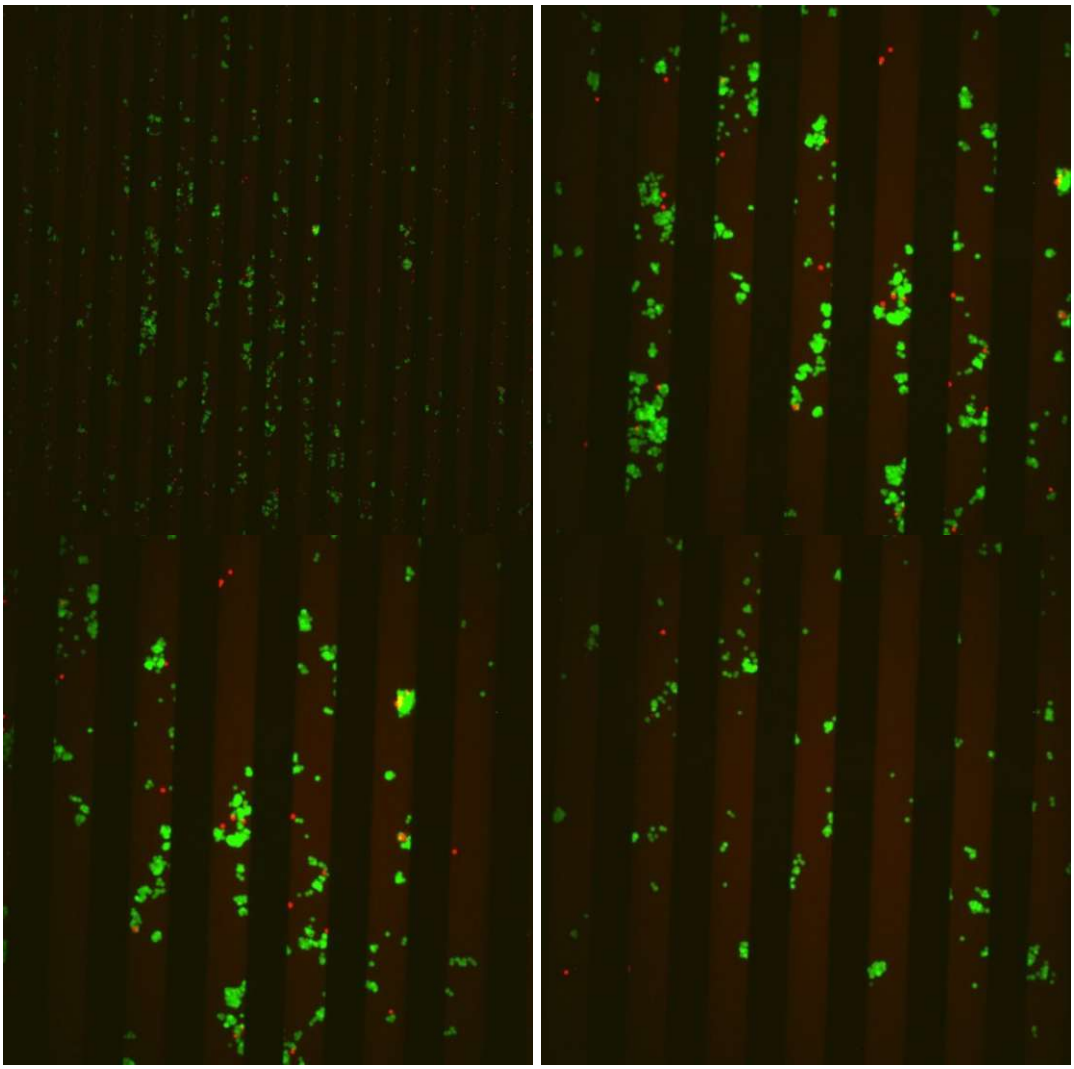

Figure 73 15V-naked 4x followed by 10x zoom:#1-1,#1-2,#1-3(clockwise), PI+Calcein, Count in Table 4

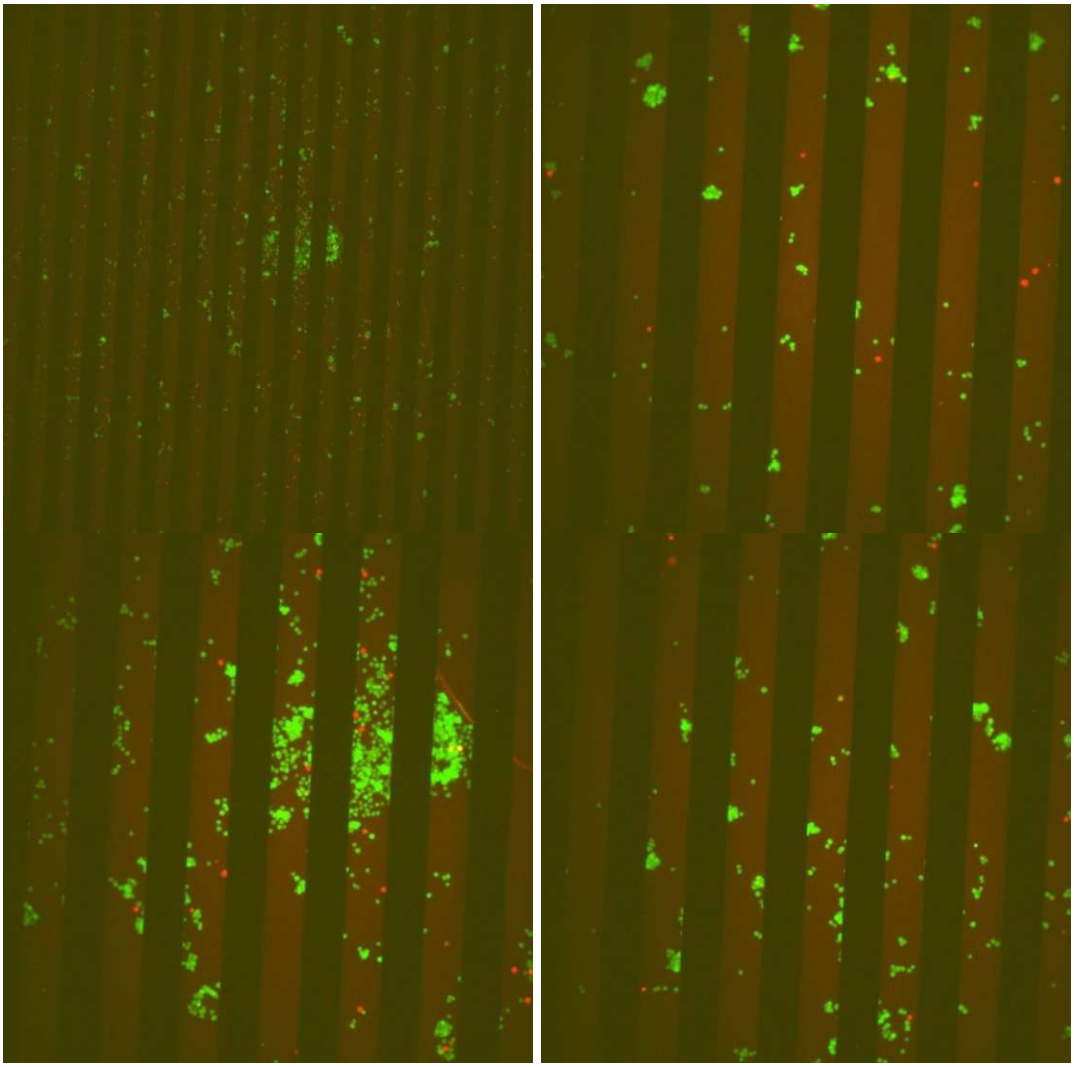

Figure 74 15V-naked 4x followed by 10x zoom:#2-1,#2-2,#2-3 (clockwise), PI+Calcein, Count in Table 4

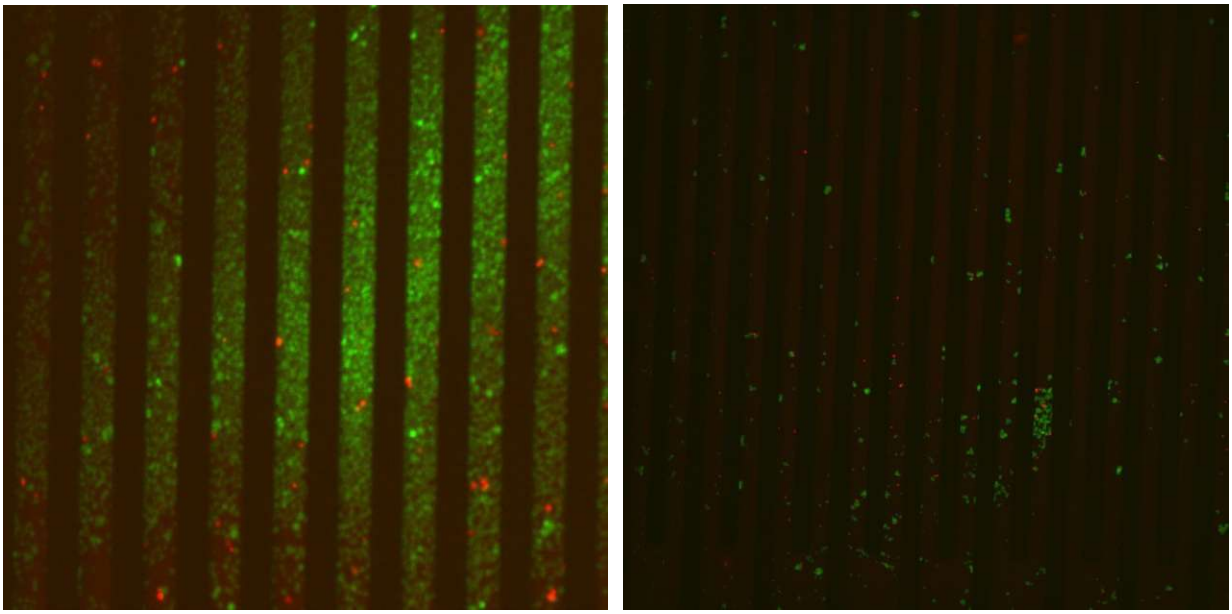

Figure 75 20V-covered electrode 10x (left) and 4x (right), PI+Calcein

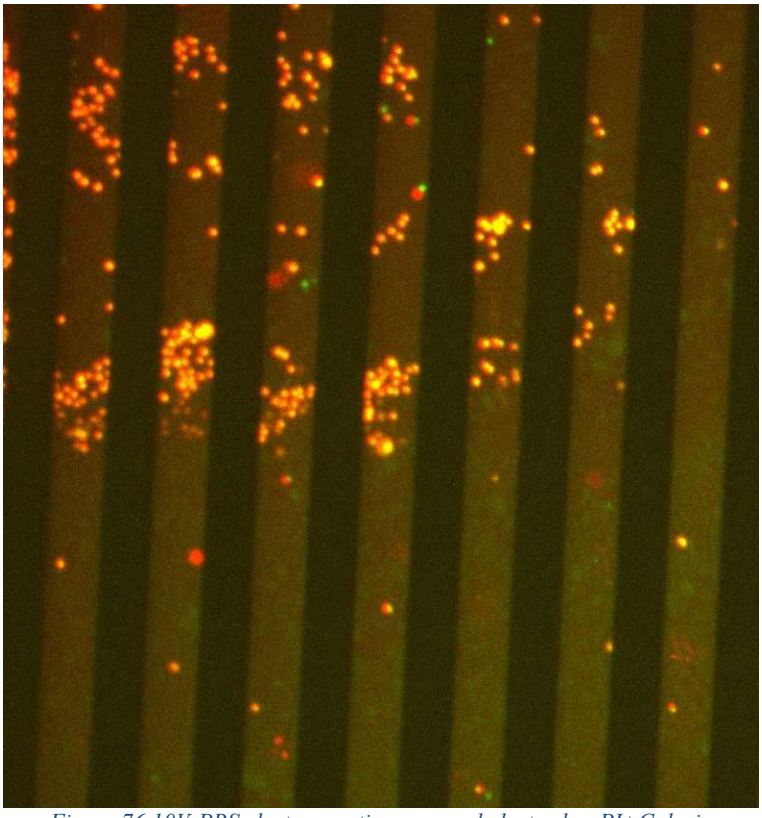

Figure 76 10V-PBS electroporation, covered electrodes, PI+Calcein

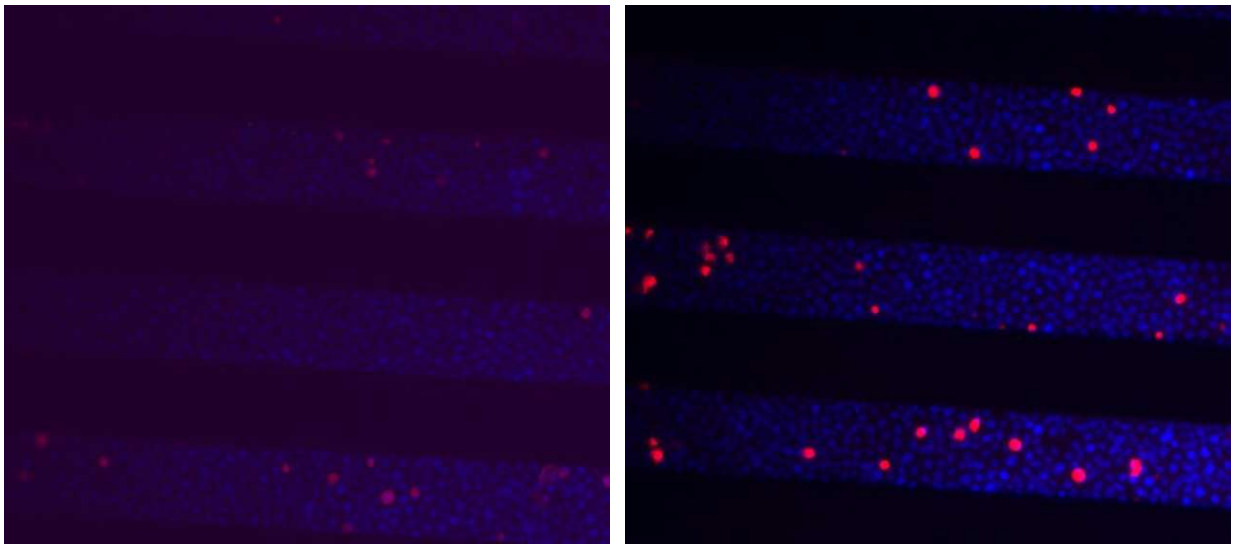

Figure 77 15V-10x nake(left) and covered (right) electrodes, PI+DAPI

Appendix- Cell count

Table 1 Cell count 10V-zoomed in area-covered electrodes

COVERED 10V	Death+electroporated(R+IR) count	Reversible electroporated count	PI- ratio
#1-1	70	30	2,33
#1-2	66	26	2,54
#1-3	37	14	2,64
#1-4	50	23	2,18
#2-1	52	19	2,74
#2-2	15	7	2,14
Average:			2,43

Table 2 Cell count 15V-zoomed in area-covered electrodes

COVER 15V	Death+electroporated(R+IR) count	Reversible electroporated count	PI-ratio
#1-1	210	86	2,44
#1-2	150	69	2,17
#1-3	68	33	2,06
#2-1	23	11	2,09
#2-2	39	19	2,05
Average:			2,16

Table 3 Cell count 10V-zoomed in area-naked electrodes

NAKED 10V	Death+electroporated(R+IR) count	Reversible electroporated count	PI-ratio
#1-1	33	10	3,3
#1-2	27	5	5.4
#1-3	35	6	5,83
#2-1	35	6	5,83
#2-2	58	13	4,46
Average:			4,96

Table 4 Cell count 15V-zoomed in area-naked electrodes

NAKED 15V	Death+electroporated(R+IR) count	Reversible electroporated count	PI-ratio
#1-1	28	9	3,11
#1-2	25	7	3,57
#1-3	8	2	4
#2-1	12	5	2,4
#2-2	28	12	2,33
#2-3	9	3	3
Average:			3,07

Literature

[1] Bejarano L., Jordão M.J.C., Joyce J.A., "Therapeutic targeting of the tumor microenvironment", (2021) Cancer Discovery, 11 (4), pp. 933 – 959, DOI: 10.1158/2159-8290.

[2] Dagogo-Jack I., Shaw A.T. "Tumour heterogeneity and resistance to cancer therapies" (2018) Nature Reviews Clinical Oncology, 15 (2), pp. 81 – 94, DOI: 10.1038/nrclinonc.2017.166

[3] Wu T., Dai Y., Tumor microenvironment and therapeutic response, (2017) Cancer Letters, 387, pp. 61 – 68, DOI: 10.1016/j.canlet.2016.01.043

[4] Knavel EM, Brace CL. Tumor ablation: common modalities and general practices. Tech Vasc Interv Radiol. 2013 Dec;16(4):192-200. doi: 10.1053/j.tvir.2013.08.002.

[5] Das R, Langou S, Le TT, Prasad P, Lin F, Nguyen TD. Electrical Stimulation for Immune Modulation in Cancer Treatments. Front Bioeng Biotechnol. 2022 Jan 11;9:795300. doi: 10.3389/fbioe.2021.795300.

[6] Oun R, Moussa YE, Wheate NJ. Correction: The side effects of platinum-based chemotherapy drugs: a review for chemists. Dalton Trans. 2018 Jun 12;47(23):7848. doi: 10.1039/c8dt90088d. Erratum for: Dalton Trans. 2018 May 15;47(19):6645-6653.

[7] Cooper, Geoffrey M. The Cell: A Molecular Approach. 2nd Edition. Sinauer Associates, 2000.

[8] Samantha F., Rebecca R., James W., Concepts of Biology ISBN 13:9781947172036 OpenStax

[9] Kanwal S, Fardini Y, Pagesy P, N'tumba-Byn T, Pierre-Eugène C, Masson E, Hampe C, Issad T. O-GlcNAcylation-inducing treatments inhibit estrogen receptor α expression and confer resistance to 4-OH-tamoxifen in human breast cancer-derived MCF-7 cells. PLoS One. 2013 Jul 11;8(7):e69150. doi: 10.1371/journal.pone.0069150.

[10] Donsì, F., Ferrari, G. & Pataro, G. Applications of Pulsed Electric Field Treatments for the Enhancement of Mass Transfer from Vegetable Tissue. Food Eng. Rev. 2, 109–130 (2010). doi: 10.1007/s12393-010-9015-3

[11] Campelo SN, Huang PH, Buie CR, Davalos RV. Recent Advancements in Electroporation Technologies: From Bench to Clinic. Annu Rev Biomed Eng. 2023 Jun 8;25:77-100. doi: 10.1146/annurev-bioeng-110220-023800. Epub 2023 Feb 28.

[12] Kotnik T., Rems L., Tarek M., Miklavcic D. Membrane Electroporation and Electropermeabilization: Mechanisms and Models (2019) Annual Review of Biophysics, 48, pp. 63 – 91 DOI: 10.1146/annurev-biophys-052118-115451

[13] Herman P. Schwan, Electrical Properties of Tissue and Cell Suspensions, Editor(s): JOHN H. LAWRENCE, CORNELIUS A. TOBIAS, Advances in Biological and Medical Physics, Elsevier, Volume 5,1957, Pages 147-209, ISSN 0065-2245, ISBN 9781483231112

[14] Edward J. Jacobs IV, Sabrina N. Campelo, Alyssa Charlton, Sara Altreuter, Rafael V. Davalos, Characterizing reversible, irreversible, and calcium electroporation to generate a burst-dependent dynamic conductivity curve, Bioelectrochemistry, Volume 155,2024,108580, ISSN 1567-5394, doi: 10.1016/j.bioelechem.2023.108580.

[15] Zhang N, Li Z, Han X, Zhu Z, Li Z, Zhao Y, Liu Z, Lv Y. Irreversible Electroporation: An Emerging Immunomodulatory Therapy on Solid Tumors. Front Immunol. 2022 Jan 7;12:811726. doi: 10.3389/fimmu.2021.811726.

[16] Frandsen, Stine K., Mille Vissing, and Julie Gehl. 2020. "A Comprehensive Review of Calcium Electroporation—A Novel Cancer Treatment Modality" Cancers 12, no. 2: 290. doi: 10.3390/cancers12020290

[17] Kurata K, Yoshimatsu S, Takamatsu H. Low-Voltage Irreversible Electroporation Using a Comb-Shaped Contact Electrode. IEEE Trans Biomed Eng. 2020 Feb;67(2):420-427. doi: 10.1109/TBME.2019.2914689. Epub 2019 May 3.

[18] Maschietto M, Dal Maschio M, Girardi S, Vassanelli S. In situ electroporation of mammalian cells through SiO2 thin film capacitive microelectrodes. Sci Rep. 2021 Jul 23;11(1):15126. doi: 10.1038/s41598-021-94620-8..

[19] Kauth, A., Mildner, AK., Hegel, L. et al. Development of Specialized Microelectrode Arrays with Local Electroporation Functionality. Ann Biomed Eng 52, 12–21 (2024). doi: 10.1007/s10439-023-03268-0

[20] Markx GH. The use of electric fields in tissue engineering: A review. Organogenesis. 2008 Jan;4(1):11-7. doi: 10.4161/org.5799.

[21] Behra Bahreyni, Chapter 2 - Microfabrication, Editor(s): Behraad Bahreyni, In Micro and Nano Technologies, Fabrication and Design of Resonant Microdevices, William Andrew Publishing, 2009, Pages 9-46, ISBN 9780815515777, doi: 10.1016/B978-081551577-7.50006-7.

[22] R.M. Pujahari, Chapter 2 - Solar cell technology, Editor(s): S.J. Dhoble, N.Thejo Kalyani, B. Vengadaesvaran, Abdul Kariem Arof, Energy Materials, Elsevier, 2021, Pages 27-60, ISBN 9780128237106, doi: 10.1016/B978-0-12-823710-6.00007-8.

[23] Kapil Gupta, Neelesh Kumar Jain, Rudolph Laubscher, Chapter 6 - Surface Property Enhancement of Gears, Editor(s): Kapil Gupta, Neelesh Kumar Jain, Rudolph Laubscher, Advanced Gear Manufacturing and Finishing, Academic Press, 2017, Pages 167-196, ISBN 9780128044605, doi: 10.1016/B978-0-12-804460-5.00006-7.

[24] Vaessen, E. M., Timmermans, R. A., Tempelaars, M. H., Schutyser, M. A., & Den Besten, H. M. (2019). Reversibility of membrane permeabilization upon pulsed electric field treatment in Lactobacillus plantarum WCFS1. Sci Rep. 2019 Dec 27;9(1):19990. doi: 10.1038/s41598-019-56299-w.

[25] Timothée Houssin, Vincent Senez,Chapter Six - Electrochemical Detection,Editor(s): Helen Bridle,Waterborne Pathogens,Academic Press,2014,Pages 147-188,ISBN 9780444595430, doi: 10.1016/B978-0-444-59543-0.00006-2.

[26] Chang L, Li L, Shi J, et al. Micro-/nanoscale electroporation. Lab on a Chip. 2016 Oct;16(21):4047-4062. DOI: 10.1039/c6lc00840b.

[27] Sherba JJ, Hogquist S, Lin H, Shan JW, Shreiber DI, Zahn JD. The effects of electroporation buffer composition on cell viability and electro-transfection efficiency. Sci Rep. 2020 Feb 20;10(1):3053. doi: 10.1038/s41598-020-59790-x.

Supplemental literature

[s1] WHO, Cancer statistic: https://www.who.int/news-room/fact-sheets/detail/cancer -Accessed 28.11.2023
[s2] World Cancer research fund International, global cancer incidence: https://www.wcrf.org/cancer-trends/worldwide-cancer-data/ -Accessed 28.11.2023
[s3] Cancer research UK: https://www.cancerresearchuk.org/about-cancer/what-is-cancer/how-cancers-grow Accessed 30.11.2023
[s4] https://www.electronics-tutorials.ws/waveforms/waveforms.html -Accessed 5.4.2024
[s5]https://www.neoti.com/led-technology-blogs/knowledge/gold-vs-copper-bonding-in-led-displays/ -Accessed 15.4.2024
[s6] Klayout:https://uhnf.egr.uh.edu/nanofabrication/lithography/klayout/ Accessed 15.4.2024
[s7] TI Prime datasheet:
https://www.microchemicals.com/products/adhesion_promotion/ti_prime.html Accessed 17.4.2024
[s8] https://www.keyence.com/ss/products/measure/sealing/coater-type/spin.jsp -Accessed 21.4.2024
[s9] AZ5214E photoresist datasheet:
https://www.microchemicals.com/de/produkte/fotolacke/az_5214_e.html -Accessed 21.4.2024
[s10] https://heidelberg-instruments.com/product/mla150/ -Accessed 21.4.2024
[s11] https://www.epfl.ch/research/facilities/cmi/equipment/photolithography/mla-150/ -Accessed 21.4.2024
[s12] https://www.microchemicals.com/micro/QDP_AZ5214E_EUvsJP_neg_2021-02-04.pdf -Accessed 21.4.2024
[s13] https://www.microchemicals.com/micro/tds_az_mif_developer.pdf -Accessed 21.4.2024
[s14] https://industry.nikon.com/de-de/produkte/industriemikroskopie/industriemikroskope/upright-eclipse-lv100nda-lv100nd/ - Accessed 21.4.2024
[s15] https://www.bruker.com/en/products-and-solutions/test-and-measurement/stylus-profilometers/dektakxt.html - Accessed 21.4.2024
[s16] https://plasma.oxinst.com/products/pecvd/plasmapro-100-pecvd Accessed 21.5.2024
[s17] https://www.microchemicals.com/micro/QDP_AZ5214E_EUvsJP_pos_2021-02-04.pdf Accessed 26.4.2024
[s18] https://en.wikipedia.org/wiki/Reactive-ion etching Accessed 20.5.2024
[s19] https://www.fluke.com/de-de/produkt/elektrische-pruefungen/digitalmultimeter/fluke-116 -Accessed 30.11.2023
[s20] https://www.pink.de/en/products/low-pressure-plasma-systems-en/v10-g.html Accessed 20.5.2024
[s21] https://www.attend.com.tw/en/product.php?act=list&cid=70 -Accessed 2.5.2024
[s22] https://www.fishersci.com/us/en/browse/90222047/electroporators?page=1 --Accessed 12.3.2024
[s23]https://single-market-economy.ec.europa.eu/single-market/european-standards/harmonised-standards/medical-devices_en -Accessed 2.12.2023
[s24] https://rigolshop.eu/product-oscilloscope-ds1000z/ds1074z-s%20plus.html -Accessed 18.4.2024
[s25] LM723 Datasheet: https://www.ti.com/lit/ds/symlink/lm723.pdf?ts=1715489581036 -Accessed 20.10.2023
[s26] B80R Datasheet: https://www.alldatasheet.com/datasheet-pdf/pdf/81722/DIOTEC/B80R.html - Accessed 20.10.2023
[s27] LM7824 Datasheet: https://www.alldatasheet.com/datasheet-pdf/pdf/33411/UTC/LM7824.html - Accessed 20.10.2023
[s28] BZX3V9 Datasheet: https://www.alldatasheet.com/datasheet-pdf/pdf/344206/DIOTECH/BZX3V9.html - Accessed 20.10.2023
[s29] 1N4007 Datasheet: https://www.vishay.com/docs/88503/1n4001.pdf - Accessed 20.10.2023

[s30] BYW81P-200 Datasheet: https://www.alldatasheet.com/datasheet-pdf/pdf/22175/STMICROELECTRONICS/BYW81P-200.html - Accessed 20.10.2023
[s31] https://www.fluke.com/en-us/product/thermal-cameras/tis55plus - Accessed 30.10.2023
[s32] https://store.arduino.cc/products/arduino-uno-rev3 - Accessed 15.10.2023
[s33]https://www.ti.com/lit/ds/symlink/ads1115.pdf?ts=1715495628740&ref_url=https%253A%252F%252Fwww.google.com%252F - Accessed 15.10.2023
[s34] https://www.handsontec.com/dataspecs/module/I2C_1602_LCD.pdf -Accessed 15.10.2023
[s35] BD241 Datasheet: https://www.alldatasheet.com/datasheet-pdf/pdf/601365/SAVANTIC/BD241.html Accessed 30.10.2023
[s36] LM308 Datasheet: https://www.analog.com/media/en/technical-documentation/data-sheets/lt0108.pdf - Accessed 30.10.2023
[s37] 2N2222 Datasheet: https://www.alldatasheet.com/view.jsp?Searchword=2n2222 Accessed 30.10.2023
[s38] BUZ21 Datasheet: https://www.alldatasheet.com/datasheet-pdf/pdf/79519/INFINEON/BUZ21.html Accessed 30.10.2023
[s39] https://www.atcc.org/products/htb-38 Accessed 26.2.2024
[s40] https://www.ols-bio.de/products/cell-counter-casy Accessed 2.3.2024
[s41] DAPI Datasheet: https://www.thermofisher.com/at/en/home/life-science/cell-analysis/fluorophores/dapi-stain.html -Accessed 11.3.2024
[s42] PI Datasheet: https://www.thermofisher.com/at/en/home/life-science/cell-analysis/fluorophores/propidium-iodide.html -Accessed 11.3.2024
[s43] https://www.microscopyu.com/museum/eclipse-te2000-inverted-microscope -Accessed 6.3.2024
[s44] https://www.geeksforgeeks.org/amperes-law/ -Accessed 5.4.2024
[s45] https://www.electrical4u.com/faraday-law-of-electromagnetic-induction/ -Accessed 5.4.2024
[s46] Calecein Datasheet: https://www.thermofisher.com/document-connect/document-connect.html?url=https://assets.thermofisher.com/TFS-Assets%2FLSG%2Fmanuals%2FMAN0019058_CalceinAM_UG.pdf -Accessed 20.3.2024

Biography

Antun Štetić was born on 30.10.1995 in the small town of Zaprešić, near Zagreb, Croatia. After finishing high school with excellent performance in physics during the matriculation exam, started to study electrical engineering at the University of Osijek. During the study, 10-month long ERASMUS exchange program was spent at TU Wien where he fell in love with biomedical engineering. After finishing a Master's degree from the University of Osijek with a specialization in communication technologies it was decided that a new degree would be achieved at TU Wien as biomedical engineer with specialization in Biomedical signals & instrumentation. During the whole study, he was always volunteering at different student organizations, while at same time being employed.

His previous thesis works were: ”Electrical circuits for capacitive-voltage transformation” (Bachelor) and “Circuits for bioimpedance measurements” (Masters).

Appreciation

Special thanks to my mentor Heinz Wanzenböck for his guidance and patience through the thesis work, Neda Karami for introducing me to the cleanroom and helping with the staining process, Sebastian Knafl for the help with working principles of clean room equipment, Sonia Prado Lopez for allowing me to use her bio-lab as well assisting with CASY measurements and experiment setup, and Seyda Khigilli for helping with tumor cell cultivation.

Special thanks to Eugenijus Kaniusas as well for introducing me to the biomedical engineering field during my Erasmus stay and inspiring me to study it.

Finally, thanks to Marko, Zdravka, Matej, Anja, Antonia, Mislav, and Mihaela for being a moral support during this process.